Imaging of the Distal Tibiofibular Syndesmosis:
Anatomy in Relation to Radiological Diagnosis

John J. Hermans

ISBN/EAN: 978-94-91211-35-5

Cover image: J.J. Hermans
Layout: Bob Kielstra, Ipskamp Drukkers B.V., Enschede, Netherlands
Printing: Ipskamp Drukkers B.V., Enschede, Netherlands

Rotterdam, 2011

Imaging of the Distal Tibiofibular Syndesmosis:
Anatomy in Relation to Radiological Diagnosis

Afbeelding van de distale tibiofibulaire syndesmose:
anatomie in relatie tot radiologische diagnose

Proefschrift

ter verkrijging van de graad van doctor aan de
Erasmus Universiteit Rotterdam
op gezag van de
rector magnificus

prof.dr. H.G. Schmidt

en volgens het besluit van het College voor Promoties.

De openbare verdediging zal plaatsvinden op

donderdag 16 juni 2011 om 9.30 uur

door

John J. Hermans
geboren te 's-Gravenhage

Promotiecommissie

Promotor:	Prof.dr. G.J. Kleinrensink
Overige leden:	Prof.dr. J.L. Bloem
	Dr. A.Z. Ginai-Karamat
	Prof.dr. P. Patka

To my parents

Contents

Chapter 1

Introduction and thesis outline

Introduction

1. Background

Injury to the distal tibiofibular syndesmosis can occur after an ankle sprain or after an acute ankle fracture. In an estimated 1-11% of all ankle sprains, injury of the distal tibiofibular syndesmosis occurs which is known as a high ankle sprain [1-3]. However, depending on the type and level of sporting activities the incidence of syndesmotic injury can be as high as 75% [4-7]. Whether acute ankle fractures are accompanied with injury of the syndesmosis depends on the type of ankle fracture. Based on radiological findings, several fracture classification systems have been developed. These classifications can aid in predicting the presence of injury to the syndesmosis in relation to the level of the fibula fracture or to the mechanism of trauma. Clinically frequently used fracture classification systems are the Danis-Weber and AO-Müller classification that pertain to the level of the distal fibula fracture, and the Lauge-Hansen classification which is based on the trauma mechanism, i.e. on the position of the foot at the moment of injury and the direction in which the talus moves within the ankle mortise [8-10]. Detailed information about the three fracture classifications can be found in tables 1-3 (*pages 16/17/18*). Despite the frequency and importance of injury of the syndesmosis, the management of this kind of injury has remained controversial [11-29].

2. Problem definition

In order to use a fracture classification which uses the distal tibiofibular syndesmosis as a point of reference, good knowledge about the syndesmosis is fundamental. This concerns not only information about the exact boundaries of the syndesmosis, but also the exact location and direction of the tibiofibular ligaments.

2.1 Boundaries of the syndesmosis

Fracture classification systems are useful because they enable one to define a fracture pattern, which subsequently forms the basis for a treatment plan. As in the Danis-Weber and AO-Müller fracture classification system the level of fibula fracture is related to the distal tibiofibular syndesmosis, one would expect that the anatomic position of the syndesmosis as well as which osseoligamentous structures are exactly involved are precisely defined [30, 31]. However, neither in anatomical textbooks (among others Lanz und Wachsmuth), nor in articles referring to the fracture classification systems are the upper and lower border of the syndesmosis mentioned [32-38]. Presumably, injury to the syndesmosis refers to injury to the tibiofibular ligaments, and most likely the anterior tibiofibular ligament. A syndesmosis is, strictly speaking, a fibrous joint in which two adjacent bones are linked by a strong membrane or ligaments. The distal tibiofibular joint is also a syndesmosis and consists of two bones and four ligaments. The distal tibia and fibula form the osseous part of the syndesmosis and are linked by the distal anterior tibiofibular ligament (ATIFL), the distal posterior tibiofibular ligament (PTIFL), the transverse ligament and the interosseous ligament [39, 40].

In order to determine what radiologists define as the tibiofibular syndesmosis, I presented an anteroposterior radiograph of a normal ankle at a congress about musculoskeletal radiology (Sandwich course 2-5 February 2010, Ede, The Netherlands). Both residents and consultants in radiology, the latter with different fields of interest and varying years of experience, were asked to define the lower and upper border of the syndesmosis (Fig. 1, *on next page*). On the first day there were 366 participants, consisting of 56% consultants and 44% residents, and on the second day there were 453 participants, consisting of 59% consultants and 41% residents.

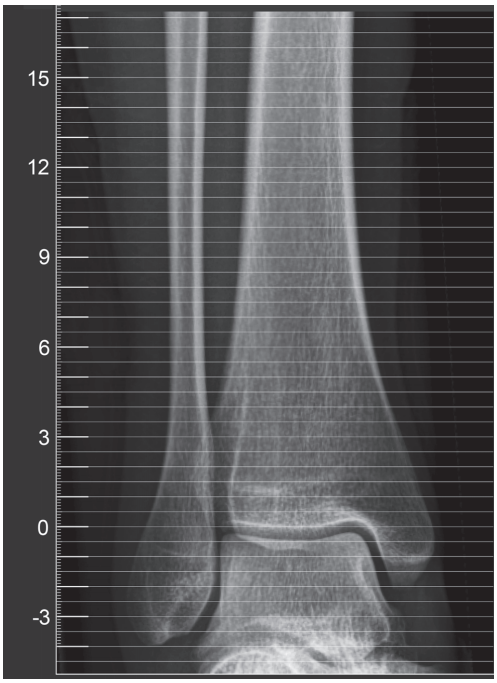

Fig. 1. Anteroposterior radiograph of a normal ankle. A vertical scale in cm allows demarcation of the lower (at 0 cm) and upper (at 8 cm) border of the syndesmosis.

The results showed a large variation in demarcation of both the lower and the upper border of the syndesmosis (Fig. 2, *continues on next page*). The lower border was more or less centred around the tibiotalar joint line and ranged from 1 cm below to 1 cm above the tibiotalar joint line in 82%. For the upper border of the syndesmosis however, the de facto upper border of the syndesmosis, i.e. at 8-9 cm above the tibiotalar joint, was chosen as the least likely possibility. Generally, when consultants were compared with residents, the position of the lower border was demarcated more or less equally. The upper border, however, showed some variation with the residents' estimation of the upper border being slightly lower positioned than that of the consultants'. This means that classification of a fibula fracture as infra- trans- or suprasyndesmotic is not uniform and could be an explanation for the observed poor to moderate interobserver variation for the Weber fracture classification [41, 42].

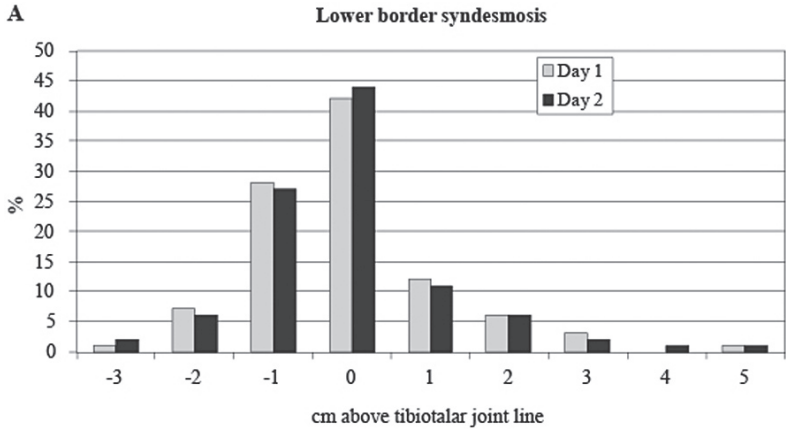

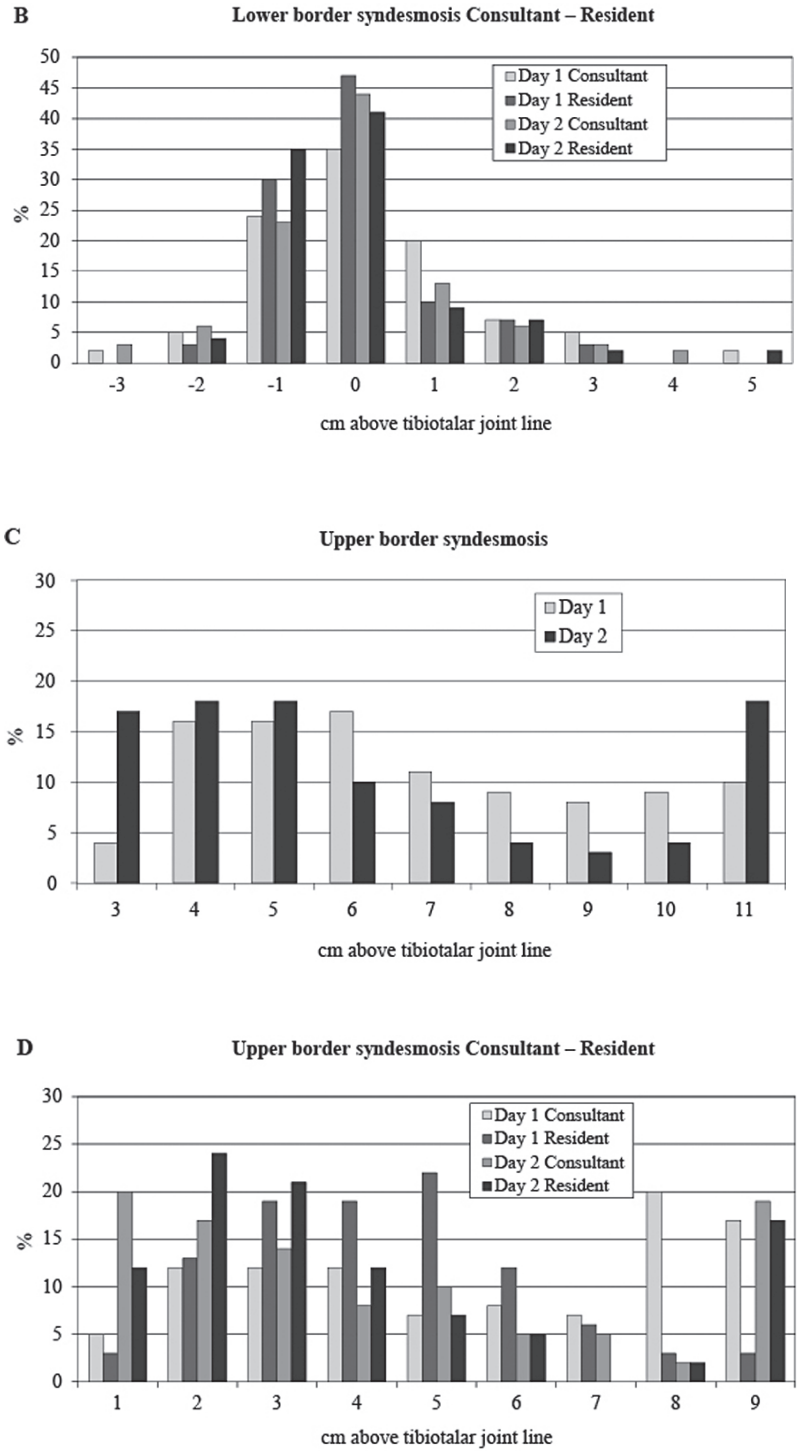

Fig. 2. Distribution of the estimated lower (*A, B*) and upper borders (*C, D*) of the syndesmosis by two groups of consultants and residents in radiology on two different days.

2.2 Position and direction of syndesmotic ligaments

Understanding the exact anatomy of both the osseous and ligamentous structures is essential for interpretation of plain radiographs, ultrasound (US), computed tomography (CT) and magnetic resonance (MR) images, in ankle arthroscopy and in therapeutic management.

Several techniques have been used to obtain a better insight into the anatomy of the osseoligamentous structures comprising the ankle syndesmosis [30, 43-49]. In human cadavers microscopic and macroscopic analysis of the bones and ligaments have shown that the distal tibiofibular joint is not only a syndesmotic joint but also a synovial joint [39].

Radiography is the most commonly used technique to image the ankle and evaluate the integrity of the syndesmosis. For that reason the congruity of the ankle mortise and the distance between the distal tibia and fibula are evaluated. Frequently used measurements include the tibiofibular clear space (TFCS), the tibiofibular overlap (TFO) and the ratio of the medial clear space and the superior clear space (MCS/SCS) (Fig. 3). A normal TFCS should be less than 6mm, and a normal TFO should be greater than 6mm [50]. The absolute value of a normal MCS should not exceed 4mm, and a normal SCS/MCS ratio is larger than one [51]. Tibiofibular overlap and medial and superior clear space are the most useful. This as one-sided traumatic absence of tibiofibular overlap may be an indication of syndesmotic injury, and a medial clear space larger than a superior clear space is indicative of deltoid injury, which could be associated with syndesmotic injury [52].

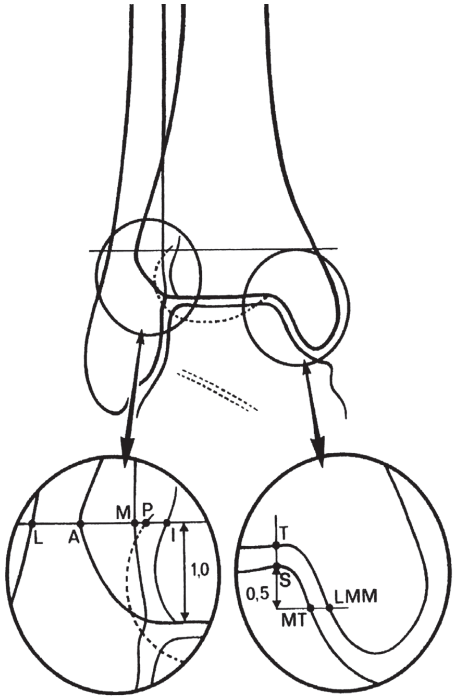

Fig 3. A schematic drawing of the ankle shows landmarks used for measurements of the different radiologic parameters. L=lateral border of the fibula; M=medial border of the fibula; A=anterior tibial tubercle; P=posterior tibial tubercle; I=floor of incisura fibularis; T=tibial plafond; S=superior point of medial talus; MT=medial side of talus; LMM=lateral side medial malleolus. AM is tibiofibular overlap (TFO). MI is tibiofibular clear space (TFCS). TS is superior clear space (SCS) and MTLMM is medial clear space (MCS). (Copy with permission from A. Beumer Clin. Orthop. Rel. Res 2004;423:227-234).

The syndesmotic ligaments have not been as extensively studied with ultrasound (US) as the medial and lateral collateral ligaments [53-56]. The anterior tibiofibular ligament is easy to depict because it lies superficially. The posterior tibiofibular ligament, however, is less easy to depict as it is not only positioned a little deeper but also because it is difficult to position

the US probe in the curved space between the Achilles tendon and the fibula. Ultrasound can clearly depict a torn anterior tibiofibular ligament in the acute stage but is less accurate after elapse of time. Furthermore, the results are dependent on the skills of the radiologist [55].
Computed tomography has been used to analyze the relation of the tibia and fibula and to determine the morphology of the fibular incisure [31, 57-59]. The fibula lies in a groove of the tibia that in most cases has a concave shape, but can be flat, and is held in this groove by the four syndesmotic ligaments that attach it to the tibia. A shallow fibular incisure might predispose to syndesmotic injury as the fibula is not held firmly in position. Also, after an acute ankle fracture it is more difficult to reposition the fibula when the tibial groove is flat. With CT, widening of the mortise exceeding 3 mm can reliably be assessed, as well as gross deformity, fibular malrotation or displacement [60]. CT can therefore be of aid in planning revision surgery.
Evaluation of the syndesmotic ligaments can be performed with arthroscopy and MRI. With arthroscopy, using either anterior or posterior portals, the anterior and posterior tibiofibular ligaments can be visualized [61, 62]. However it is not possible to visualize the entire anterior tibiofibular ligament as it lies intra-articularly for only 20% [63]. Furthermore, due to its anatomical position, only the inferior part of the posterior tibiofibular ligament can be seen, i.e. the transverse ligament, whereas the interosseous ligament, extending above the syndesmotic recess between the distal tibia and fibula, cannot be visualized at all. During arthroscopy widening of the tibiofibular syndesmosis can be tested using a bone hook. When a bone hook with a width of 3 mm can be turned around in the space between the distal tibia and fibula the suspicion of syndesmotic injury is raised (unpublished data A. Beumer, M.P. Heijboer, Department of Orthopaedics, Erasmus University Medical Center).
The value of MRI in acute and chronic syndesmotic injuries has been described in several articles [5, 64-66]. Vogl et. al. performed a contrast-enhanced MRI in 38 patients with an acute ankle trauma and clinical suspicion of a lesion in the syndesmosis, in which a tear of the ATIFL markedly enhanced in T1-weighted images [67]. Muratli et. al. used MR arthrography in the first few days after injury in 15 patients with a Weber type B or C ankle fracture to demonstrate leakage of contrast into the tibiofibular space as a sign of syndesmotic diastasis [68].
Several authors paid attention to the position of the ligaments paraxial to the imaging plane and concluded that axial imaging with the foot in full dorsiflexion provided optimal views of the anterior and posterior tibiofibular ligaments [69, 70].
Until now the usual three orthogonal planes, i.e. axial, coronal and sagittal planes, have been used to depict the tibiofibular ligaments. A basic concept in visualizing a ligament with MRI is that the plane of imaging should be along the longitudinal axis of the ligament. When the image plane is oblique to this axis the ligament is not depicted along its entire length but only partially. This could lead to interpretation of an intact ligament as a ruptured ligament. Therefore, as the anterior and posterior distal tibiofibular ligament run in an oblique plane, imaging in the axial plane can result in false positive findings [64, 66, 71]. The transverse ligament lies in the axial plane and can therefore be depicted with the standard axial view. The interosseous ligament extends between the distal tibia and fibula and can be depicted in a coronal plane.

3. Focus area

Knowledge about the detailed anatomy of the distal tibiofibular ligaments in relation to different imaging modalities plays an important role in evaluation of imaging findings in both acute and chronic injury. In this thesis special attention is paid to the anatomy of the distal tibiofibular syndesmosis which served as a basis to improve depiction of the syndesmotic ligaments with MRI. As only with MRI it is possible to obtain information about all four tibiofibular ligaments, as well as the osseous structures and their relationships.

4. Goal

The goal of this thesis is to improve knowledge of the anatomy of the distal tibiofibular syndesmosis and apply this knowledge in clinically used fracture classification systems.

5. Outline of the thesis

In chapter one an overview of the literature is given about imaging techniques of the syndesmosis of the ankle. In chapter two a pictorial review reveals the normal anatomy of the distal tibiofibular syndesmosis based on a review of the literature, supplemented with our own findings at microscopy and macroscopy. In chapter three, MR-plastination-arthrography is presented as a new technique to correlate plastination slices with the intra- and extraarticular anatomy of the distal tibiofibular syndesmosis as seen with MRI. These anatomic findings lead to the development of a new oblique imaging plane for MRI. In chapter four this new oblique MR imaging plane is used to depict, in healthy volunteers, the anterior and posterior tibiofibular ligaments. In chapter five the additional value of this oblique imaging plane in detection of syndesmotic injury is demonstrated in patients with an acute ankle fracture. In chapter six three frequently used fracture classifications (Weber, AO-Müller and Lauge-Hansen) were compared to MRI, regarding their ability to predict injury of the syndesmosis in acute ankle fractures.

Table 1. Weber fracture classification.

Type	**Fracture description**
A	Fibula fracture below the level of the syndesmosis
B	Fibula fracture at the level of the syndesmosis: - juxtasyndesmotic: syndesmosis intact - transsyndesmotic: syndesmosis injured
C	Fibula fracture above level of the syndesmosis, and may be as high as just below the fibular head (Maisonneuve fracture)

Table 2. AO-Müller fracture classification (malleolar segment type 44).

Category A	injury below the level of the distal tibiofibular syndesmosis (infrasyndesmotic).
A.1	*isolated infrasyndesmotic lesion*
A.1.1	rupture of the lateral collateral ligament.
A.1.2	avulsion of the tip of the lateral malleolus
A.1.3	transverse fracture of the lateral malleolus
A.2	*infrasyndesmotic lesion associated with a fracture of the medial malleolus*
A.2.1	rupture of the lateral collateral ligament together with a fracture of the medial malleolus
A.2.2	avulsion of the tip of the lateral malleolus together with a fracture of the medial malleolus
A.2.3	transverse fracture of the lateral malleolus together with a fracture of the medial malleolus
A.3	*infrasyndesmotic lesion together with a postero-medial fracture*
A.3.1	rupture of the lateral collateral ligament together with a postero-medial fracture
A.3.2	avulsion of the tip of the lateral malleolus together with a postero-medial fracture
A.3.3	transverse fracture of the lateral malleolus together with a postero-medial fracture
Category B	injury at the level of the distal tibiofibular syndesmosis (transsyndesmotic)
B.1	*isolated transsyndesmotic fibular fracture*
B.1.1	simple fracture of the fibula
B.1.2	simple fibular fracture with a rupture of the anterior syndesmosis
B.1.3	multifragmentary fibular fracture
B.2	*transsyndesmotic fibular fracture with a medial lesion*
B.2.1	simple fracture of the fibula with rupture of the anterior syndesmosis and a rupture of the medial collateral ligament
B.2.2	simple fibular fracture with rupture of the anterior syndesmosis and a fracture of the medial malleolus
B.2.3	multifragmentary fibular fracture with a medial lesion
B.3	*transyndesmotic fibular fracture with a medial lesion and a Volkmann's fracture*
B.3.1	simple fracture of the fibula with rupture of the medial collateral ligament and a Volkmann fracture
B.3.2	simple fracture of the fibula with a fracture of the medial malleolus and a Volkmann fracture
B.3.3	multifragmentary fibular fracture with a fracture of the medial malleolus and a Volkmann fracture
Category C	injury above the level of the distal tibiofibular syndesmosis (suprasyndesmotic)
C.1	*simple suprasyndesmotic fracture of the fibular diaphysis*
C.1.1	simple fibular diaphyseal fracture with rupture of the medial collateral ligament
C.1.2	simple fibular diaphyseal fracture with a fracture of the medial malleolus
C.1.3	simple fibular diaphyseal fracture with a fracture of the medial malleolus and a Volkmann fracture (Dupuytren)
C.2	*multifragmentary suprasyndesmotic fracture of the fibular diaphysis*
C.2.1	multifragmentary fracture of the fibular diaphysis with rupture of the medial collateral ligament
C.2.2	multifragmentary fracture of the fibular diaphysis with a fracture of the medial malleolus
C.2.3	multifragmentary fracture of the fibular diaphysis with a Medial lesion and a Volkmann fracture (Dupuytren)
C.3	*proximal fibular lesion (Maisonneuve)*
C.3.1	Maisonneuve fracture without shortening and without a Volkmann Fracture
C.3.2	Maisonneuve fracture with shortening without a Volkmann fracture
C.3.3	Maissonneuve fracture wih a medial lesion and a Volkmann fracture

Table 3. The Lauge-Hansen fracture classification describes the mechanisms of ankle fractures, based on the position of the foot at the time of injury and the direction in which the talus moves within the ankle mortise. It defines both the bony and ligamentous injury. The following five groups of ankle fractures can be discerned: supination-adduction, supination-eversion, pronation-abduction, pronation-eversion and pronation-dorsiflexion. Depending on the degree of severity the main groups can be further divided into stages.

Type of injury Foot position/ direction of force	**Pathology**
Supination adduction	1) Transverse fracture fibula at or distal to the level of the tibiofibular joint/ tear of collateral ligaments 2) Vertical, oblique fracture of the medial malleolus/ tear of the deltoid ligament
Supination eversion (external rotation)	1) Disruption of the anterior tibiofibular ligament or an avulsion of its tibial attachment (*Tillaux fracture*) or fibular attachment (*Wagstaffe-Le Fort fracture*) 2) Spiral, oblique fracture of the distal fibula. The fracture line runs from proximal posterior to distal anterior at a variable distance from the tibiotalar joint 3) Disruption of the posterior tibiofibular ligament or fracture of the posterior malleolus 4) Fracture of the medial malleolus or rupture of the deltoid ligament
Pronation abduction	1) Transverse fracture of the medial malleolus or rupture of the deltoid ligament 2) Rupture of the anterior and posterior syndesmotic ligaments or avulsion fracture of their insertion(s) 3) Short, oblique fracture of the fibula 0,5-1cm above the distal articular surface of the tibia
Pronation eversion (external rotation)	1) Transverse fracture of the medial malleolus or disruption of the deltoid ligament 2) Disruption of the anterior tibiofibular ligament. The ligament may avulse its tibial attachment (*Tillaux fracture*) 3) High oblique, spiral fibular fracture. No fracture is less than 2,5 cm above the tibiotalar joint. The fracture pattern runs from proximal anterior to distal posterior. The fibula may fracture proximally at the neck (*Maisonneuve fracture*) 4) Rupture of posterior tibiofibular ligament or avulsion fracture of the posterolateral tibia
Pronation dorsiflexion/ pilon fracture	1) Fracture of the medial malleolus 2) Fracture of the anterior margin of the tibia 3) Supramalleolar fracture of the fibula 4) Transverse fracture of the posterior tibial surface

References

1. Gerber JP, Williams GN, Scoville CR, Arciero RA, Taylor DC. Persistent disability associated with ankle sprains: a prospective examination of an athletic population. Foot Ankle Int. 1998; 19(10):653-660.
2. Hopkinson WJ, St Pierre P, Ryan JB, Wheeler JH. Syndesmosis sprains of the ankle. Foot Ankle. 1990; 10(6):325-330.
3. Cedell CA. Ankle lesions. Acta Orthop Scand. 1975; 46(3):425-445.
4. Wright RW, Barile RJ, Surprenant DA, Matava MJ. Ankle syndesmosis sprains in national hockey league players. Am J Sports Med. 2004; 32(8):1941-1945.
5. Brown KW, Morrison WB, Schweitzer ME, Parellada JA, Nothnagel H. MRI findings associated with distal tibiofibular syndesmosis injury. AJR Am J Roentgenol. 2004; 182(1):131-136.
6. Crim JR. Winter sports injuries. The 2002 Winter Olympics experience and a review of the literature. Magn Reson Imaging Clin N Am. 2003; 11(2):311-321.
7. Weissman JA, Lazis AK. [The radiological features of the distal tibio-fibular syndesmosis (author's transl)]. Rofo. 1980; 133(1):46-51.
8. Lauge-Hansen N. Fractures of the ankle. II. Combined experimental-surgical and experimental-roentgenologic investigations. Arch Surg. 1950; 60(5):957-985.
9. Weber BG. Die Verletzungen des oberen Sprunggelenkes. Zweite, überarbeitete und ergänzte Auflage ed: Hans Huber Bern Stuttgart Wien, 1972.
10. Müller ME, Nazarian S, Koch P, Schatzker J. The comprehensive classification of fractures of long bones. Berlin: Springer-Verlag, 1990.
11. Xu YQ, Zhan BL, He FX, Wei HD. [Surgical treatment of pronation and supination external rotation trimalleolar fractures]. Zhongguo Gu Shang. 2008; 21(4):300-301.
12. Weening B, Bhandari M. Predictors of functional outcome following transsyndesmotic screw fixation of ankle fractures. J Orthop Trauma. 2005; 19(2):102-108.
13. Stark E, Tornetta P, 3rd, Creevy WR. Syndesmotic instability in Weber B ankle fractures: a clinical evaluation. J Orthop Trauma. 2007; 21(9):643-646.
14. Porter DA. Evaluation and treatment of ankle syndesmosis injuries. Instr Course Lect. 2009; 58:575-581.
15. Miller AN, Carroll EA, Parker RJ, Helfet DL, Lorich DG. Posterior malleolar stabilization of syndesmotic injuries is equivalent to screw fixation. Clin Orthop Relat Res. 2009; 468(4):1129-1135.
16. Kukreti S, Faraj A, Miles JN. Does position of syndesmotic screw affect functional and radiological outcome in ankle fractures? Injury. 2005; 36(9):1121-1124.
17. Kennedy JG, Soffe KE, Dalla Vedova P, Stephens MM, O'Brien T, Walsh MG, et al. Evaluation of the syndesmotic screw in low Weber C ankle fractures. J Orthop Trauma. 2000; 14(5):359-366.
18. Kaukonen JP, Lamberg T, Korkala O, Pajarinen J. Fixation of syndesmotic ruptures in 38 patients with a malleolar fracture: a randomized study comparing a metallic and a bioabsorbable screw. J Orthop Trauma. 2005; 19(6):392-395.
19. Hovis WD, Kaiser BW, Watson JT, Bucholz RW. Treatment of syndesmotic disruptions of the ankle with bioabsorbable screw fixation. J Bone Joint Surg Am. 2002; 84-A(1):26-31.
20. Heim D, Schmidlin V, Ziviello O. Do type B malleolar fractures need a positioning screw? Injury. 2002; 33(8):729-734.
21. Hamid N, Loeffler BJ, Braddy W, Kellam JF, Cohen BE, Bosse MJ. Outcome after fixation of ankle fractures with an injury to the syndesmosis: the effect of the syndesmosis screw. J Bone Joint Surg Br. 2009; 91(8):1069-1073.
22. Gardner MJ, Brodsky A, Briggs SM, Nielson JH, Lorich DG. Fixation of posterior malleolar fractures provides greater syndesmotic stability. Clin Orthop Relat Res. 2006; 447:165-171.
23. Donatto KC. Ankle fractures and syndesmosis injuries. Orthop Clin North Am. 2001; 32(1):79-90.
24. Dattani R, Patnaik S, Kantak A, Srikanth B, Selvan TP. Injuries to the tibiofibular syndesmosis. J Bone Joint Surg Br. 2008; 90(4):405-410.
25. Cottom JM, Hyer CF, Philbin TM, Berlet GC. Treatment of syndesmotic disruptions with the Arthrex Tightrope: a report of 25 cases. Foot Ankle Int. 2008; 29(8):773-780.
26. Beumer A, Heijboer RP, Fontijne WP, Swierstra BA. Late reconstruction of the anterior distal tibiofibular syndesmosis: good outcome in 9 patients. Acta Orthop Scand. 2000; 71(5):519-521.
27. Bai XD, Xing GY, Yang CD, Ye QB. Operative treatment for separation of distal tibiofibular syndesmosis. Chin J Traumatol. 2006; 9(3):175-180.
28. Amendola A, Williams G, Foster D. Evidence-based approach to treatment of acute traumatic syndesmosis (high ankle) sprains. Sports Med Arthrosc. 2006; 14(4):232-236.
29. Tejwani NC, McLaurin TM, Walsh M, Bhadsavle S, Koval KJ, Egol KA. Are outcomes of bimalleolar fractures poorer than those of lateral malleolar fractures with medial ligamentous injury? J Bone Joint Surg Am. 2007; 89(7):1438-1441.
30. Bartonicek J. Anatomy of the tibiofibular syndesmosis and its clinical relevance. Surg Radiol Anat. 2003; 25(5-6):379-386.
31. Hocker K, Pachucki A. [The fibular incisure of the tibia. The cross-sectional position of the fibula in distal syndesmosis]. Unfallchirurg. 1989; 92(8):401-406.
32. Kelikian H, Kelikian S. Disorders of the ankle. Philadelphia, London, Toronto: W.B. Saunders Company, 1985.
33. Lanz vT, Wachsmuth W. Praktische Anatomie. zweite neubearbeite Auflage ed. Berlin-Heidelberg-New York: Springer-Verlag, 1972.
34. Kopsch F. Lehrbuch und Atlas der Anatomie des Menschen. 12. ed. Leipzig: Georg Thieme, 1922.

35. Gardner E, Gray DJ, O'Rahilly R. Anatomy: a regional study of human structure. 4th ed. Philadelphia, London, Toronto: W.B. Saunders Company, 1975.
36. Kapandji IA. Funktionelle Anatomie der Gelenke. Schematisierte und kommentierte Zeichnungen zur menslichen Biomechanik: Ferdinand Enke Verlag; 1985:148-165.
37. Lutz W. Zur Struktur der unteren Tibiofibularverbindung und der Membrana interossea cruris. Anat Entwickl Gesch. 1942; 111:315-321.
38. Ashhurst APC, Bromer RS. Classification and mechanism of fractures of the leg bones involving the ankle: based on a study of three hundred cases from Episcopal Hospital. Arch Surg. 1922; 4:51-129.
39. Ebraheim NA, Taser F, Shafiq Q, Yeasting RA. Anatomical evaluation and clinical importance of the tibiofibular syndesmosis ligaments. Surg Radiol Anat. 2006; 28(2):142-149.
40. Bartonicek J. [Syndesmosis tibiofibularis. II. A contribution to clinical anatomy]. Acta Chir Orthop Traumatol Cech. 1982; 49(5):374-381.
41. Thomsen NO, Overgaard S, Olsen LH, Hansen H, Nielsen ST. Observer variation in the radiographic classification of ankle fractures. J Bone Joint Surg Br. 1991; 73(4):676-678.
42. Michelson JD, Magid D, McHale K. Clinical utility of a stability-based ankle fracture classification system. J Orthop Trauma. 2007; 21(5):307-315.
43. Nikolopoulos CE, Tsirikos AI, Sourmelis S, Papachristou G. The accessory anteroinferior tibiofibular ligament as a cause of talar impingement: a cadaveric study. Am J Sports Med. 2004; 32(2):389-395.
44. Boonthathip M, Chen L, Trudell DJ, Resnick DL. Tibiofibular syndesmotic ligaments: MR arthrography in cadavers with anatomic correlation. Radiology. 2010; 254(3):827-836.
45. Link SC, Erickson SJ, Timins ME. MR imaging of the ankle and foot: normal structures and anatomic variants that may simulate disease. AJR Am J Roentgenol. 1993; 161(3):607-612.
46. Lee SH, Jacobson J, Trudell D, Resnick D. Ligaments of the ankle: normal anatomy with MR arthrography. J Comput Assist Tomogr. 1998; 22(5):807-813.
47. Xenos JS, Hopkinson WJ, Mulligan ME, Olson EJ, Popovic NA. The tibiofibular syndesmosis. Evaluation of the ligamentous structures, methods of fixation, and radiographic assessment. J Bone Joint Surg Am. 1995; 77(6):847-856.
48. Akseki D, Pinar H, Yaldiz K, Akseki NG, Arman C. The anterior inferior tibiofibular ligament and talar impingement: a cadaveric study. Knee Surg Sports Traumatol Arthrosc. 2002; 10(5):321-326.
49. Ray RG, Kriz BM. Anterior inferior tibiofibular ligament. Variations and relationship to the talus. J Am Podiatr Med Assoc. 1991; 81(9):479-485.
50. Harper MC, Keller TS. A radiographic evaluation of the tibiofibular syndesmosis. Foot Ankle. 1989; 10(3):156-160.
51. Pettrone FA, Gail M, Pee D, Fitzpatrick T, Van Herpe LB. Quantitative criteria for prediction of the results after displaced fracture of the ankle. J Bone Joint Surg Am. 1983; 65(5):667-677.
52. Beumer A, van Hemert WL, Niesing R, Entius CA, Ginai AZ, Mulder PG, et al. Radiographic measurement of the distal tibiofibular syndesmosis has limited use. Clin Orthop Relat Res. 2004(423):227-234.
53. Krappel F, Schmitz R, Harland U. [Sonographic diagnosis of anterior syndesmosis rupture]. Z Orthop Ihre Grenzgeb. 1997; 135(2):116-119.
54. Milz P, Milz S, Putz R, Reiser M. 13 MHz high-frequency sonography of the lateral ankle joint ligaments and the tibiofibular syndesmosis in anatomic specimens. J Ultrasound Med. 1996; 15(4):277-284.
55. Milz P, Milz S, Steinborn M, Mittlmeier T, Putz R, Reiser M. Lateral ankle ligaments and tibiofibular syndesmosis. 13-MHz high-frequency sonography and MRI compared in 20 patients. Acta Orthop Scand. 1998; 69(1):51-55.
56. Milz P, Milz S, Steinborn M, Mittlmeier T, Reiser M. [13-MHc high frequency ultrasound of the lateral ligaments of the ankle joint and the anterior tibia-fibular ligament. Comparison and results of MRI in 64 patients]. Radiologe. 1999; 39(1):34-40.
57. Ebraheim NA, Lu J, Yang H, Rollins J. The fibular incisure of the tibia on CT scan: a cadaver study. Foot Ankle Int. 1998; 19(5):318-321.
58. Elgafy H, Semaan HB, Blessinger B, Wassef A, Ebraheim NA. Computed tomography of normal distal tibiofibular syndesmosis. Skeletal Radiol. 2010; 39(6):559-564.
59. Taser F, Shafiq Q, Ebraheim NA. Three-dimensional volume rendering of tibiofibular joint space and quantitative analysis of change in volume due to tibiofibular syndesmosis diastases. Skeletal Radiol. 2006; 35(12):935-941.
60. Ebraheim NA, Lu J, Yang H, Mekhail AO, Yeasting RA. Radiographic and CT evaluation of tibiofibular syndesmotic diastasis: a cadaver study. Foot Ankle Int. 1997; 18(11):693-698.
61. Golano P, Mariani PP, Rodriguez-Niedenfuhr M, Mariani PF, Ruano-Gil D. Arthroscopic anatomy of the posterior ankle ligaments. Arthroscopy. 2002; 18(4):353-358.
62. Takao M, Ochi M, Naito K, Iwata A, Kawasaki K, Tobita M, et al. Arthroscopic diagnosis of tibiofibular syndesmosis disruption. Arthroscopy. 2001; 17(8):836-843.
63. Stoller DW. Magnetic Resonance Imaging in Orthopaedics and Sports Medicine. 3rd ed. Philadelphia - Baltimore: Lippincott -Williams- Raven, 2007.
64. Oae K, Takao M, Naito K, Uchio Y, Kono T, Ishida J, et al. Injury of the tibiofibular syndesmosis: value of MR imaging for diagnosis. Radiology. 2003; 227(1):155-161.
65. Cerezal L, Llopis E, Canga A, Rolon A. MR arthrography of the ankle: indications and technique. Radiol Clin North Am. 2008; 46(6):973-994, v.
66. Kim S, Huh YM, Song HT, Lee SA, Lee JW, Lee JE, et al. Chronic tibiofibular syndesmosis injury of ankle: evaluation with contrast-enhanced fat-suppressed 3D fast spoiled gradient-recalled acquisition in the steady state MR imaging. Radiology. 2007; 242(1):225-235.

67. Vogl TJ, Hochmuth K, Diebold T, Lubrich J, Hofmann R, Stockle U, et al. Magnetic resonance imaging in the diagnosis of acute injured distal tibiofibular syndesmosis. Invest Radiol. 1997; 32(7):401-409.
68. Muratli HH, Bicimoglu A, Celebi L, Boyacigil S, Damgaci L, Tabak AY. Magnetic resonance arthrographic evaluation of syndesmotic diastasis in ankle fractures. Arch Orthop Trauma Surg. 2005; 125(4):222-227.
69. Schneck CD, Mesgarzadeh M, Bonakdarpour A, Ross GJ. MR imaging of the most commonly injured ankle ligaments. Part I. Normal anatomy. Radiology. 1992; 184(2):499-506.
70. Muhle C, Frank LR, Rand T, Ahn JM, Yeh LR, Trudell D, et al. Tibiofibular syndesmosis: high-resolution MRI using a local gradient coil. J Comput Assist Tomogr. 1998; 22(6):938-944.
71. Takao M, Ochi M, Oae K, Naito K, Uchio Y. Diagnosis of a tear of the tibiofibular syndesmosis. The role of arthroscopy of the ankle. J Bone Joint Surg Br. 2003; 85(3):324-329.

Chapter 2

Anatomy of the distal tibiofibular syndesmosis in adults: a pictorial essay with a multimodality approach

John J. Hermans
Annechien Beumer
Anton A.W. de Jong
Gert-Jan Kleinrensink

Journal of Anatomy 2010 Dec; 217(6):633-45

Abstract

A syndesmosis is defined as a fibrous joint in which two adjacent bones are linked by a strong membrane or ligaments. This definition also applies for the distal tibiofibular syndesmosis, which is a syndesmotic joint formed by two bones and four ligaments. The distal tibia and fibula form the osseous part of the syndesmosis and are linked by the distal anterior tibiofibular ligament (ATIFL), the distal posterior tibiofibular ligament (PTIFL), the transverse ligament and the interosseous ligament. Although the syndesmosis is a joint, in literature the term syndesmotic injury is used to describe injury of the syndesmotic ligaments.
In an estimated 1-11% of all ankle sprains, injury of the distal tibiofibular syndesmosis occurs. Forty percent of patients do still have complaints of ankle instability six months after an ankle sprain. This could be due to widening of the ankle mortise as a result of increased length of the syndesmotic ligaments after acute ankle sprain. Since widening of the ankle mortise by 1mm decreases the contact area of the tibiotalar joint with 42%, this could lead to instability and hence an early osteoarthritis of the tibiotalar joint.
In fractures of the ankle, syndesmotic injury occurs in about 50% of type Weber B and in all of type Weber C fractures. However, it seems in discussing syndesmotic injury, the exact proximal and distal boundaries of the distal tibiofibular syndesmosis are not well defined. There is no clear statement in the Ashhurst and Bromer etiological, the Lauge-Hansen genetic or the Danis-Weber topographical fracture classification about the extent of the syndesmosis. This joint is also not clearly defined in anatomical textbooks, such as Lanz and Wachsmuth. Kelikian and Kelikian postulate that the distal tibiofibular joint begins at the level of origin of the tibiofibular ligaments from the tibia and ends where these ligaments insert into the fibular malleolus.
As the syndesmosis of the ankle plays an important role in the stability of the talocrural joint, understanding of the exact anatomy of both the osseous and ligamentous structures is essential in interpreting plain radiographs, CT and MR images, in ankle arthroscopy and in therapeutic management.
With this pictorial essay we try to fill the hiatus in anatomic knowledge and provide a detailed anatomic description of the syndesmotic bones with the incisura fibularis, the syndesmotic recess, synovial fold and tibiofibular contact zone and the four syndesmotic ligaments. Each section describes a separate syndesmotic structure, followed by its clinical relevance and discussion of remaining questions.

Introduction

A syndesmosis is defined as a fibrous joint in which two adjacent bones are linked by a strong membrane or ligaments. This definition also applies for the distal tibiofibular syndesmosis, which is a syndesmotic joint formed by two bones and four ligaments. The distal tibia and fibula form the osseous part of the syndesmosis and are linked by the distal anterior tibiofibular ligament (ATIFL), the distal posterior tibiofibular ligament (PTIFL), the transverse ligament and the interosseous ligament. Although the syndesmosis is a joint, in literature the term syndesmotic injury is used to describe injury of the syndesmotic ligaments. To avoid confusion we will do the same.

In an estimated 1-11% of all ankle sprains, injury of the distal tibiofibular syndesmosis occurs[1]. Forty percent of patients do still have complaints of ankle instability six months after an ankle sprain. This could be due to widening of the ankle mortise as a result of increased length of the syndesmotic ligaments after acute ankle sprain. As widening of the ankle mortise by 1mm decreases the contact area of the tibiotalar joint with 42% [2, 3], this could lead to instability and hence an early osteoarthritis of the tibiotalar joint.

Syndesmotic injury can occur after trauma of the ankle, both with or without a fracture of the osseous part. In fractures of the ankle, syndesmotic injury occurs in about 50% of type Weber B and in all of type Weber C fractures, whereas in ankle sprains without fracture syndesmotic injury accounts for 1-11% of all injuries (Hopkinson et al., 1990).

However, in discussing syndesmotic injury it seems the exact proximal and distal boundaries of the distal tibiofibular syndesmosis are not well defined. There is no clear statement in the Ashhurst & Bromer (1922) etiological, Lauge-Hansen (1950) genetic or Weber [4] topographical fracture classifications, concerning the exact extent of the syndesmosis. This joint is also not clearly defined in anatomical textbooks, such as Lanz and Wachsmuth [5]. Kelikian and Kelikian (1985) postulate that the distal tibiofibular joint begins at the level of origin of the tibiofibular ligaments from the tibia and ends where these ligaments insert into the fibular malleolus[6].

As the syndesmosis of the ankle plays an important role in the stability of the talocrural joint, understanding of the exact anatomy of both the osseous and ligamentous structures is essential for interpretation of plain radiographs, CT and MR images, in ankle arthroscopy and in therapeutic management.

With this pictorial essay we try to fill the hiatus in anatomic knowledge and provide a detailed anatomic description of the syndesmotic bones with the incisura fibularis, the syndesmotic recess, synovial fold and tibiofibular contact zone and the four syndesmotic ligaments. Each section below describes a separate syndesmotic structure, followed by its clinical relevance and discussion of remaining questions.

Syndesmotic bones and incisura fibularis

Anatomy

At the apex of the syndesmosis, the crista interossea tibiae, i.e. the lateral ridge of the tibia, bifurcates caudally into an anterior and posterior margin (Fig. 1, *see next page*). The anterior margin ends in the anterolateral aspect of the tibial plafond called the anterior tubercle (Chaput's tubercle). The posterior margin ends in the posterolateral aspect of the tibial plafond called the posterior tubercle. The anterior and posterior margin of the distal tibia enclose a concave triangle, with its apex 6-8cm above the level of the talocrural joint [6]. The base of the triangle is formed by the anterior and posterior tubercle of the tibia with the incisura tibialis in between. The anterior tubercle is more prominent than the posterior tubercle and protrudes further laterally and overlaps the medial two thirds of the supramalleolar shaft of the fibula [6].

The fibular part of the syndesmosis is congruent with its tibial counterpart. The crista interossea fibularis, i.e. the ridge on the medial aspect of the fibula, also bifurcates into an anterior and posterior margin and forms a convex triangle that is located above the articular facet on the lateral malleolus. The base of the fibular triangle is formed by the anterior tubercle (Wagstaffe-Le Fort tubercle) and the, almost negligible, posterior tubercle. The apex of the fibular triangle and the apex of the tibial triangle are situated at the same level. The convex shape of the distal fibula matches the concave incisura tibialis.

The incisura tibialis is also known under a variety of other names: the incisura fibulae, fibular incisure of the tibia, incisural notch, fibular notch of the tibia, peroneal groove of the tibia and syndesmotic notch. According to international terminology (Terminologia anatomica) its official name is incisura fibularis tibiae. Whenever the incisura tibialis is flattened, i.e. less concave, the distal fibula accordingly becomes less convex. The depth of the incisura tibialis increases from proximal to distal and its shape varies from concave (60-75%) to shallow (25-40%) giving the syndesmosis a rectangular shape with irregular forms [7, 8]. Its depth varies from 1.0 to 7.5 mm [9, 10] and is a little less in women than in men [11].

Clinical relevance

The size and shape of the incisura tibialis play an important role in ankle injury. The anterior tibial tubercle is larger than the posterior tubercle and prevents forward slipping of the distal fibula, while the diminutive posterior tubercle allows backward dislocation of the distal fibula. In fibula fractures caused by external rotation, the posterior tubercle functions as a fulcrum and the distal fibula spins around its longitudinal axis in a lateral direction [6]. A shallow incisura tibialis may predispose to recurrent ankle sprains [12] or syndesmotic injury with fracture-dislocation [13]. After an acute ankle fracture, good repositioning of the fibula is necessary to create a good alignment and rotation of the fibula in the incisura tibialis, in order to maintain a good position of the talus in the tibiofibular joint or ankle mortise. When the talus moves 1 mm laterally, the contact area of the tibiotalar articulation decreases by 42% [3]. This could lead to early osteoarthritis of the tibiotalar joint.

It is difficult to determine the correct alignment of the fibula on a plain X-ray of the ankle. Several measurements have been introduced to assess the integrity of the syndesmosis and stability of the ankle on X-rays, such as the tibiofibular overlap (TFO) [14, 15], the tibiofibular clear space (TFCS) [15-17] and the ratio between the medial and superior clear space (MCS/SCS) [18]. However, compared with MRI, CT and peroperative findings, these measurements are not very accurate [19, 20]. Therefore in patients with suspected instability of

the distal tibiotalar joint a CT or MRI should be performed to evaluate more accurately the position of the fibula in the incisura tibialis [21].

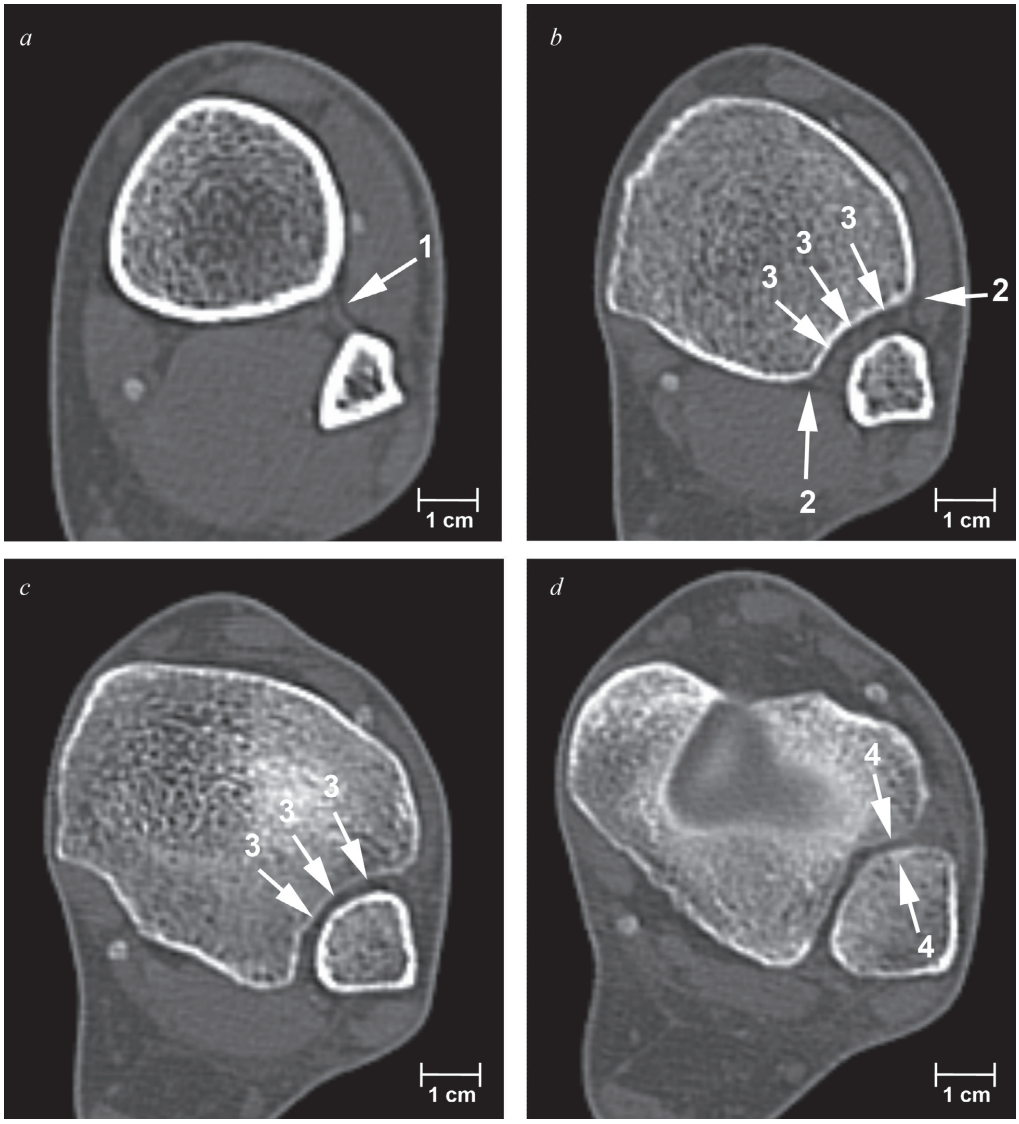

Fig. 1. Axial CT images at the level of the distal tibiofibular joint from (*a*) proximal to (*d*) distal (male, 53 years). The interosseous membrane (1) is visible between the tibial and fibular crest (*a*). A little lower, the tibial crest forms an anterior and posterior margin (2). The lateral aspect of the distal fibula is convex and fits into the concave tibial incisure. The fascicles of the interosseous ligament bridge the fibular incisure and run obliquely upward from the fibula towards the tibia. In the axial plane, the obliquely running fibres are depicted as small dots (3). The interosseous ligament extends till 1cm above the tibiotalar joint. In (*c*) the full length and maximal depth of the incisure are visible. At the level of the tibiotalar joint the anterior aspect of the fibular incisure flattens again to form the contact area with the fibula (4), which is also flat at its antero-medial border.

Tibiofibular contact zone

Anatomy

At the base of the syndesmosis there is a small area where the tibia and fibula are in direct contact. This area is called the tibiofibular contact zone. Its facets are covered with a small strip of hyaline cartilage with a thickness of about 0.5–1.0 mm [5, 6, 22, 35]. (Fig. 2 and Fig. 3, *on next page*). The tibial cartilage rim is a continuation of the cartilage covering the tibial plafond and is 3–9 mm in length and about 2–5 mm in height. The rim of fibular cartilage is continuous with the articular facet of the fibular malleolus.

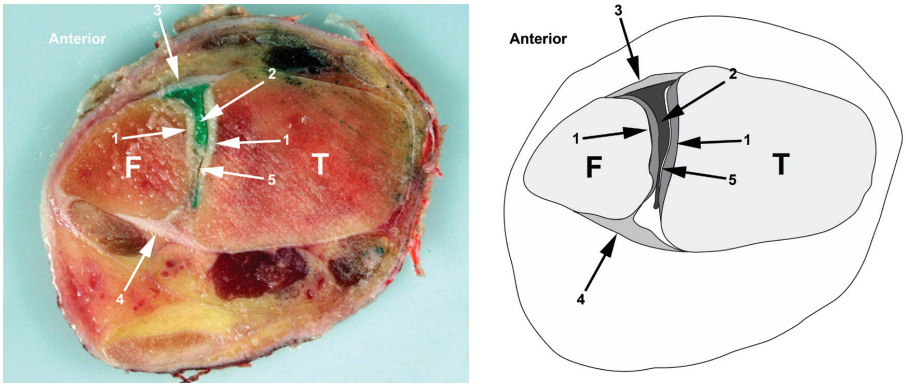

Fig. 2. A 45° oblique slice through the right distal tibiofibular syndesmosis of a fresh frozen anatomic specimen (male, 85 years). A thin layer of cartilage (1) covers the lateral tibia and the medial fibula at the level of the tibiofibular contact zone. In between is the syndesmotic recess, which is filled with intra-articularly injected green coloured resin (2) and abuts the posterior margin of the ATIFL (3). In the middle of the recess and just anterior to the PTIFL (4), some fibres of the interosseous ligament (5) are visible. F, fibula; T, tibia.

Clinical relevance

There is little information about the variation in size and presence of the cartilage-covered tibiofibular contact area and little is known about its function. The contact zone is not always present [22].

The minimal size of the cartilaginous facets could be explained by the fact that the main forces acting on the distal tibiofibular articulation are strain forces [23]. The two bones can come into direct contact in maximal plantar flexion when the fibula rotates internally and shifts anteriorly.

Although this articulation can be seen as only a minor joint concerning the size of its cartilage surface, this bony connection can play an important role in the detection of malalignment of the malleolar mortise in ankle fractures or in anatomically based reconstructive surgery of the anterior syndesmosis. In this respect a detailed knowledge of the three dimensional situation after fracture of this joint is of great importance. The articular facets might help as landmarks for accurate repositioning of the lateral malleolus in the incisura fibularis [22].

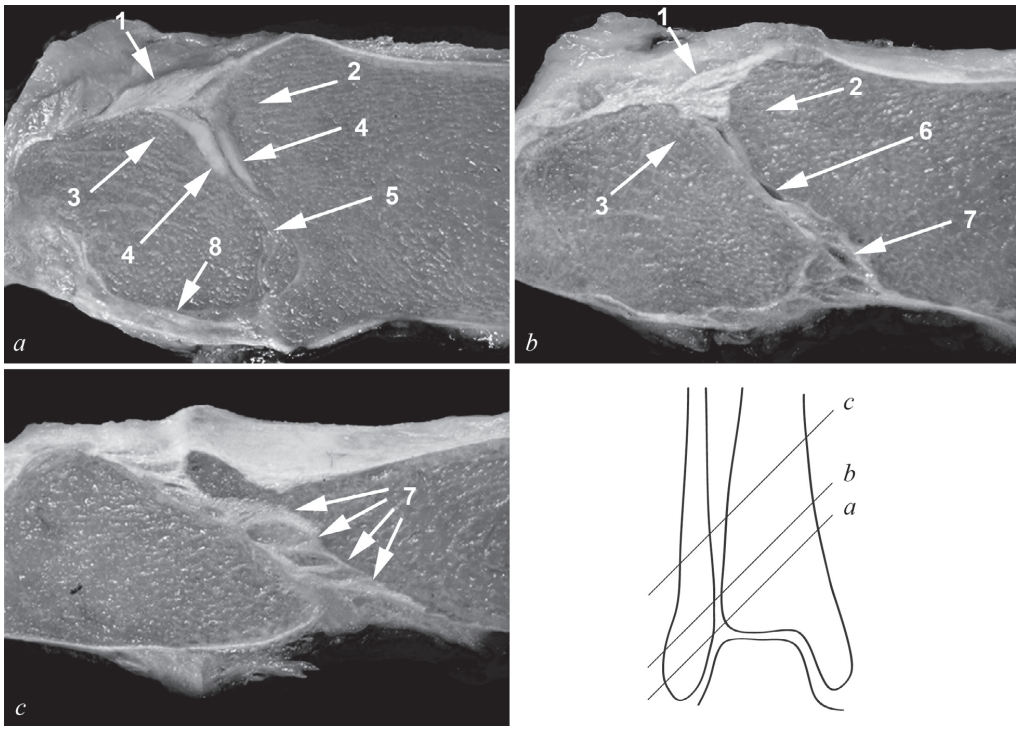

Fig. 3. A 45° oblique slice through the distal tibiofibular joint of a fresh frozen specimen (male, 86 years). The ATIFL has a triangular aspect and consists of multiple tight fibres interspersed with some fat (1). The fibres start at the broad-based anterior tibial tubercle (Chaput) (2) and converge towards the fibular tubercle (Wagstaffe - Le Fort) (3). Just behind the ATIFL is the small cartilage-covered tibiofibular contact zone (4), which abuts the fat pad (5) of the synovial recess (6). The posterior fibres of the interosseous ligament (7) gradually coalesce with the PTIFL (8). In (*c*) the network of thin fibro-fatty fibres forming the interosseous ligament is visible. The schematic drawing shows the level of oblique dissection.

Syndesmotic recess (Recessus tibiofibularis)

Anatomy

A syndesmotic recess is nearly always present between the distal tibia and fibula [5, 33] (Fig. 4, 5). This synovial lined plica extends from the tibiotalar joint and varies in size. Cranially, it is bordered by the distal aspect of the interosseous ligament. Medially, the plica is directly attached to the distal tibia with a small amount of connective tissue. Laterally, a fat containing synovial fold is interposed between the synovial lining and the fibula, which contains loose connective tissue with an abundance of vessels and occasionally some small nerves [22, 24] (Fig. 6, 7, *see next pages*). The synovial recess is attached to the fibula just proximal to the most superior border of the lateral malleolar articular surface and extends posteriorly with diffuse attachment to the entire posterior margin of the transverse ligament [32, 33] (Fig. 8, *see next pages*).

The antero-posterior borders of the syndesmotic recess are variable and depend on the presence of a tibiofibular contact area anteriorly and a synovial fold or fat pad posteriorly. Regarding the anterior border, the plica extends to the posterior aspect of the ATIFL when the tibiofibular contact area is absent (Fig. 9, *on next pages*). Posteriorly, when the fat pad is small or absent, the plica borders on the anterior lining of the PTIFL (Fig. 10, *on next pages*). Its

antero-posterior length varies from 10 to 15 mm [22].The width of the syndesmotic recess is 2 mm and its height varies from 4 to 25 mm [6, 22, 24-28].

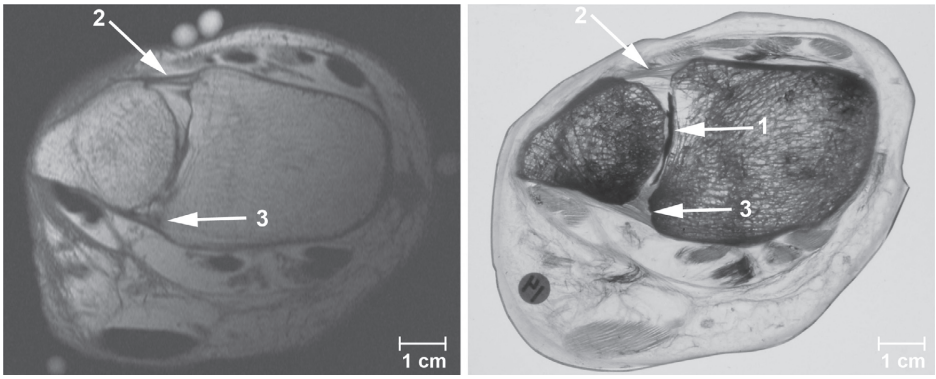

Fig. 4. Correlation between MR image (*left*) and plastinated slice (*right*) at the same level through the tibiofibular syndesmosis (female, 84 years).The intra-articularly injected green dye is visible in the tibiofibular recess (1), which extends between the anterior (2) and posterior (3) tibiofibular ligament.As the MR image is obtained without intra-articular contrast, the recess is not visible here.The incisura fibularis is shallow with an irregular contour.

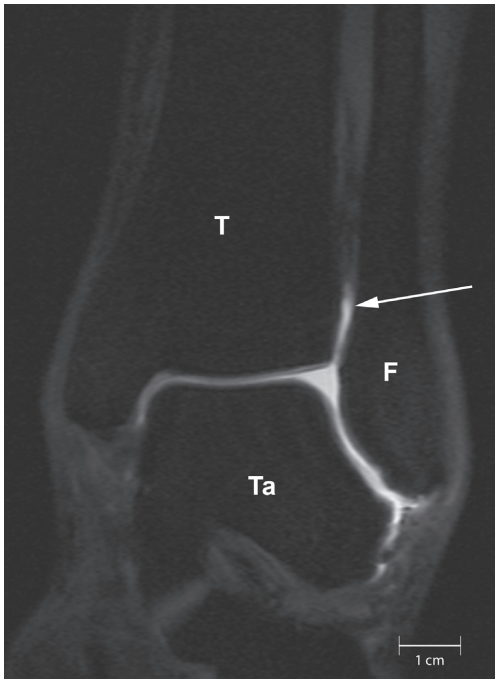

Fig. 5. MR-arthrography of the tibiotalar joint with a coronal view of the syndesmotic recess (female, 43 years).This recess is visible as a vertical, contrast-filled pouch between the distal part of the tibia and fibula (arrow). F, fibula;T, tibia;Ta, talus.

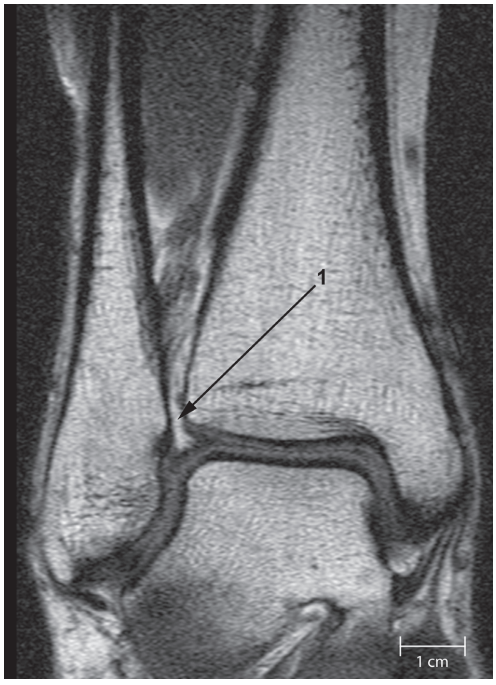

Fig. 6. Coronal proton-density-weighted MR image (female, 23 years).The fat-containing synovial fold (1) protrudes from the incisura fibularis into the lateral superior tibiotalar joint space. During dorsal flexion of the foot, the talus pushes the tibia and fibula outwards, therewith increasing the space of the tibial incisure. This leads to retraction of the fatpad, as can be seen during arthroscopy.

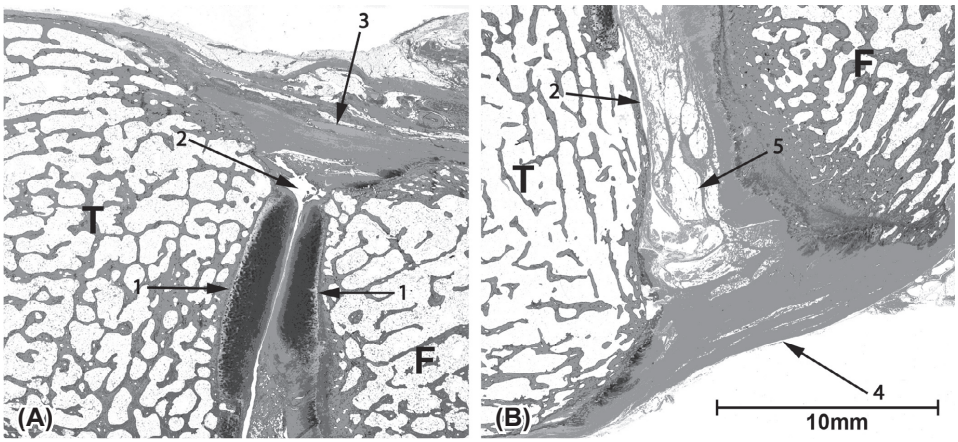

Fig. 7. Microscopy (haematoxylin-azophloxin; female, 89 years). Oblique slice at the level of the anterior (*A*) and posterior (*B*) distal tibiofibular syndesmosis.The tibial and fibular facets of the tibiofibular contact zone are covered with a thin layer of cartilage (1).The small recess (2) between the two facets extends anteriorly to the posterior aspect of the ATIFL (3), and posteriorly almost to the anterior aspect of the PTIFL (4).The synovial fold (5), consisting of fat and loose connective tissue, is attached to the fibula and is continuous with the anterior aspect of the PTIFL.The synovial recess (2) is covered by a single cell layer of synoviocytes and is directly attached to the tibia. F, fibula;T,tibia.

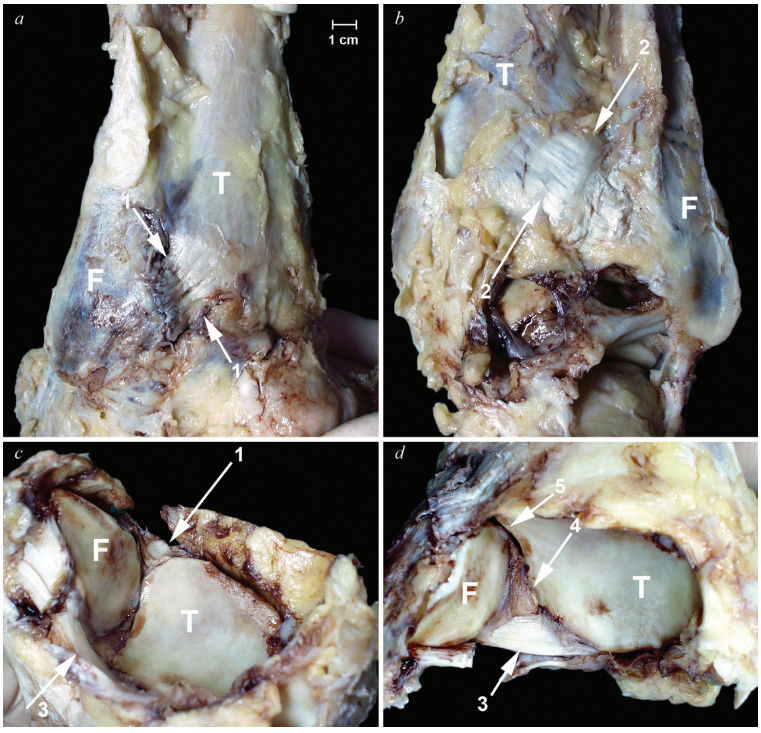

Fig. 8. Exposure of syndesmotic ligaments in a dissected right ankle (male, 92 years). (*a*) The trapezoid multifascicular anterior tibiofibular ligament (ATIFL) (1) runs obliquely upwards from the anterior fibular tubercle towards the anterior tibial tubercle. (*b*) The band-like posterior tibiofibular ligament (PTIFL) (2) runs obliquely upwards from the posterior fibular tubercle towards the posterior tibial tubercle. (*c*) View from below after removal of the talus shows the curved and horizontally running transverse ligament (3) and the inferior margin of the ATIFL. In (*d*) fat (4) from the synovial fold is visible in the tibial incisure between the transverse ligament and the small contact area between the tibia and fibula (5). F, fibula; T , tibia.

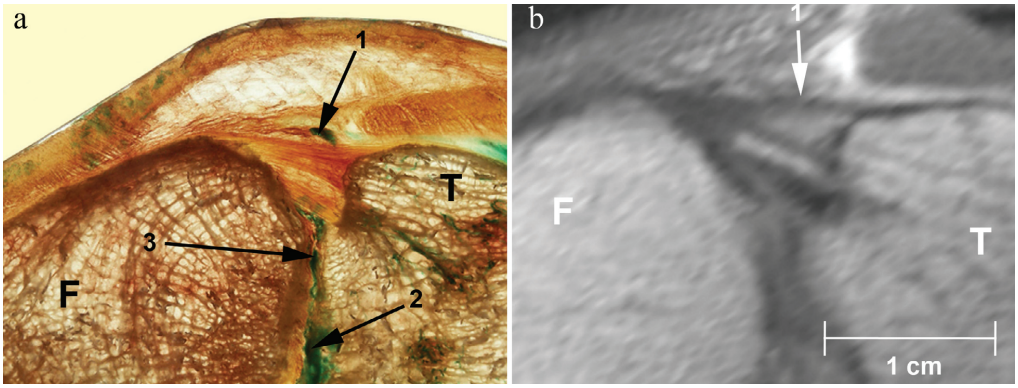

Fig. 9. Correlation between detailed view of ATIFL (1) in a 45° oblique plastinated slice (*a*) and an MR image (*b*) taken at exactly the same level (male, 71 years). Green coloured resin is visible in the syndesmotic recess (2) which abuts the posterior margin of the multifascicular ATIFL (1). There is a small tibiofibular contact zone devoid of cartilage just posteriorly of the ATIFL (3). F, fibula; T, tibia.

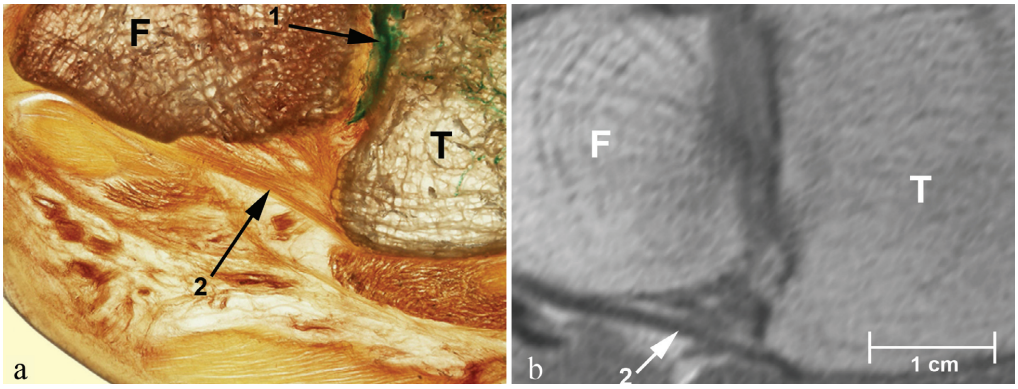

Fig. 10. Correlation between detailed view of PTIFL in a 45° oblique plastinated slice (*a*) and an MR image (*b*) taken at exactly the same level (male, 71 years). Green coloured resin is visible in the syndesmotic recess (1) which abuts the anterior margin of the multifascicular PTIFL (2). F, fibula; T, tibia.

Clinical relevance

In acute injury to the syndesmosis, i.e. injury mostly to the ATIFL, the syndesmotic recess can tear. In the acute setting, arthrography of the tibiotalar joint would demonstrate leakage of contrast fluid into the incisura tibialis or, depending on the extent of injury, into the interosseous ligament between the tibia and fibula, or even outside the borders of the ATIFL and PTIFL [29, 30].

The syndesmotic recess runs the risk of being traversed during the insertion of fine wires when using external fixators for the treatment of fractures or placement of a set screw. To minimize the risk of septic arthritis of the ankle due to pin tract infections, it is best to avoid areas of capsular extensions [31].

In chronic injury of the syndesmosis, the synovial lining may become irregular due to inflammation. Kim et al. (2007) speculated that in contrast enhanced MRI, an abnormal upward extension of enhancing tissue surrounding the syndesmotic recess could be an ancillary sign of syndesmotic instability caused by syndesmotic disruption[24].

In inflammation of the syndesmosis, such as rheumatoid arthritis, scalloping of the medial border of the distal fibula can occur due to chronic erosion, secondary to hyperplastic synovial villi and invasive pannus in a 'bare area" devoid of articular cartilage. The scalloped defects measured 7–23 mm in length [32].
With dorsiflexion the synovial fold retracts between the tibia and fibula, and is pushed downward during plantar flexion of the foot. This movement of the fatpad can be easily seen during ankle arthroscopy. In healthy volunteers the height of the fat pad protruding from the incisura tibialis into the tibiotalar joint varied from 0 to 7 mm (Hermans JJ, Beumer A, Kleinrensink GJ, unpublished MRI data). The synovial fold or fat pad is therefore a normal finding and should not be mistaken for synovial thickening. Both its gross appearance and histologic structure may indicate that this fold functions like a meniscus and is needed for stability and proper function [33].

The Syndesmotic ligaments

Anterior tibiofibular ligament (Ligamentum tibiofibulare anterius)
Anatomy
About 20% of the distal anterior tibiofibular ligament (ATIFL) is intra-articular [34]. The ATIFL extends in an oblique way from the anterior tubercle of the distal tibia, on average 5 mm above the articular surface, to the anterior tubercle of the distal fibula, running from proximal-medial to distal-lateral and crossing the antero-lateral corner of the talus (Fig. 8, *see previous pages*). The angle formed by a line along the tibial plafond in the coronal view and a line along the ATIFL varies between 30 to 50º [9, 22, 35, 36]. Posteriorly, it forms an angle of 65º with the sagittal plane [35]. The ATIFL has a multifascicular aspect, caused by fatty tissue interposed between the multiple collagen bundles (Fig. 3, 4, 9, *see previous pages*). Viewed in a coronal plane, it is composed of three bundles, separated by 2-mm-wide gaps that converge slightly in the latero-distal direction and consequently give the ATIFL a trapezoid shape [22, 35].
The upper part is the shortest (6.0–8.9 mm), with a width of 4.0–4.9 mm and thickness of 1.8–3.0 mm. It originates just above the anterior tubercle of the tibia and is attached just above the anterior tubercle of the fibula. Sometimes it is divided into two stronger fascicles. The middle, and strongest, part runs between the anterior tubercle of the tibia and fibula. It measures about 12.0–15.5 mm in length, 8.3–10.0 mm in width and of 2.6–4.0 mm in thickness. It is sometimes divided into three or four smaller ligaments. The lower part, which is the longest, extends just below the anterior tubercles and measures 17.0–20.6 mm in length, 3.8–4.0 mm in width and 2.0–2.2 mm in thickness.
An accessory antero-inferior tibiofibular ligament, also called Bassett´s ligament, which runs inferior and parallel to the ATIFL, is described in literature. This accessory ligament, not demonstrated in this pictorial essay, can be identified in 21–92% of dissected ankles of human anatomic specimen or MRI studies [37-43]. The fibular attachment of Bassett's ligament is distal-medial to the ATIFL and its fibres blend with the tibial attachment of the distal fibres of the ATIFL. The ligament is 17–22 mm in length, 1–2 mm in thickness, and 3–5 mm in width [37, 39]. It is not covered by synovial tissue, is intra-articular and crosses the proximo-lateral margin of the ankle and comes into contact with the lateral talar trochlea during dorsiflexion.

Clinical relevance

Bartonicek (2003) described a meniscoid structure just behind the ATIFL[22]. It is possible that he in fact thereby encountered one of the shorter deep fibres of the ATIFL. On axial MRI the ATIFL is triangular-shaped and shows more than one fascicle. Nikolopoulos (2004) demonstrated that in five ankles the ATIFL appeared to consist of two layers, one deep and one superficial, which were separated by a thin fibrofatty septum[39]. Brostroem (1964) mentioned that the superficial anterior fibres are 2-3 cm long and the deeper posterior fibres somewhat shorter[44]. As 20% of the ATIFL lies intra-articularly, the most inferior and deepest fibres are easily seen with arthroscopy and should not be interpreted as a meniscus or scar tissue.

It is easier to get a good depiction of the transverse cross-sectional area of the ATIFL with MRI than with gross macroscopy. Although the ATIFL is described as a flat band on dissection [45], on a transverse cross section with MRI or plastination it looks more triangular [46]. In our experience we have never seen a separate superficial and deep layer of the ATIFL. In both the coronal, axial and oblique MR images the ATIFL consists of a variable number of contiguous fibrous fibres separated by fat, which could give the impression of a multilayered structure. The number of fascicles can vary from a few thick fibres to up to seven thin fibres.

The ATIFL is the weakest of the four syndesmotic ligaments and is the first to yield to forces that create an external rotation of the fibula around its longitudinal axis [6].

It is important to distinguish the accessory ligament from the ATIFL because it can potentially cause anterolateral ankle impingement and pain in the presence of a normal ATIFL due to synovitis and scarring in the anterolateral groove and cartilage abnormalities in the anterolateral talar dome [37]. Resection of the accessory ligament does not lead to instability and relieves pain in patients with chronic ankle complaints after ankle sprain [41].

In patients with chronic instability of the syndesmosis, an anatomical reconstruction of the anterior syndesmosis can be considered. The widened syndesmosis can be reduced, followed by medial reinsertion of a bone block with the tibial insertion of the intact but elongated ATIFL [47].

As the ATIFL is located superficially, just beneath the skin, it can be well visualized with ultrasound. With high frequency US (15MHz), injuries of the ATIFL can be detected with an accuracy of 85% [48]. As the ATIFL runs obliquely, MR images in an axial plane could lead to depiction of a partly interrupted ligament, leading to a false positive diagnosis of a ruptured ligament. Using an additional oblique image plane of about 45 degrees reduces this problem [49].

Posterior tibiofibular ligament (Ligamentum tibiofibulare posterius)

Anatomy

The PTIFL is a strong ligament that extends from the posterior tibial malleolus to the posterior tubercle of the fibula and runs from proximal-medial to distal-lateral (Fig. 8, *see previous pages*). It forms a 20–40º angle with the horizontal plane and a 60–85º angle with the sagittal plane [9, 35]. Its lower part, or transverse ligament, runs more horizontally than the PTIFL [22]. The PTIFL has a similar shape and structure as the ATIFL. It is triangular with a broad base at the tibial insertion. Its fascicles more or less converge to the posteromedial aspect of the fibula (Fig. 4, 10, *see previous pages*). Therefore the length of the proximal fibres is shorter than the distal fibres; respectively 9.7 ± 6.9 mm (3.4–21.2 mm) and 21.8 ± 7.5 mm (6.4–32.5 mm). The mean width of the ligament is 17.4 ± 3.5 mm (11.1–21.5 mm), with a tibial insertion thickness of 6.4 ± 1.9 mm (4.4–9.0 mm) and fibular insertion thickness of 9.7 ± 1.7 mm (8.0–11.4 mm) [35, 39]. The PTIFL, like the ATIFL, is multifascicular and consists of multiple collagen bundles interspersed with fat. Its most distal fibres are in close contact

with the transverse ligament and some fibres from the fibular insertion sometimes even appear to be continuous with it [35].

Clinical relevance
According to the fracture classification of Lauge-Hansen, rupture of the posterior syndesmosis, i.e. the PTIFL or avulsion fracture of the PTIFL, can occur in supination-eversion, pronation-eversion or pronation-abduction injury of the ankle. As the PTIFL is a thick and strong ligament, excessive stress results more often in a posterior malleolus avulsion fracture than in a rupture of the ligament [50]. With direct reduction of the posterior malleolus avulsion fracture, the syndesmosis can be stabilized. However, this is only feasible when the PTIFL is intact [19].

Transverse ligament (Ligamentum tibiofibulare transversum)
Anatomy
The transverse ligament runs horizontally between the proximal margin of the fibular malleolar fossa and the dorso-distal rim of the tibia and may extend as far as the dorsal aspect of the medial malleolus (Fig. 11, 12, *see next pages*). Its length varies from 22 to 43 mm [35, 39]. It is a thick, round ligament that deepens the posteroinferior rim of the tibia and forms a labrum analogue (Fig. 8, *see previous pages* and Fig. 13, *see next pages*). Some fibres of the posterior talofibular ligament coalesce with the most distal fibres of the transverse ligament and form the so called tibial slip, or intermalleolar ligament (IML) (Fig. 14, *see next pages*). According to Oh et al. (2006) the intermalleolar ligament is a separate anatomic entity and almost invariably present in 81.8% of 77 specimens [51, 52]. The IML arises slightly proximal to the origin of the posterior talofibular ligament in the malleolar fossa and distal to the origin of the transverse ligament [53]. Its shape varies from a thick string to a band, with a length of 39.2 mm (28.2–44.9 mm), a width of 3.7 mm (0.8–8.8 mm), and a thickness of 2.8 mm (0.4–5.8 mm), and occasionally extends into the joint. The medial insertion sometimes consists of two or three slips. The medial arising sites of the IML include both the medial and lateral border of the medial malleolar sulcus, through the septum between the M. flexor digitorum longus and M. tibialis posterior, or the medial part of the posterior margin of the tibia [52]. The IML runs parallel to the transverse ligament, from which it is always separated by a triangular or quadrilateral-shaped soft tissue space. During plantar flexion the IML becomes less taut and approximates the transverse ligament [51].

Clinical relevance
In the literature there is controversy whether the transverse ligament and distal posterior tibiofibular ligament form one anatomic unit or are two distinct structures. Golano et al. (2002) stated that the transverse ligament is the deep part of the posterior tibiofibular ligament[51], whereas Lee et al. (1998) demonstrated that MR arthrography allowed resolution of the superficial and deep component of the posterior tibiofibular ligament[54].
Even more controversy exists about the tibial slip and intermalleolar ligament. Bartonicek (2003) considered the tibial slip as a reinforced strip of the joint capsule[22], whereas others showed that the intermalleolar ligament is a separate anatomic structure with diverse morphologic features [51, 52]. The observed frequency of the IML varies from 19% in MRI of the ankle to 82% in dissected anatomical specimens [51-53, 55]. This difference could be due to difference in used techniques, like MRI, dissection, cryosection or arthroscopy, the number of patients or specimens used or the position of the foot during investigation.

The space between the transverse ligament and IML makes the posterolateral approach in ankle arthroscopy most suitable for avoiding ligamentous structures. During anterior ankle arthroscopy with standard antero-medial or antero-lateral ports, the transverse and intermalleolar ligament are visible but not the posterior tibiofibular ligament. To visualize the PTIFL, posterior arthroscopy or endoscopy is necessary. The intermalleolar ligament can be the cause of the posterior impingement syndrome in ballet dancers, where in extreme plantar flexion, entrapment or even a bucket handle tear of the ligament can occur [52, 53].

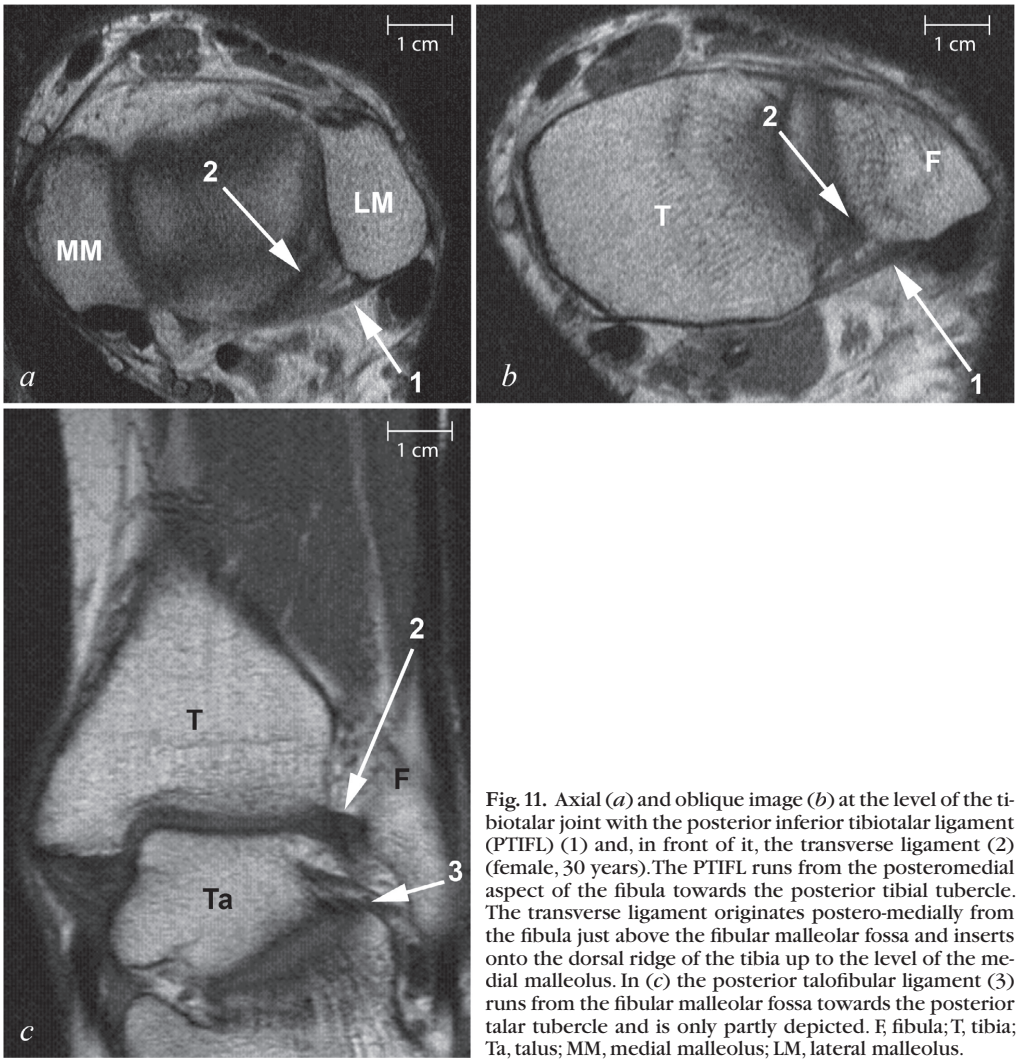

Fig. 11. Axial (*a*) and oblique image (*b*) at the level of the tibiotalar joint with the posterior inferior tibiotalar ligament (PTIFL) (1) and, in front of it, the transverse ligament (2) (female, 30 years). The PTIFL runs from the posteromedial aspect of the fibula towards the posterior tibial tubercle. The transverse ligament originates postero-medially from the fibula just above the fibular malleolar fossa and inserts onto the dorsal ridge of the tibia up to the level of the medial malleolus. In (*c*) the posterior talofibular ligament (3) runs from the fibular malleolar fossa towards the posterior talar tubercle and is only partly depicted. F, fibula; T, tibia; Ta, talus; MM, medial malleolus; LM, lateral malleolus.

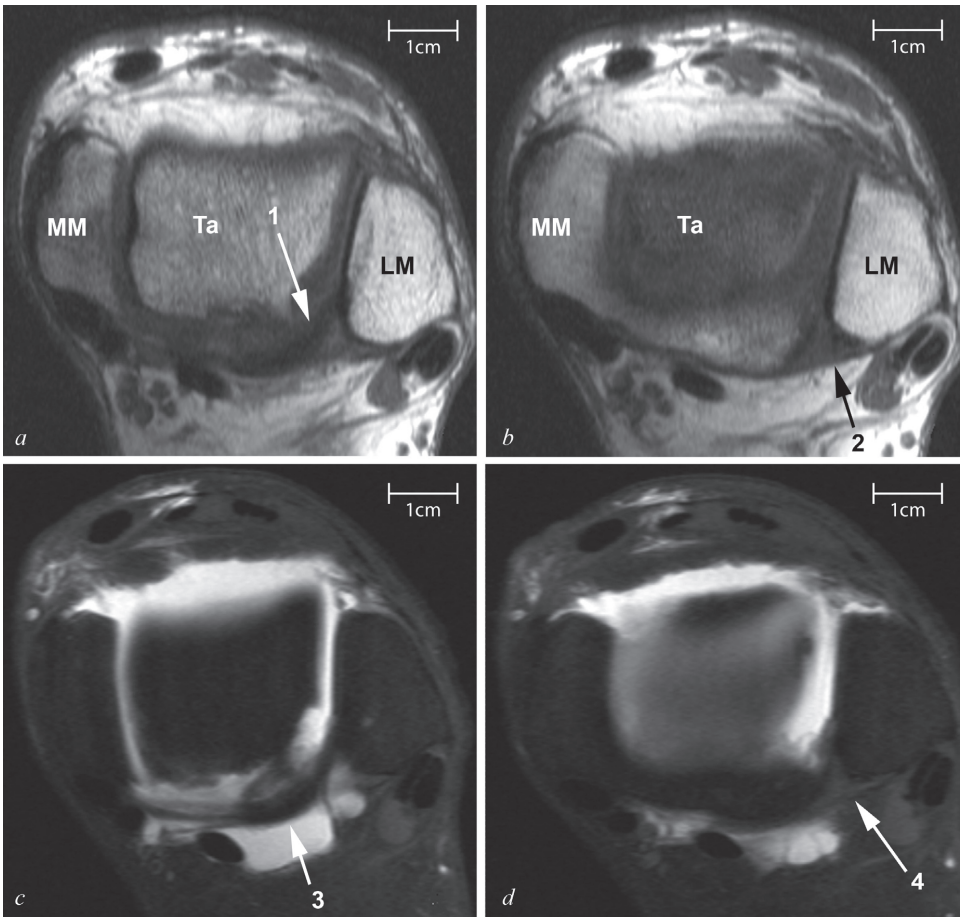

Fig. 12. Axial proton-density-weighted MR images (*a, b*) and axial T1-weighted MR images with fat suppression with intra-articular contrast (*c, d*) at the level of the tibiotalar joint, in the same patient (female, 47 years). The transverse ligament (1) originates postero-medially from the fibula, just above the fibular fossa, and inserts on the dorsal ridge of the tibia. It forms a labrum-like structure to keep the talus from moving posteriorly (*a*). The posterior tibiofibular ligament (PTIFL) (2) is visible 5 mm above this level, which originates from the postero-medial corner of the fibular malleolus and inserts on the posterior tibial tubercle (*b*). The transverse ligament (3), extends like a thick band along the entire border of the posterior tibial ridge, where it serves as a labrum for the talus (*c*). The PTIFL (4) is short and triangular-shaped and bridges the fibula and tibia posteriorly (*d*). MM, medial malleolus; LM, lateral malleolus; Ta, talus.

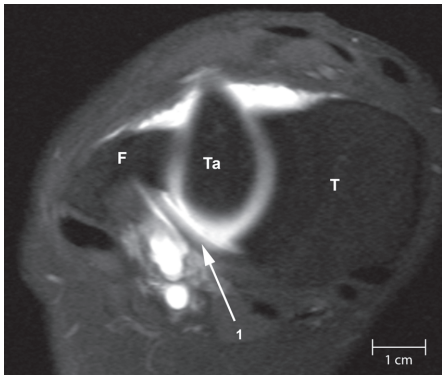

Fig. 13. MR arthrogram with an oblique image at the level of the tibiotalar joint shows the curved transverse ligament (1) running from the posteromedial aspect of the fibula to the posterior inferior rim of the tibia (female, 16 years). F, fibula; T, tibia; Ta, talus.

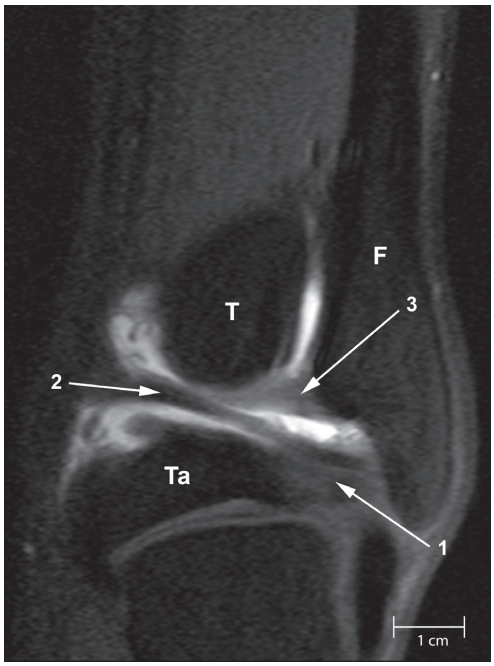

Fig. 14. MR-arthrogram: coronal T1-weighted image with fat suppression and with intra-articular contrast in the tibiotalar joint (male, 23 years). The fibula (F), the posterior malleolus of the tibia (T) and the posterior body of the talus (Ta) are visible. The posterior talofibular ligament (TFP) (1) runs more or less horizontally from the fibular fossa to the posterior process of the talus. Just above the origin of the TFP in the fibular fossa, the intermalleolar ligament originates (2), extending medially and fusing with the transverse ligament (3) at the medial aspect of the posterior ridge of the distal tibia. The transverse ligament runs between the posteromedial fibula, just above the fibular fossa, and the posterior ridge of the distal tibia. F, fibula; T, tibia; Ta, talus.

Interosseous ligament (Ligamenta tibiofibularia)

Anatomy

The interosseous membrane (Membrana interossea cruris) extends between the tibia and fibula, and at its lowermost end thickens and gives rise to a spatial network of pyramidal shape. This network is filled with fatty tissue and steep running fascicles and forms the interosseous ligament (Fig. 1, 2, 4, *see previous pages*). Most fibres run in a latero-distal and anterior direction from the tibia to the fibula, although some fibres on the anterior aspect run in the reverse direction. The most distal fibres attach to the tibia at the anterior tubercle level and descend straight to the fibula, where they attach just above the level of the talocrural joint. The most proximal fibres attach to the tibia at the apex of the incisura tibialis [22, 35]. The length of fibres gradually increases from proximal to distal, with a proximal length of 6.6 ± 1.3 mm (5.8–7.6 mm) and distal length of 10.4 ± 3.1 mm (8.2–12.6 mm). The thickness of the interosseous ligament is 4.7 ± 1.1 mm (3.8–5.3 mm), its width at the fibular attachment 21.2 ± 1.7 mm (20.0–22.5 mm) and its width at the tibial attachment 17.7 ± 1.0 mm (17.1–18.5 mm). The measurements of Nikolopoulos et. al. (2004) differ a little from these values (length 3–6 mm, thickness 2–4 mm and width 2–4 mm)[39]. However the trend of these data is the same. The presence of the interosseous ligament is variable. In some individuals it is absent, whereas in others it is rather markedly present, especially in those with a flattened incisura of the tibia and fibula. The area underneath the interosseous ligament is generally filled with the synovial plica from the tibiotalar joint [22, 35].

Clinical relevance

Not only is there a gradual transition of the interosseous membrane into the interosseous ligament [25], but there also appears to be a continuous transition between the interosseous tibiofibular ligament and the ATIFL and PTIFL. However, Bartonicek (2003) describes that on a sagittal section the ATIFL is sharply separated from the anterior surface of the interosseous ligament by a narrow gap[22].

The interosseous ligament is thought to act as a ´spring´, allowing for slight separation between the medial and lateral malleolus during dorsiflexion at the talocrural joint, and thus for some wedging of the talus in the mortise. This is also reflected in the change of shape, reflecting the tension in the ATIFL and PTIFL, as can be observed with ultrasound during plantar- and dorsiflexion of the foot (Fig. 15).

The interosseous ligament not only functions as a buffer, neutralizing forces during for instance the 'heel strike' phase in walking, but also has a function in stabilizing the talocrural joint during loading [7, 9, 56]. Haraguchi et al. (2009) described that the distal tibiofibular ligaments and interosseous membrane were loaded throughout the stance phase, which provides a theoretical basis for evidence of syndesmosis screw breakage or loosening[57]. In anatomical specimens the relative importance of the individual syndesmotic ligaments to syndesmotic stability was found to be 35% for ATIFL, 33% for the transverse ligament, 22% for the interosseous ligament and 9% for the PTIFL [58].

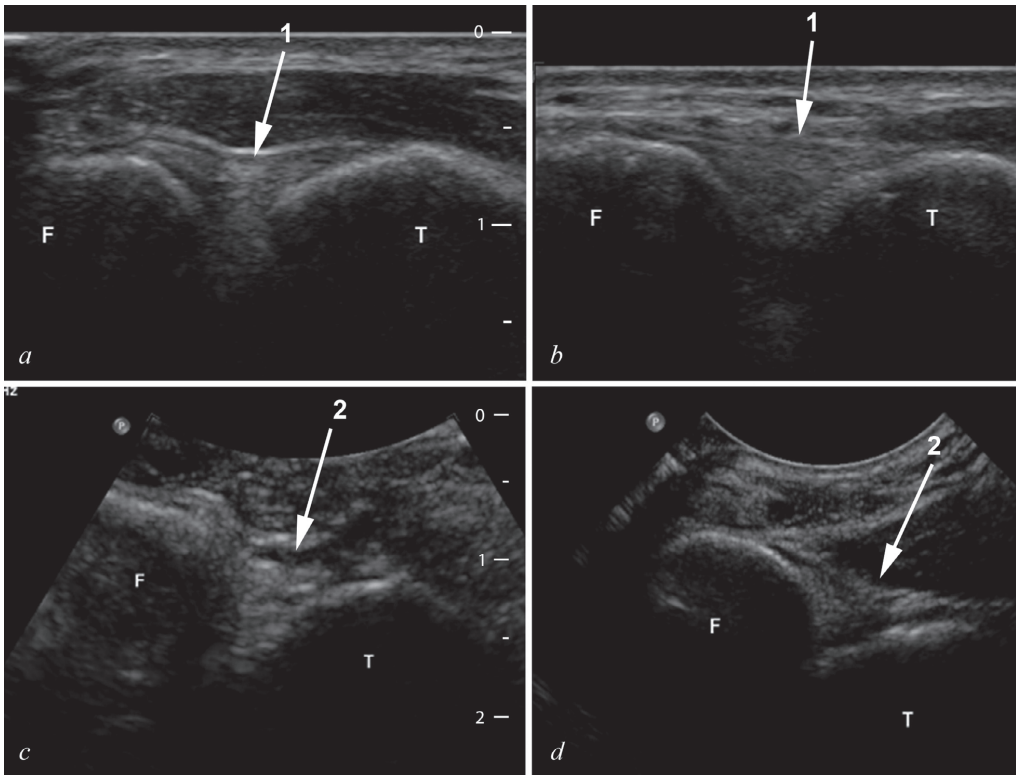

Fig. 15. Ultrasound images of anterior (1) (*a, b*) and posterior (2) (*c, d*) tibiofibular ligament (female, 20 years). In plantar flexion the ATIFL is slack (*a*). In dorsiflexion the talus pushes the tibia and fibula outwards, with stretching of the anterior tibiofibular ligament as a result (*b*). The same mechanism applies for the PTIFL. In plantar flexion the ligament is slack with a resulting increase echogenicity (*c*). In dorsiflexion the fibres are stretched and are more longitudinally aligned (*d*). F, fibula; T, tibia.

Conclusion

As the syndesmosis plays an important role in stability after acute or chronic osseoligamentous injury, understanding of the anatomy is essential in both diagnostic imaging and therapeutic management. In this article we described in detail the anatomy of the separate osseoligamentous structures of the distal tibiofibular joint, which is a complex syndesmotic joint, and discussed the clinical relevance of these structures.

References

1. Hopkinson WJ, St Pierre P, Ryan JB, Wheeler JH. Syndesmosis sprains of the ankle. Foot Ankle. 1990; 10(6):325-330.
2. Harris J, Fallat L. Effects of isolated Weber B fibular fractures on the tibiotalar contact area. J Foot Ankle Surg. 2004; 43(1):3-9.
3. Ramsey PL, Hamilton W. Changes in tibiotalar area of contact caused by lateral talar shift. J Bone Joint Surg Am. 1976; 58(3):356-357.
4. Weber BG. Die Verletzungen des oberen Sprunggelenkes. Zweite, überarbeitete und ergänzte Auflage ed: Hans Huber Bern Stuttgart Wien, 1972.
5. Lanz vT, Wachsmuth W. Praktische Anatomie. zweite neubearbeite Auflage ed. Berlin-Heidelberg-New York: Springer-Verlag, 1972.
6. Kelikian H, Kelikian S. Disorders of the ankle. Philadelphia, London, Toronto: W.B. Saunders Company, 1985.
7. Hocker K, Pachucki A. [The fibular incisure of the tibia. The cross-sectional position of the fibula in distal syndesmosis]. Unfallchirurg. 1989; 92(8):401-406.
8. Elgafy H, Semaan HB, Blessinger B, Wassef A, Ebraheim NA. Computed tomography of normal distal tibiofibular syndesmosis. Skeletal Radiol. 2010; 39(6):559-564.
9. Grass R. [Injuries of the inferior tibiofibular syndesmosis]. Unfallchirurg. 2000; 103(7):519.
10. Sora MC, Strobl B, Staykov D, Forster-Streffleur S. Evaluation of the ankle syndesmosis: a plastination slices study. Clin Anat. 2004; 17(6):513-517.
11. Yildirim H, Mavi A, Buyukbebeci O, Gumusburun E. Evaluation of the fibular incisura of the tibia with magnetic resonance imaging. Foot Ankle Int. 2003; 24(5):387-391.
12. Mavi A, Yildirim H, Gunes H, Pestamalci T, Gumusburun E. The fibular incisura of the tibia with recurrent sprained ankle on magnetic resonance imaging. Saudi Med J. 2002; 23(7):845-849.
13. Ebraheim NA, Lu J, Yang H, Rollins J. The fibular incisure of the tibia on CT scan: a cadaver study. Foot Ankle Int. 1998; 19(5):318-321.
14. Pettrone FA, Gail M, Pee D, Fitzpatrick T, Van Herpe LB. Quantitative criteria for prediction of the results after displaced fracture of the ankle. J Bone Joint Surg Am. 1983; 65(5):667-677.
15. Harper MC, Keller TS. A radiographic evaluation of the tibiofibular syndesmosis. Foot Ankle. 1989; 10(3):156-160.
16. Leeds HC, Ehrlich MG. Instability of the distal tibiofibular syndesmosis after bimalleolar and trimalleolar ankle fractures. J Bone Joint Surg Am. 1984; 66(4):490-503.
17. Sclafani SJ. Ligamentous injury of the lower tibiofibular syndesmosis: radiographic evidence. Radiology. 1985; 156(1):21-27.
18. Beumer A, van Hemert WL, Niesing R, Entius CA, Ginai AZ, Mulder PG, et al. Radiographic measurement of the distal tibiofibular syndesmosis has limited use. Clin Orthop Relat Res. 2004(423):227-234.
19. Miller AN, Carroll EA, Parker RJ, Helfet DL, Lorich DG. Posterior malleolar stabilization of syndesmotic injuries is equivalent to screw fixation. Clin Orthop Relat Res. 2009; 468(4):1129-1135.
20. Nielson JH, Gardner MJ, Peterson MG, Sallis JG, Potter HG, Helfet DL, et al. Radiographic measurements do not predict syndesmotic injury in ankle fractures: an MRI study. Clin Orthop Relat Res. 2005(436):216-221.
21. Taser F, Shafiq Q, Ebraheim NA. Three-dimensional volume rendering of tibiofibular joint space and quantitative analysis of change in volume due to tibiofibular syndesmosis diastases. Skeletal Radiol. 2006; 35(12):935-941.
22. Bartonicek J. Anatomy of the tibiofibular syndesmosis and its clinical relevance. Surg Radiol Anat. 2003; 25(5-6):379-386.
23. Tillmann B, Bartz B, Schleicher A. Stress in the human ankle joint: a brief review. Arch Orthop Trauma Surg. 1985; 103(6):385-391.
24. Kim S, Huh YM, Song HT, Lee SA, Lee JW, Lee JE, et al. Chronic tibiofibular syndesmosis injury of ankle: evaluation with contrast-enhanced fat-suppressed 3D fast spoiled gradient-recalled acquisition in the steady state MR imaging. Radiology. 2007; 242(1):225-235.
25. Kopsch F. Lehrbuch und Atlas der Anatomie des Menschen. 12. ed. Leipzig: Georg Thieme, 1922.
26. Olson RW. Ankle arthrography. Radiol Clin North Am. 1981; 19(2):255-268.
27. Pavlov H. Ankle and subtalar arthrography. Clin Sports Med. 1982; 1(1):47-69.
28. Arner O, Ekengren K, Hulting B, Lindholm A. Arthrography of the talocrural joint: anatomic, roentgenographic, and clinical aspects. Acta Chir Scand. 1957; 113(3):253-259.
29. van Moppes FI, Meijer F, van den Hoogenband CR. Arthrographic differential diagnosis between ruptures of the anterior talofibular ligament, the joint capsule and the anterior tibiofibular ligament. Rofo. 1980; 133(5):534-539.
30. Wrazidlo W, Karl EL, Koch K. [Arthrographic diagnosis of rupture of the anterior syndesmosis of the upper ankle joint]. Rofo. 1988; 148(5):492-497.
31. Lee PT, Clarke MT, Bearcroft PW, Robinson AH. The proximal extent of the ankle capsule and safety for the insertion of percutaneous fine wires. J Bone Joint Surg Br. 2005; 87(5):668-671.
32. Karasick D, Schweitzer ME, O'Hara BJ. Distal fibular notch: a frequent manifestation of the rheumatoid ankle. Skeletal Radiol. 1997; 26(9):529-532.
33. Sabacinski KA, Walter JH, Jr., Saffo GM. Anatomical and histologic investigation of the syndesmotic area in the ankle joint. J Am Podiatr Med Assoc. 1990; 80(4):204-210.
34. Stoller DW. Magnetic Resonance Imaging in Orthopaedics and Sports Medicine. 3rd ed. Philadelphia - Baltimore: Lippincott -Williams- Raven, 2007.
35. Ebraheim NA, Taser F, Shafiq Q, Yeasting RA. Anatomical evaluation and clinical importance of the tibiofibular syndesmosis ligaments. Surg Radiol Anat. 2006; 28(2):142-149.

36. Kapanji I. Funktionelle Anatomie der Gelenke: Ferdinand Enke Verlag, 1985.
37. Subhas N, Vinson EN, Cothran RL, Santangelo JR, Nunley JA, 2nd, Helms CA. MRI appearance of surgically proven abnormal accessory anterior-inferior tibiofibular ligament (Bassett's ligament). Skeletal Radiol. 2008; 37(1):27-33.
38. Akseki D, Pinar H, Yaldiz K, Akseki NG, Arman C. The anterior inferior tibiofibular ligament and talar impingement: a cadaveric study. Knee Surg Sports Traumatol Arthrosc. 2002; 10(5):321-326.
39. Nikolopoulos CE, Tsirikos AI, Sourmelis S, Papachristou G. The accessory anteroinferior tibiofibular ligament as a cause of talar impingement: a cadaveric study. Am J Sports Med. 2004; 32(2):389-395.
40. Ray RG, Kriz BM. Anterior inferior tibiofibular ligament. Variations and relationship to the talus. J Am Podiatr Med Assoc. 1991; 81(9):479-485.
41. Akseki D, Pinar H, Bozkurt M, Yaldiz K, Arac S. The distal fascicle of the anterior inferior tibio-fibular ligament as a cause of anterolateral ankle impingement: results of arthroscopic resection. Acta Orthop Scand. 1999; 70(5):478-482.
42. Bassett FH, 3rd, Gates HS, 3rd, Billys JB, Morris HB, Nikolaou PK. Talar impingement by the anteroinferior tibiofibular ligament. A cause of chronic pain in the ankle after inversion sprain. J Bone Joint Surg Am. 1990; 72(1):55-59.
43. Nikolopoulos CE. Anterolateral instability of the ankle joint: an anatomical, experimental, and clinical study. Athens, Greece: University of Athens; 1982.
44. Brostroem L. Sprained Ankles. I. Anatomic Lesions in Recent Sprains. Acta Chir Scand. 1964; 128:483-495.
45. Muhle C, Frank LR, Rand T, Ahn JM, Yeh LR, Trudell D, et al. Tibiofibular syndesmosis: high-resolution MRI using a local gradient coil. J Comput Assist Tomogr. 1998; 22(6):938-944.
46. Hermans JJ, Wentink N, Kleinrensink GJ, Beumer A. MR-plastination-arthrography: a new technique used to study the distal tibiofibular syndesmosis. Skeletal Radiol. 2009; 38(7):697-701.
47. Beumer A, Heijboer RP, Fontijne WP, Swierstra BA. Late reconstruction of the anterior distal tibiofibular syndesmosis: good outcome in 9 patients. Acta Orthop Scand. 2000; 71(5):519-521.
48. Milz P, Milz S, Steinborn M, Mittlmeier T, Reiser M. [13-MHc high frequency ultrasound of the lateral ligaments of the ankle joint and the anterior tibia-fibular ligament. Comparison and results of MRI in 64 patients]. Radiologe. 1999; 39(1):34-40.
49. Hermans JJ, Ginai AZ, Wentink N, Hop WC, Beumer A. The additional value of an oblique image plane for MRI of the anterior and posterior distal tibiofibular syndesmosis. Skeletal Radiol. 2010.
50. Van de Perre S, Vanhoenacker FM, De Vuyst D, Parizel R. Imaging anatomy of the ankle. JBR-BTR. 2004; 87(6):310-314.
51. Golano P, Mariani PP, Rodriguez-Niedenfuhr M, Mariani PF, Ruano-Gil D. Arthroscopic anatomy of the posterior ankle ligaments. Arthroscopy. 2002; 18(4):353-358.
52. Oh CS, Won HS, Hur MS, Chung IH, Kim S, Suh JS, et al. Anatomic variations and MRI of the intermalleolar ligament. AJR Am J Roentgenol. 2006; 186(4):943-947.
53. Rosenberg ZS, Cheung YY, Beltran J, Sheskier S, Leong M, Jahss M. Posterior intermalleolar ligament of the ankle: normal anatomy and MR imaging features. AJR Am J Roentgenol. 1995; 165(2):387-390.
54. Lee SH, Jacobson J, Trudell D, Resnick D. Ligaments of the ankle: normal anatomy with MR arthrography. J Comput Assist Tomogr. 1998; 22(5):807-813.
55. Milner CE, Soames RW. Anatomy of the collateral ligaments of the human ankle joint. Foot Ankle Int. 1998; 19(11):757-760.
56. Heim U. [Malleolar fractures]. Unfallheilkunde. 1983; 86(6):248-258.
57. Haraguchi N, Armiger RS, Myerson MS, Campbell JT, Chao EY. Prediction of three-dimensional contact stress and ligament tension in the ankle during stance determined from computational modeling. Foot Ankle Int. 2009; 30(2):177-185.
58. Ogilvie-Harris DJ, Reed SC, Hedman TP. Disruption of the ankle syndesmosis: biomechanical study of the ligamentous restraints. Arthroscopy. 1994; 10(5):558-560.

Chapter 3

MR-plastination-arthrography: a new technique used to study the distal tibiofibular syndesmosis

John J. Hermans
Noortje Wentink
Gert-Jan Kleinrensink
Annechien Beumer

Skeletal Radiology 2009 Jul; 38(7): 697-701

Abstract

Objective: The purpose of this study was to describe a new technique called MR plastination arthrography to study both intra- and extra-articular anatomy.

Materials and Methods: In six human cadaveric lower legs MR arthrography was performed in either a one-step or two-step procedure. In the former a mixture of diluted Gadolinium and dyed polymer was injected. In the latter the dyed polymer was injected after arthrography with diluted Gadolinium. Three-millimeter slices of these legs, obtained in a plane identical to that of the MR images, were plastinated according to the E12 technique of von Hagens. The plastination slices were subsequently compared with the MR images.

Results: The one-step procedure resulted in an inhomogeneous arthrogram. The two-step procedure resulted in a good correlation between the high-resolution MR images and plastination slices, as expressed by a good comparison of anatomic detail of the small syndesmotic recess.

Conclusion: Images of the distal tibiofibular syndesmosis obtained with plastination arthrography correlated well with images acquired by MR arthrography when performed in a two-step procedure.

Introduction

MR arthrography is an accepted technique to study intra-articular pathology. In patients with an injury of the distal tibiofibular syndesmosis the joint space and its recesses may be involved. Therefore the normal anatomy not only of the syndesmotic ligaments but also of the joint space and of the height and contour of the syndesmotic recess is of interest. One way to study the anatomy is by using the technique of plastination, in which biologic tissues are impregnated by curable polymers [1]. This results in dry, odorless, and durable specimens that have intact gross and microscopic anatomy. However the joint space itself and its recesses are not easily recognized because in the process of plastination the joint fluid is removed. Therefore we decided to combine plastination with arthrography. In this way, both the joint space and its outlining structures can be depicted.
In this article we describe our experiences with two techniques of plastination arthrography. The images obtained by plastination arthrography were correlated with images of MR arthrography and were used to study the normal anatomy of the distal tibiofibular syndesmosis.

Materials and Methods

We used six fresh frozen human cadaveric lower legs, which were amputated through the knee joint. The specimens were thawed 12 - 24 hours before scanning. In all specimens both a conventional MR as well as a MR arthrography were performed. As contrast agent we used Gadolinium (Magnevist® dimeglumingadopentetate, Schering, Germany; Gd) in MR and dyed polymer in plastination. After MR imaging the leg was frozen again for a week at –20°C in order for the intra-articular polymer to cure. After this, 3 mm slices of fresh frozen legs were obtained in a 45º oblique axial plane identical to that of the MR images. These slices were then plastinated according to the E12 technique of von Hagens. The plastination slices were subsequently compared with MR images.
The injection of contrast fluid for MR-plastination arthrography was performed in either a one-step or a two-step procedure. In the one-step procedure MR arthrography was performed after a single injection with a mixture of NaCl (0.9%), Gd, and dyed polymer. In the two-step procedure injection of a mixture of NaCl (0.9%) and Gd for MR arthrography was followed by removal of the Gd and a second injection of dyed polymer for plastination arthrography. To prevent artifacts at the level of the anterior syndesmosis, injection was performed between the tendon of the anterior tibial muscle and the medial malleolus at the level of the talocrural joint.
For the one step procedure it was necessary to find the optimal concentration of Gd and the optimal curation speed of the polymer solution. Two series with each nine different Gd concentrations were made in test tubes. The dilutions of Gd in these tubes increased from 1:50 – 1:250 with steps of 25, with NaCl (0.9%) as the diluting agent. The first series was made with a fast curing polymer, the second series with a slow curing polymer. The slow curing polymer was made with half the amount of hardening component (Biodur Härter E2) of that used in the fast curing polymer.
The 18 test tubes were scanned axially using T1 weighted FFE images (TR = 5.1 ms, TE = 1.8 ms, α = 55º), a 128 x 256 matrix, NSA =1, and one slice with a thickness of 10 mm at a 1.5T MRI (Gyroscan, Philips, Best, The Netherlands). The tubes were scanned at 2-minute intervals for a period of 8.5 h. The change in signal intensity with time was plotted in time-intensity

curves. The time available to perform MR-plastination-arthrography was determined by the time the signal of the mixture had faded for 50%.
A 1.5T MR (Gyroscan, Philips, Best, The Netherlands) and C3 surface coil around the cadaver ankles were used to obtain high-resolution images of the distal tibiofibular syndesmosis. The syndesmosis was scanned in a coronal, an axial and an oblique axial plane. The latter plane had shown to give the best images of the syndesmosis in a previous study [2, 3]. T1-weighted images were acquired with a matrix of 512 x 512, a field of view of 120–140 mm and 2.5 mm slice thickness. For the MR arthrography T1-weighted images with spectral fat suppression (SPIR) were obtained using a matrix of 512 x 512, a field of view of 120–140 mm and 3.0 mm slice thickness. With these scan parameters an in plane resolution of about 250 x 250 µm was realized. Cod oil markers were fixed to the leg before scanning started in order to be able to define the exact plane in which the ankle had to be sawed [4].

Results

With time the signal intensity of the mixtures of Gd and polymer decreased as is demonstrated by the time-intensity curves (Fig. 1). The time-intensity curves showed the following: the decrease in signal intensity was initially greater in the fast-curing polymer than in the slow-curing polymer; after 512 minutes both polymers still had not completely solidified as the signal intensity of both the fast and slow curing polymer had not reached zero yet; at higher dilutions the decrease in signal intensity occurred at a greater rate than at lower dilutions.

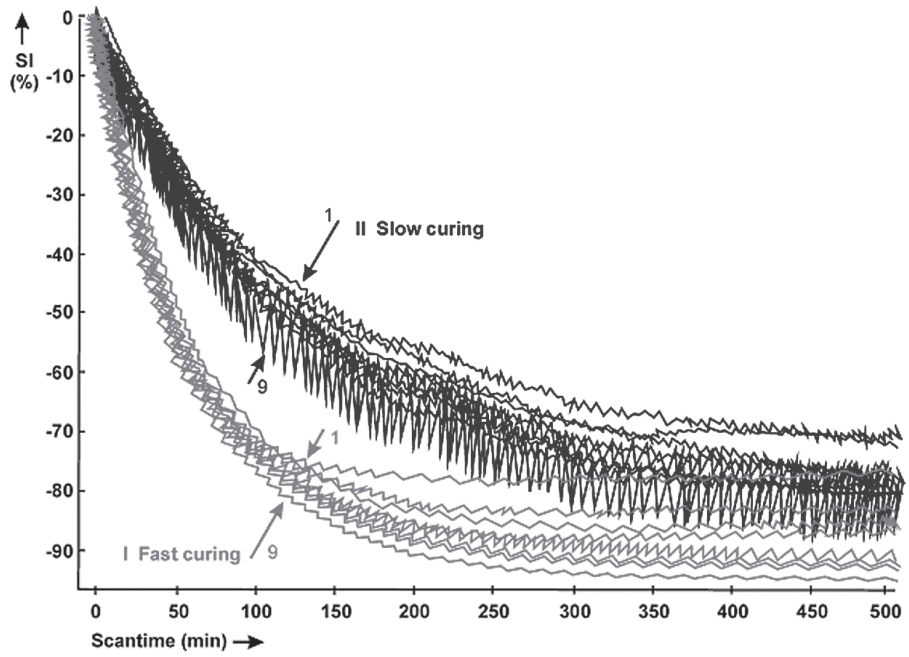

Fig. 1. Signal intensity (SI (%)) versus scan time (min) of two series of mixtures with polymer and Gadolinium (Gd) with different curing speed. *I* = fast curing; *II* = slow curing polymer. Each series contains nine different Gd dilutions varying from 1:50 to 1:250, in steps of 25 (1-9).

MR-plastination-arthrography was performed in either a one- or a two-step procedure. For the one-step procedure we used the mixture with the slow curing polymer with 1:50 diluted Gd. Although this procedure resulted in a good plastination arthrogram, the MR arthrogram appeared to be inhomogeneous (Fig. 2).

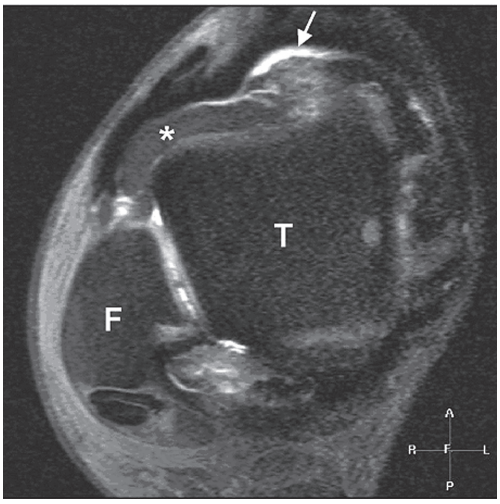

Fig. 2. Axial T1-w image with fat suppression after an intra-articular injection with a mixture of diluted Gd and polymer (one-step procedure). F, fibula; T, talus. The arthrogram is inhomogeneous: there are both areas with high signal intensity (*arrow*) as well as areas with signal voids (*asterisk*).

For the two-step MR plastination arthrography, we first performed a conventional MR arthrogram with 1: 250 diluted Gd, followed by an intra-articular injection of dyed polymer. This resulted in both a homogeneous MR arthrogram as well as a good plastination arthrogram.
The images acquired after the two-step MR plastination arthrography were compared with the plastination arthrography and showed an excellent correlation (Fig. 3). The talocrural joint space and its recesses were filled with contrast agent in the MR arthrogram and with dyed polymer in the plastination arthrogram. The syndesmotic recess was clearly visible in both the MR and the plastination arthrogram and the inner boundaries of the joint could easily be identified. The noncontrast enhanced MR images demonstrated ligaments, muscles, tendons and the neurovascular bundles in great detail. The same structures were clearly recognizable in the plastinated slices.
Directly behind the anterior tibiofibular ligament was a small fat pad, which protruded variably into the talocrural joint (Fig. 4). In the T1-weighted images, the fat pad had the same signal intensity as the subcutaneous fat. In the MR arthrogram, a technique with fat suppression was used. The fat could now be seen as a signal void abutting the posterior border of the anterior tibiofibular ligament and indenting the syndesmotic recess (Fig. 3).
The anterior and posterior tibiofibular ligaments were only partially depicted in the axial images of the talocrural joint. However, in the oblique plane, running 45° in caudal-cranial direction from the lateral malleolus and related to the tibia plafond, the syndesmotic ligaments were depicted in their entire length (Fig 5, *see next pages*).
The transverse ligament was best seen in an axial image since it runs parallel to the tibial plafond between the medial and lateral malleolus, and forms a labrum like structure at the posterior distal tibia. We cannot present a plastination image of this ligament in the axial plane since we only made images in the aforementioned oblique plane. The interosseous membrane was well visualized in both the axial and the oblique plane since it constitutes a continuous sheet between the crest of the tibia and fibula.

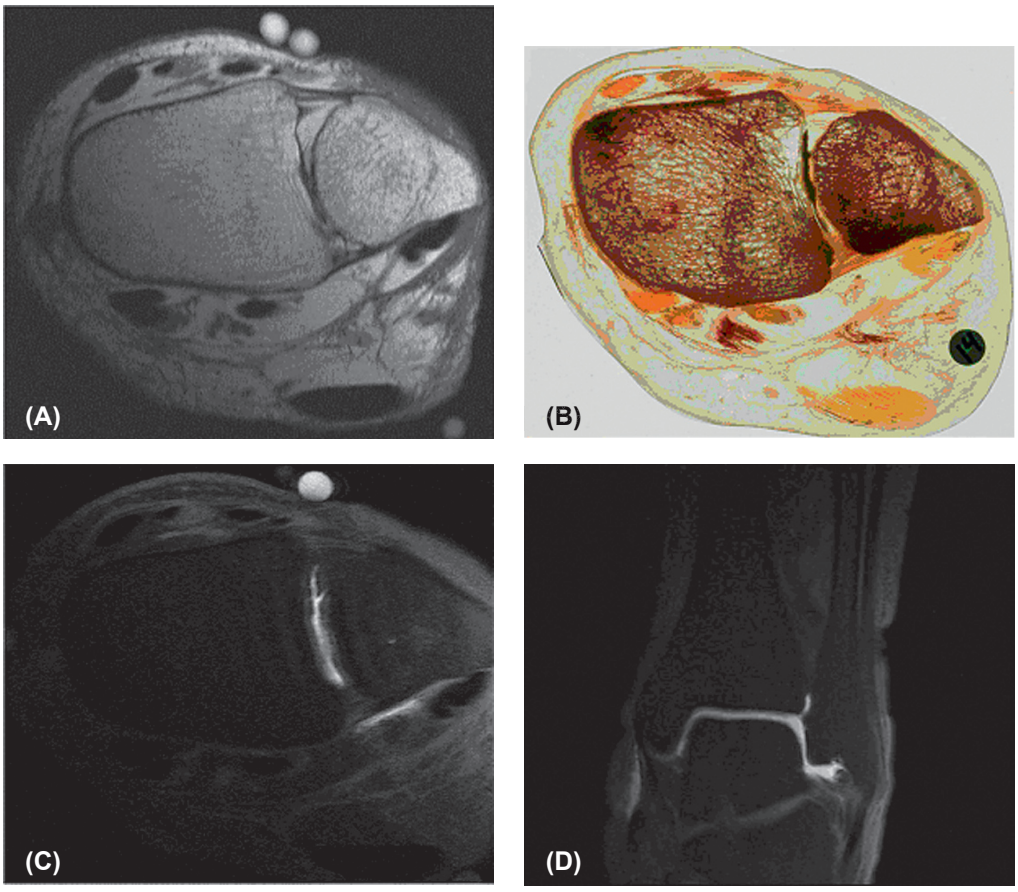

Fig. 3. Correlation between noncontrast enhanced MRI (*A*), plastination arthrography (*B*), and MR arthrography (*C, D*) at the level of the syndesmosis. The green dye (*B*) and contrast (*C, D*) are visible in the syndesmotic recess. The recess is not visible in the noncontrast MRI (*A*). The anterior and posterior tibiofibular ligaments outline the syndesmotic recess. The fat pad is visible behind the anterior tibiofibular ligament (*A, B*). The cod oil markers are visible as white balls on the skin (*A, C*).

Fig. 4. Coronal T1-w image. A small fat pad (*arrow*) protrudes into the tibiotalar joint.

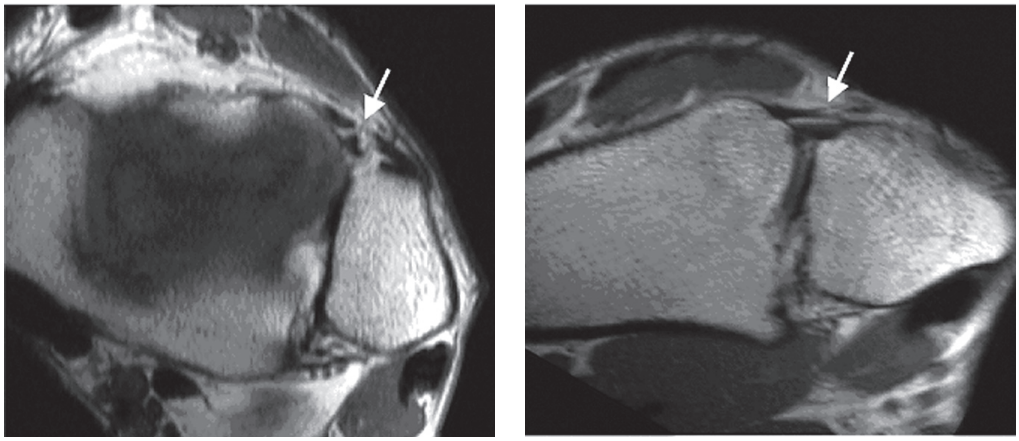

Fig. 5. Axial (*left*) and 45° oblique (*right*) T1-w image. In the axial image the anterior tibiofibular ligament looks interrupted (*arrow*). In the oblique image the ligament is depicted along its entire length (*arrow*).

Discussion

Several techniques can be used to perform MR arthrography. All techniques however are based on the presence of an intra-articular contrast-enhancing agent and on distension of the joint. A joint effusion or haemarthros, due to an acute or chronic injury of the joint, leads to distension of the joint with the intra-articular fluid acting as a natural contrast agent. Another way to perform an arthrogram is by injecting a saline solution into the joint and injecting Gd intravenously. The most commonly used technique however, is an intra-articular injection of a diluted Gd solution [5]. This results in a high intra-articular signal and therefore a good depiction of the intra-articular anatomy.

Until now no technique was available to perform plastination arthrography. Plastination is a process in which tissues are dehydrated and impregnated with a polymer. It is an excellent method to study anatomy, but as fluids are taken out of the tissues during the process, it is difficult to study intra-articular anatomy. Plastination arthrography could be the solution for this problem. When a polymer is added to the Gd solution there will be a decrease in signal intensity with time because curing of the polymer results in an increasing solidity of the mixture. This decrease in signal intensity goes on until, finally, there is a signal void.

In order to be able to perform MR arthrography we looked for that specific mixture of Gd and polymer, which would give us the maximum time window to scan before the signal intensity, dropped below a visible level. The mixture showing the highest signal intensity for the longest period of time was the slow-curing polymer with a 1:50 diluted Gd solution. At 50% decrease of the initial signal intensity, this Gd-polymer mixture was still clearly visible. The 50% reduction in signal intensity was reached after 150 minutes. Since we needed circa 50 minutes to prepare the Gd-polymer mixtures before we could start MRI scanning, the total available time window before the signal intensity dropped below a visible level added up to 200 minutes. This gave us ample time to perform the MR imaging.

The most convenient way to perform MR Plastination arthrography is with a single intra-articular injection of a mixture of Gd and polymer. Such a mixture did not give a good result in this study. Although the joint could be clearly visualized, the arthrogram was inhomogeneous. As such it was not possible to study the joint lining and syndesmotic recess. There could be

a number of reasons for this phenomenon.
Firstly, the ongoing process of curing could be the cause of this inhomogeneous arthrogram. However, this is not likely since all images were acquired within approximately 110 min after we started the preparation of the Gd-polymer while the total available time window amounted 200 minutes.
Secondly the presence of joint fluid and/or the presence of tissues forming the joint lining may give an additional interaction between the Gd and polymer. This could lead to a faster decrease of signal intensity in the joint than was observed in the test tubes. Moreover the curing process itself may be an inhomogeneous process.
Changing the order of mixing the components of the polymer solution with the hardening component (Biodur Härter E2) added last however, did not result in a more homogenous arthrogram. We therefore changed towards a two-step procedure with a conventional MR arthrogram as a first step, followed by an intra-articular injection of a dyed polymer and plastination of the leg.
The obliquely running anterior and posterior tibiofibular ligaments are only partially visible in axial images of the talocrural joint. This may lead to the erroneous interpretation of a rupture of these ligaments. Generally, a ligament is best depicted in a plane along its length. We therefore scanned and sawed the specimen in an oblique plane, which was defined with the aid of markers containing cod oil, which were attached to the skin of the cadaveric leg.
This article shows that the study of clinically relevant anatomical structures clearly improves by using plastination arthrography. This can best be done following the two-step procedure. The first step was the MR arthrogram with a 1:250 diluted Gd solution; the second step the plastination arthrogram with a dyed polymer. With this technique we achieved an excellent correlation between MR images and plastinated slices of the distal tibiofibular syndesmosis. MR-plastination-arthrography demonstrated the clinically relevant syndesmotic recess, the fat pad, and the tibiofibular ligaments in great detail. This technique can be applied to study the anatomy of any synovial joint. However, it is essential to obtain plastination slices in the same plane as the imaging slices. To optimize this technique for each joint may be a subject for future studies.

References

1. von Hagens G, Tiedemann K, Kriz W. The current potential of plastination. Anat Embryol (Berl). 1987; 175(4):411-421.
2. Hermans JJ, Beumer A. MRI characteristics of chronic syndesmotic injuries. Tenth Scientific Meeting and Exhibition. Honolulu, Hawaii, USA 2002.
3. Beumer A, Hermans JJ, Niesten DD, Heijboer MP. Late reconstruction of the anterior tibiofibular syndesmosis for ankle diastasis with talar shift in a 12-year-old boy. Foot and Ankle Surgery. 2005; 11:49-53.
4. Entius CAC, Kuiper JW, Koops W, de Gast A. A new positioning technique for comparing sectional anatomy of the shoulder with sectional diagnostic modalities: Magnetic resonance Imaging (MRI), Computed Tomography (CT) and Ultrasound (US). J Int Soc Plastination. 7:23-26.
5. Lee SH, Jacobson J, Trudell D, Resnick D. Ligaments of the ankle: normal anatomy with MR arthrography. J Comput Assist Tomogr. 1998; 22(5):807-813.

Chapter 4

The additional value of an oblique image plane for MRI of the anterior and posterior distal tibiofibular syndesmosis

John J.Hermans
Abida Z. Ginai
Noortje Wentink
Wim C.J. Hop
Annechien Beumer

Skeletal Radiology 2011 Jan; 40: 75-83

Abstract

Objective: The optimal MRI scan planes of collateral ligaments of the ankle have been described extensively, with the exception of the syndesmotic ligaments. We assessed the optimal scan plane for depicting the distal tibiofibular syndesmosis.

Materials and Methods: In order to determine the optimum oblique caudal-cranial and lateral-medial MRI scan plane, two fresh frozen cadaveric ankles were used. The angle of the scan plane that demonstrated the anterior and posterior distal tibiofibular ligament uninterrupted in their full length was determined. In a prospective study this oblique scan plane was then used in addition to the axial and coronal planes, for MRI scans of both ankles in 21 healthy volunteers. Two observers independently evaluated the ATIFL and PTIFL regarding the continuity of the individual fascicles, thickness and wavy contour of the ligaments in both the axial and oblique plane. Kappa was calculated to determine the interobserver agreement. McNemar's test was used to statistically quantify the significance of the two scan planes.

Results: In the axial plane the ATIFL was in 31% (13/42) partly and in 69% (29/42) completely discontinuous; in the oblique plane the ATIFL was continuous in 88% (37/42) and partly discontinuous in 12% (5/42). Compared to the axial plane, the oblique plane demonstrated significantly less discontinuity ($p<0.001$), but not significantly less thickening ($p=1.00$) or less wavy contour ($p=0.06$) of the ATIFL. In the axial scan plane the PTIFL was continuous in 76% (32/42), partially discontinuous in 19% (8/42) and completely discontinuous in 5% (2/42); in the oblique plane the PTIFL was continuous in 100% (42/42). Compared to the axial plane, the oblique plane demonstrated significantly less discontinuity ($p=0.002$), but not significantly less thickening ($p=1.00$) or less wavy contour ($p=0.50$) of the PTIFL. The interobserver agreement score and kappa (κ) regarding the continuity for the ATIFL in the axial and oblique plane was 91% ($\kappa = 0.79$) resp. 91% ($\kappa = 0.55$); for the PTIFL it was 86% ($\kappa = 0.65$) resp. 100% (κ = not defined).

Conclusion: Until now the ATIFL and PTIFL have been scanned in the usual orthogonal scan planes. The advantage of MRI scanning in an oblique image plane of about 45 degrees lies in a better evaluation of the ligaments compared to the axial plane, particularly a better interpretation of ligament continuity, thickening and wavy contour. This may lead to a reduction in false positive results, especially regarding partial or complete ligament ruptures. This can be of considerable aid in therapeutic management.

Introduction

Injury of the distal tibiofibular syndesmosis occurs in approximately 1-11% of all ankle sprains [1-3]. This number may increase to more than 40% in those actively involved in high contact or collision sporting activities [4].

Syndesmotic instability in adults can be due to widening of the ankle mortise (complete tibiofibular diastasis) or to posterior translation and external rotation of the fibula (anterior tibiofibular diastasis). The latter is more common and more difficult to recognize. The chronic instability results from increased length of the syndesmotic ligaments that have healed elongated after an acute rupture that was not adequately treated [5-7]. Lateral shift of the talus more than 2 mm and external rotation of the talus larger than five degrees, reduce the mean joint contact area and increase the contact pressure in the ankle [8, 9]. Since widening of the ankle mortise by 1mm decreases the contact area of the tibiotalar joint with 42% [10] this could lead to an early osteoarthritis of the tibiotalar joint.

Radiography, arthrography, ultrasound and CT have been used to assess the integrity of the syndesmosis. Several authors have described that radiography has limited use in the assessment of syndesmotic integrity [11-13]. Conventional X-ray arthrography is not routinely used anymore as it is an invasive examination, although it clearly displays syndesmotic and other ligamentous injuries [14-16]. Ultrasound can clearly depict a torn tibiofibular ligament in the acute stage but is less accurate after elapse of time and the results are very dependent on the skills of the radiologist [17]. With the use of CT, widening of the mortise exceeding 3 mm can reliably be assessed as well as gross deformity [18]. However external rotation of the distal fibula, such as seen in anterior tibiofibular diastasis, is not easily recognised, due to the "round" shape of the fibula at that level.

The value of MRI in acute and chronic syndesmotic injuries has been described in several papers [19-23]. In these papers the usual three orthogonal scan planes (axial, coronal and sagittal) and the position of the foot during imaging (neutral, 10-20 degrees dorsiflexion or 40-50 degrees plantar flexion) have been used to evaluate the optimal scan plane of both the collateral and the syndesmotic ankle ligaments [21, 23]. However, since the anterior and posterior distal tibiofibular ligament run obliquely to the orthogonal planes [24], the axial scan plane may lead to a false-positive interpretation regarding the presence of a syndesmotic injury when MRI results are compared with operative findings [20, 25].

In the present study we assessed the additional value of an oblique scan plane for depicting the anterior and posterior distal tibiofibular syndesmotic ligaments in cadaveric specimens and validated this in healthy volunteers. The clinical relevance is illustrated with three clinical cases.

Materials and Methods

In two fresh frozen cadaveric lower legs, amputated below the knee, we obtained images of the ankle in a 1.5T MR (Philips Gyroscan, Best, The Netherlands). The legs were thawed for 24 hours before scanning. We used a wrap around surface coil (E1 coil). A T1-weighted turbo spin echo (TSE) sequence was used (TR 500ms; TE 15ms; TF 5) with a FOV of 12 x 12 cm, a matrix of 512 x 512 and slice thickness of 2.5 mm with a gap of 0.2 mm and NSA of 2.
The images were acquired in the axial, coronal, sagittal and several oblique planes, with the foot in neutral position. The oblique image plane was defined in the coronal and sagittal plan scans. In the coronal view the acute angle of the oblique plane was related to the tibial plafond and ran caudal-cranially and lateral-medially through the distal fibula. The angle of the oblique plane varied from 30-60 degrees with steps of 5 degrees (Fig. 1a). In the sagittal view the direction of the oblique plane ran parallel to a line along the inferior border of the anterior and posterior tibia (Fig. 1b). The angle of the scan plane that demonstrated the multiple fascicles of the anterior (ATIFL) and posterior distal tibiofibular ligament (PTIFL) uninterrupted in their full length was defined as the optimal angle. The optimal angle was defined by consensus by two observers (JH, NW).

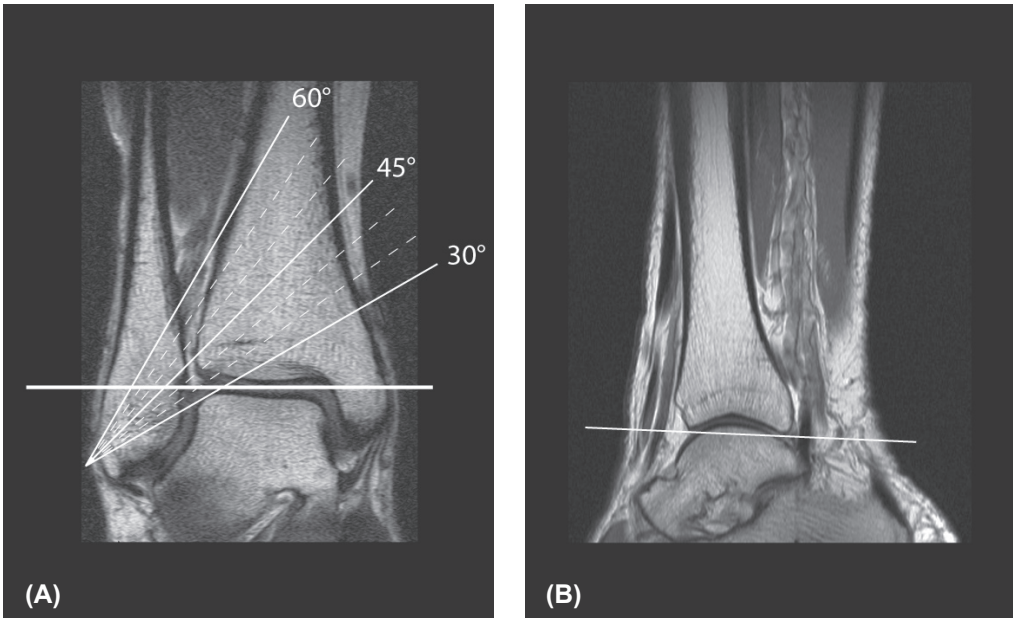

Fig. 1 Coronal (*A*) and sagittal (*B*) MR images, which indicate the angle of the oblique image plane for the anterior and posterior distal tibiofibular ligament. In the coronal plane the angle varied from 35 to 60°, with steps of 5°. In the sagittal view the direction of the oblique plane runs parallel to a line along the inferior border of the anterior and posterior tibia.

After determination of the optimal angle of the oblique MRI scan plane, this plane was used additionally to the axial and coronal views to scan the syndesmosis of both ankles in 21 healthy volunteers (9 males; range 21-30 yrs and 12 females; range 21-30 yrs). Inclusion criteria for the volunteers were: age over 18 years, no history of trauma in the past year, no previous surgery and no inflammatory disease of the ankle or foot. The same MR scanner and

T1-w TSE sequences as in the cadaveric legs were applied. The anterior and posterior distal tibiofibular ligaments were evaluated with respect to continuity of the separate fascicles, thickening of the fascicles and a wavy contour of the ligament [26]. Regarding the continuity of the fascicles the ATIFL and PTIFL were assigned a score in both the axial and the oblique image plane: "zero" when none of the fascicles of the ligament between the tibia and fibula were interrupted (i.e. continuous), "one" when one or more, but not all of the fascicles, were interrupted (i.e. partly interrupted) and "two" when all fascicles were interrupted (i.e. completely interrupted). Thickening of the fascicles and a wavy contour of the ligament were scored as either present or absent.

The images were independently analyzed by two musculoskeletal radiologists with 10 (JH) and 30 (AG) years experience. The interobserver agreement was determined by the kappa agreement score (0.00 – 0.20: poor; 0.21 – 0.40: fair; 0.41 – 0.60 moderate; 0.61 – 0.80 good; 0.81 – 0.90: very good; 0.91 – 1.00: extra good). McNemar's test was used to statistically quantify the significance of the axial and oblique scan planes regarding the continuity, thickening and wavy contour, of the anterior and posterior distal tibiofibular ligament, with a p-value less than 0.05 considered as significant. Statistical analysis was performed with Statistical Package for Social Sciences (SPSS) 15.0.

In three clinical cases the additional value of the oblique scan plane is demonstrated with respect to diagnosis and treatment.

Results

Cadaveric ankles

When the ankle joint was imaged in the axial plane the fascicles of the anterior distal tibiofibular ligament appeared to be discontinuous between the anterior tubercle of the tibia and the anterior tubercle of the fibula. This apparent discontinuity slowly decreased when the 30 degrees angle of the scan plane was increased with steps of five degrees. At about 35 degrees the uninterrupted ATIFL became visible and showed the multifascicular aspect of the ligament to good advantage. With a scan angle greater than 55 degrees the fascicles appeared to be discontinuous again. The plane of 45 degrees also demonstrated the posterior distal tibiofibular ligament in its full length. In both the coronal and sagittal plane the ATIFL and PTIFL were not depicted with as much detail as in the oblique plane.

Volunteers

The interobserver agreement was calculated with kappa and the agreement score (Table 1). The axial scan plane demonstrated a partial (Fig. 2) or complete discontinuity (Fig. 3, *see next page*) of the ATIFL in 31% (13/42) respectively in 69% (29/42) of the twenty one volunteers. In the 45 degrees oblique scan plane the ATIFL was continuous in 88% (37/42) and partially discontinuous in 12% (5/42). In the oblique plane the fascicles were more often continuous than in the axial plane ($p<0.001$). When compared to the axial plane, the oblique plane demonstrated less thickening (5% resp. 2%; $p=1.00$) and less wavy contour (24% resp. 12%; $p=0.06$) of the ATIFL, but both were not significant (Table 2).

Table 1 Agreement score [AS (%)] and kappa (κ), regarding continuity, thickening, and wavy contour of the anterior tibiofibular ligament (ATIFL) and posterior tibiofibular ligament (PTIFL) in the axial and oblique planes of both ankles in 21 volunteers.

	ATIFL				PTIFL			
	Axial		Oblique		Axial		Oblique	
	AS (%)	κ	AS (%)	κ	AS (%)	κ	AS (%)	κ
Continuity	91	0.79	91	0.55	86	0.65	100	not determined
Thickening	91	0.46	95	0.48	95	0.72	98	0.79
Wavy	91	0.77	98	0.90	88	0.23	95	not determined

Table 2. Frequencies of ligament characteristics of ATIFL and PTIFL in the axial and oblique planes of both ankles in 21 volunteers.The fascicles are continuous (CO), or partially or completely interrupted (PI resp. CI).

	ATIFL				PTIFL			
Axial\Oblique	CO	PI	CI		CO	PI	CI	
Continuous (CO)	0	0	0	0	32	0	0	32
Partially interrupted (PI)	12	0	1	13	8	0	0	8
Completely interrupted (CI)	25	0	4	29	2	0	0	2
	37	0	5	42	42	0	0	42

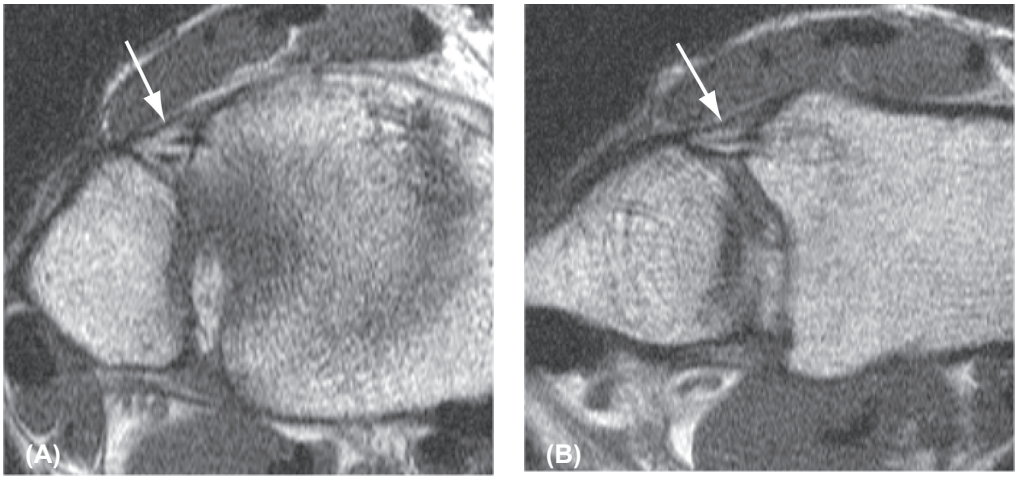

Fig. 2 Axial (*A*) and oblique (*B*) T1-weighted turbo spin echo (TSE) image of the anterior distal tibiofibular ligament in a healthy volunteer. In the axial image (*A*) two of the three visible fascicles of the anterior tibiofibular ligament (ATIFL) are partially interrupted (arrow). In the oblique image (*B*) all three fascicles are continuous and visible along their entire length.Therefore, partial discontinuity of the fascicles of the ATIFL cannot be used as a parameter for a partial rupture of the anterior syndesmosis, when scanned in an axial plane.

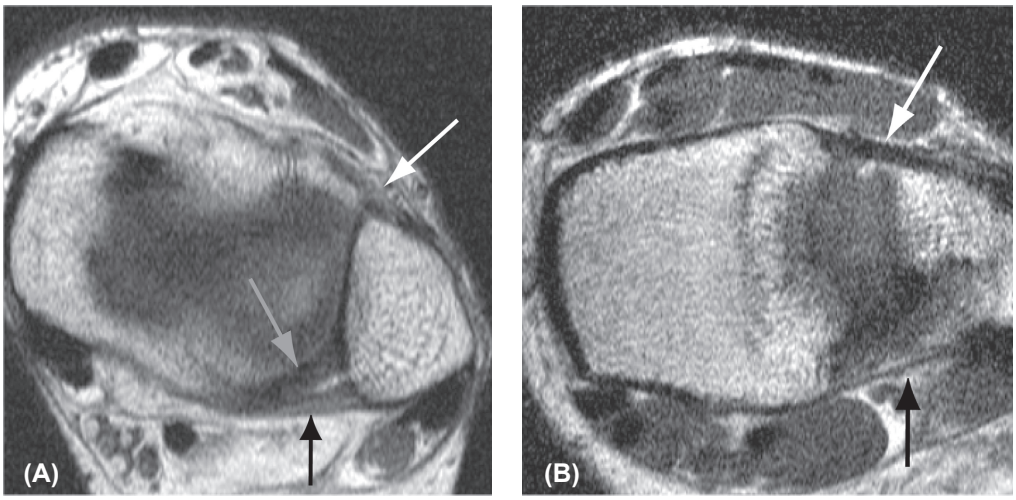

Fig. 3 Axial (*A*) and oblique (*B*) T1-weighted TSE image of the anterior distal tibiofibular ligament in a healthy volunteer. The axial image (*A*) shows a discontinuous aspect of the inferior fascicle of the ATIFL, also called Bassett's ligament (white arrow). In the oblique image (*B*) a thick continuous Bassett's ligament is visible. Posteriorly the transverse ligament (gray arrow) and posterior tibiofibular ligament (PTIFL; black arrow) are depicted; in the oblique plane (*B*) only the lowermost fascicle of the PTIFL is depicted at this level.

In the axial scan plane the PTIFL was continuous in 76% (32/42), partially discontinuous in 19% (8/42) and completely discontinuous in 5% (2/42). In the oblique plane the PTIFL was continuous in 100% (42/42) (Fig. 4). In the oblique plane the fascicles were more often continuous than in the axial plane ($p=0.002$). When compared to the axial plane, the oblique plane demonstrated less thickening (10% resp. 7%; $p=1.00$) and less wavy contour (5% resp. 0%; $p=0.50$) of the PTIFL, but both were not significant (Table 2, *see previous page*).

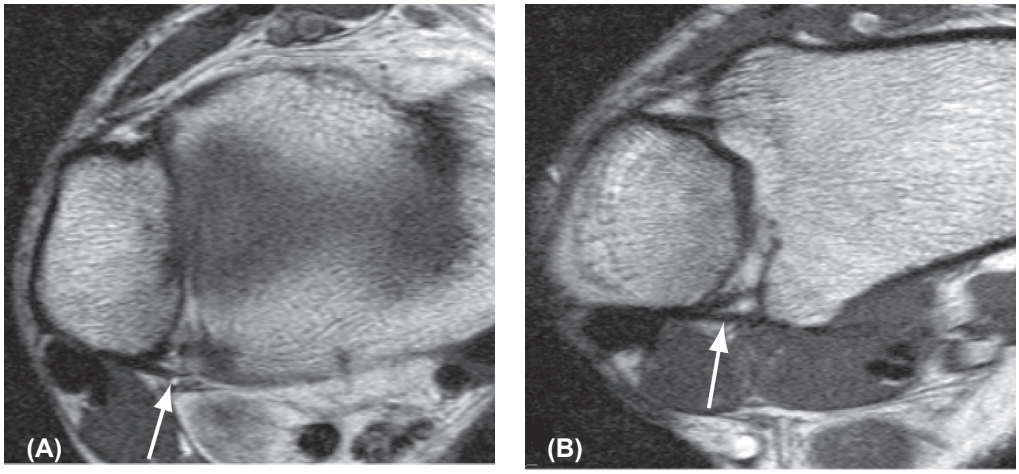

Fig.4 Axial (*A*) and oblique (*B*) T1-weighted TSE image of the posterior distal tibiofibular ligament (*arrow*) in a healthy volunteer. In the axial image (*A*) the discontinuous fascicles of the PTIFL are visible, whilst in the oblique image (*B*) the fascicles are intact. Therefore, in the oblique image plane the posterior syndesmosis is demonstrated to its better advantage.

Clinical cases

The clinical relevance of the oblique scan plane for the syndesmosis is demonstrated with three cases.The first case is a 37 year old patient with a sprain of her ankle (Fig. 5). On the T2-weighted turbo spin echo (TSE) images in the axial plane the ATIFL appeared discontinuous. In the oblique scan plane however the anterior syndesmosis was continuous.Therefore the ATIFL was not completely ruptured as suggested by the image in the axial plane.Although an isolated rupture of the ATIFL can be treated nonoperatively, it preferably should be treated in a plaster, whilst a sprain, i.e. a partial rupture of the anterior syndesmosis, can be treated functionally [27]. Additional finding of interest was a bone bruise of the distal tibia as indicated by the high signal intensity area on the coronal STIR (i.e. short tau inversion recovery) image (Fig.6c).

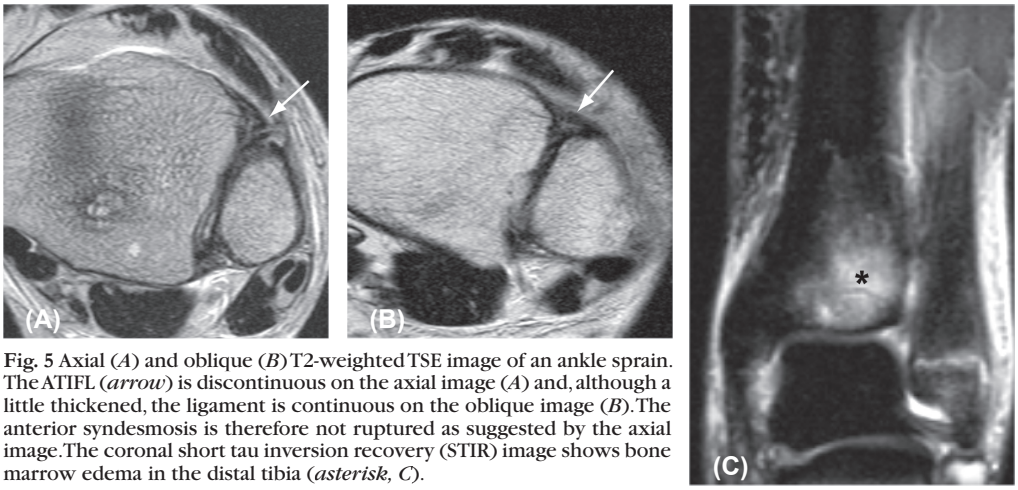

Fig. 5 Axial (*A*) and oblique (*B*) T2-weighted TSE image of an ankle sprain. The ATIFL (*arrow*) is discontinuous on the axial image (*A*) and, although a little thickened, the ligament is continuous on the oblique image (*B*).The anterior syndesmosis is therefore not ruptured as suggested by the axial image.The coronal short tau inversion recovery (STIR) image shows bone marrow edema in the distal tibia (*asterisk, C*).

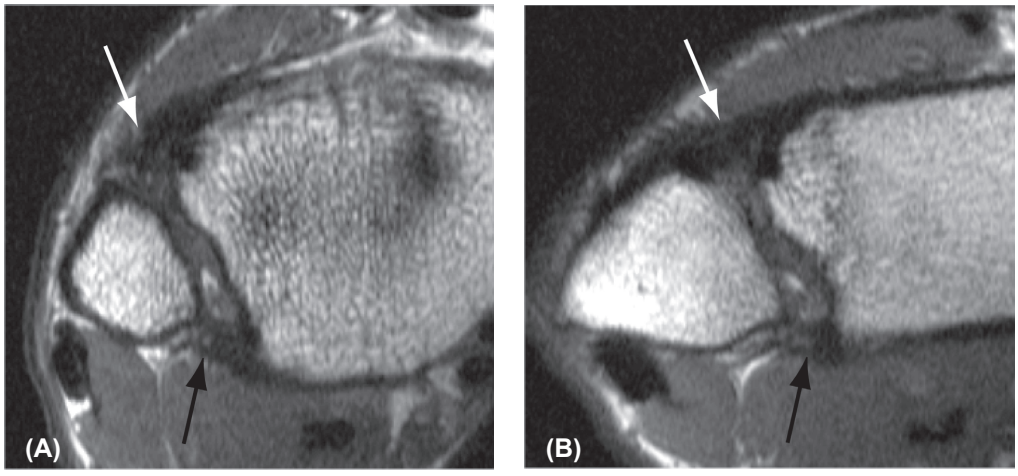

Fig. 6 Axial (*A*) and oblique (*B*) T1-weighted TSE image of a chronic injury of the ATIFL.The axial image shows a thickened and discontinuous aspect of the ATIFL (*white arrow;A*). However, in the oblique image the ligament is continuous, although quite thickened (*white arrow; B*). The two fascicles of the PTIFL are continuous, but slightly thickened in both the axial and oblique planes (*black arrow*).

The second case is a 44 year old man who complained of chronic instability after he had sprained his ankle about a year ago (Fig. 6, *see previous page*). The T1-weighted turbo spin echo (TSE) axial image showed a thickened and discontinuous aspect of the ATIFL, while in the oblique image the ATIFL was continuous. The anterior syndesmosis was thickened due to fibrosis that makes the fascicles of the ligament no longer individually visible. In the chronic situation an anatomic reconstruction is the best treatment if the ATIFL is continuous. If not salvage surgery such as tenodesis or arthrodesis may be performed. These surgeries relieve the instability but alter the biomechanics [5].

The third case is a 12 year old boy with an acute sprain of his left ankle (Fig. 7). He sustained a sprain of the same ankle 8 months previously. Extensive imaging (X-Ray, CT and MR) finally demonstrated an old avulsion fracture of the anterior tubercle of the distal fibula (Wagstaffe-Lefort) The oblique plane demonstrated an intact anterior distal tibiofibular ligament attached to an avulsion fracture of the anterior fibula, whereas axial images at adjacent levels of the distal tibiofibular joint showed the avulsion fracture of the anterior aspect of the fibula with a discontinuous aspect of the ATIFL. Based on this information the surgeon could fixate the avulsed fibular fragment with a staple and stabilize the syndesmosis with a setscrew, after debridement of the medial gutter to allow the talus to resume its normal position. Without the information obtained from the oblique MRI plane, a more substantial reconstructive surgery would have been planned.

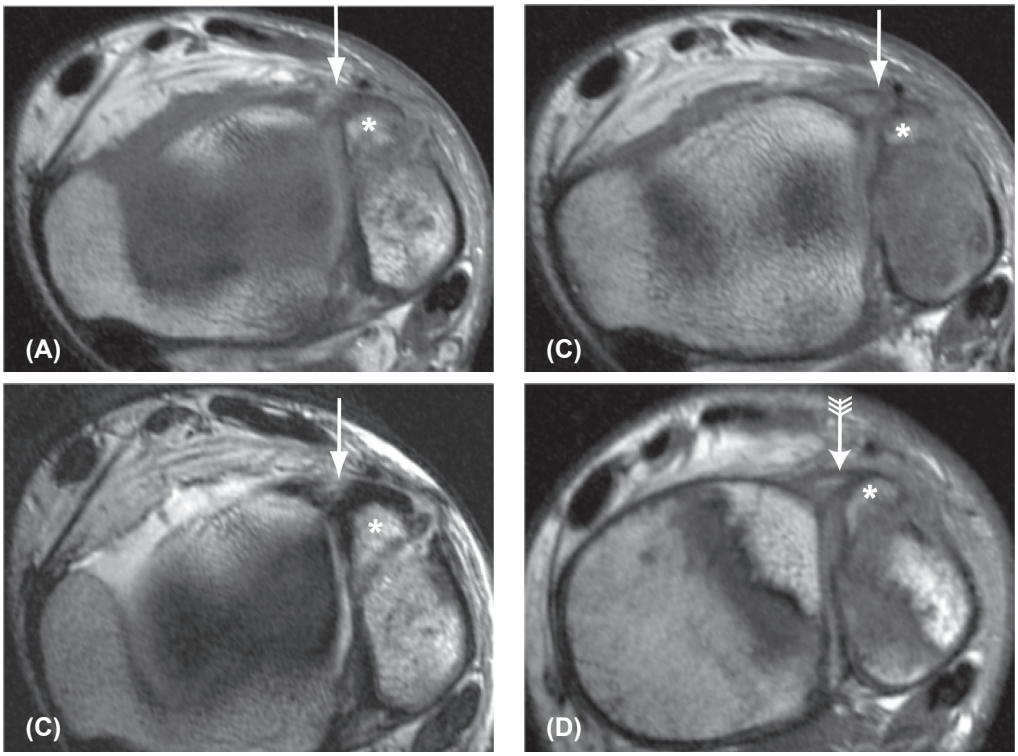

Fig. 7 Axial (*A, B*) and oblique (*D*) proton density and axial (*C*) T2-weighted TSE images of a 12-year-old boy. The two axial proton density-weighted images, at two adjacent levels of the distal tibiofibular joint (*A, B*), demonstrate the avulsion fracture of the anterior aspect of the fibula (*Wagstaffe-Lefort, asterisk*), with a discontinuous aspect of the anterior distal tibiofibular ligament (*arrow*). The axial T2-weighted image (*C*) also shows the fibular avulsion fracture and interrupted anterior syndesmosis. However, on the oblique proton density image (*D*) the fibular avulsion fragment (*asterisk*) is attached to an intact anterior distal tibiofibular ligament (*arrow*).

Discussion

Many studies have been carried out to determine the optimal plane for scanning the lateral collateral ankle ligaments with MRI. Only a few studies have been performed regarding the optimal scan plane for the syndesmotic ligaments [21, 23]. According to the literature the axial and coronal scan planes are optimal for depicting the ATIFL, PTIFL and transverse ligaments, and the axial plane for the interosseous ligament. The basic concept is that a ligament is depicted best when the scan plane runs parallel to the direction of that ligament. Since the ATIFL and PTIFL run in an oblique direction with respect to the tibial plafond, imaging of the ATIFL and PTIFL should be optimal in an oblique plane, instead of the commonly used axial and coronal planes. As one can expect, an obliquely running ligament will likely show a partial or complete discontinuity when imaged in an axial plane.

The ATIFL has antero-posteriorly a triangular shape, is about 1 cm in height and has a thickness of 5 mm. It consists of 3 bundles, separated by 2 mm wide gaps that slightly converge in the laterodistal direction [24]. The superficial anterior fibers are 2 to 3 cm long, the deeper posterior fibers are somewhat shorter [3]. It extends in an oblique way between the anterior tubercle of the distal tibia and the anterior tubercle of the distal fibula and runs from medial-superior to lateral-inferior and crosses the anterolateral corner of the talus. The angle formed between a line along the tibial plafond in the coronal view and a line along the anterior distal tibiofibular ligament varies from 30-50 degrees [24, 28-30].

The PTIFL has a quadrilateral shape, is about 1 cm in height, 6 mm thick and 18 mm wide. Its fibers extend between the posterior tibial malleolus and posterior tubercle of the fibula from medial-superior to lateral-inferior. It runs slightly more horizontally than the anterior tibiofibular ligament [24].

Based on these data it seems a logical step to introduce an oblique image plane for depicting the ATIFL and PTIFL. To find the optimal angle of this oblique plane we first used two cadaveric lower legs. We increased the angle gradually from 30 till 60 degrees with steps of five degrees. In the range of 35-55 degrees, the individual fascicles of both the ATIFL and PTIFL were visible in their entire length. We finally chose an angle of 45 degrees (in consensus JH, NW) as the optimal angle for the oblique image plane, as this angle has an upper and lower range of about 10 degrees without the risk of not depicting the ligaments properly.

In our volunteers we analyzed the ATIFL and PTIFL with regard to continuity, thickening and a wavy aspect of the ligament, since these are characteristics of ligamentous injury [26]. In the axial plane the ATIFL and PTIFL were continuous in 0% respectively 76%, while they were continuous in 88% resp. 100% in the oblique plane. In the axial plane the fascicles were depicted as partly or completely interrupted. This could easily give the impression of a rupture of the ligament [25]. An example of this problem is demonstrated in the paper by Oae et al (Radiol 2003), where axial MRI images showed a rupture of the ATIFL in one patient and a rupture of the PTIFL in another, both of which proved to be incorrect at ankle arthroscopy. Since the range in the angle of the anterior distal tibiofibular ligament varies, it sometimes will happen that not all of its fascicles lie in the oblique image plane of 45 degrees, as occurred in 12% of the healthy volunteers.

Other characteristics of an injured ligament are thickening and a wavy aspect. In two volunteers, one or more of the fascicles of the ATIFL appeared to be thickened in the axial plane (in only one in the oblique plane). Basset described a thick inferior fascicle of the ATIFL as a possible cause of anterolateral tibiotalar impingement [31]. The ATIFL consisted of two or three rather thick fascicles in some, and multiple thin fascicles in other volunteers. Since

none of the volunteers had a history of serious ankle trauma or current ankle complaints, it is reasonable to assume that a thickened aspect of one or more of the fascicles, especially when present in both ankles, could be a normal variant. Possibly the ATIFL is composed of a variable number of fascicles, with variable thickness, instead of the three mentioned by Bartonicek [24]. SubHas et. al. also mention a thickened inferior ligament (i.e. Bassett) in the presence of a normal ATIFL [32].
In a few cases the ATIFL or PTIFL demonstrated a wavy aspect in the axial plane, in 10 resp. 2 cases, and remained wavy in the oblique plane, in 2 resp. 0 cases (Fig. 8). It is not clear why the wavy aspect of these ligaments, as observed in the axial plane, disappeared in the oblique plane. Possibly, insertion of the ligament on a slightly protruding tibial and fibular tubercle gives this impression. A wavy aspect of the syndesmotic ligaments has until now been interpreted as a sign of injury and could therefore also lead to false positive findings.

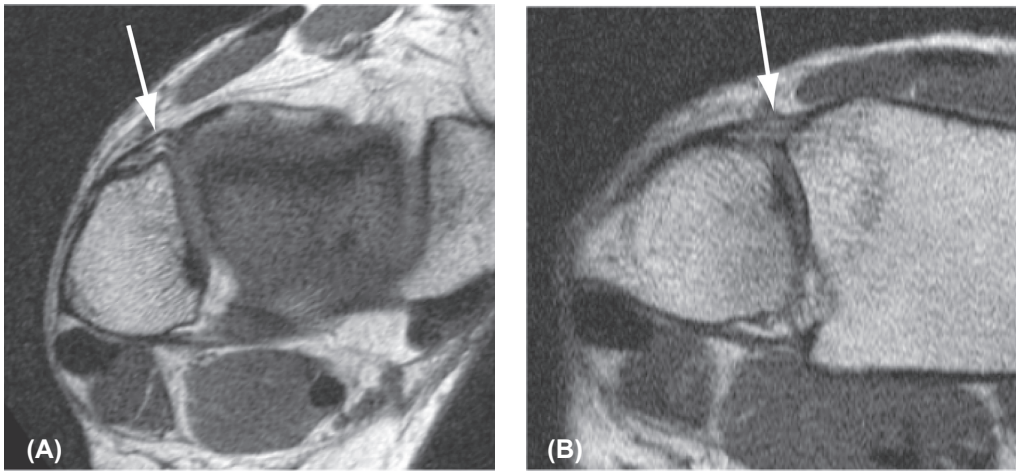

Fig. 8 Axial (*A*) and oblique (*B*) T1-weighted TSE image of the ATIFL (*arrow*) in a healthy volunteer. The ATIFL has a wavy aspect on the axial image (*A*) and a straight aspect on the oblique image (*B*). The continuity and multifascicular aspect of the ATIFL are better demonstrated on the oblique image. A wavy aspect of the ATIFL can thus not be used as a parameter for injury of the ATIFL, in an axial scan plane.

Although the agreement score regarding the different characteristics of the ATIFL and PTIFL was generally good (86% - 100%), the kappa value (κ) however varied from fair to good (0,23 – 0,90) (Table 1, *see previous page*). For example the agreement score regarding continuity of the PTIFL in the oblique plane was 100%, while kappa was only 0,65. Discrepancies between the percentage agreement and kappa values in our case can be explained by the skewed distribution of categories. In such cases kappa is known to have poor properties as an index for measuring agreement. In two cases, continuity and wavy aspect of the PTIFL in the oblique plane, the value for kappa could not even be determined [33].
We compared the oblique plane only with the axial plane and not with the coronal plane. The oblique and axial plane differ in only one parameter i.e. the angle in which the ligaments are depicted, while the cross sectional direction is the same, whilst the oblique and coronal plane differ in two parameters, i.e. both a different cross sectional direction as well as a different plane. Although the coronal view is good for depicting the multifascicular aspect of the ATIFL and PTIFL, in our volunteers the fascicles of the ATIFL and PTIFL were never entirely

visible along their full length between their insertion on the tibia and fibula. The coronal plane is therefore less suited for analysis of traumatic changes.
Our study has several shortcomings. First, we only used two cadaveric legs. It would be better to determine the range of angles of the ATIFL and PTIFL in a larger number cadaveric legs or volunteers. Maybe the ATIFL and PTIFL should each be scanned with a different optimal angle? Second, ideally the best way to analyze the ATIFL and PTIFL would be to determine the exact angle of both ligaments in each individual separately.This would mean that in each individual first an axial and coronal dataset should be acquired. Subsequently in the axial plane the angle with the coronal plane could be established and next in the coronal images the angle with the axial plane. However this would make it an elaborate and time consuming procedure and not very practical. We therefore chose a fixed angle of 45 degrees for the oblique MRI scan plane and accept a small percentage (12%) of partly interrupted ligaments.
Third, although the volunteers are healthy, it is unlikely they never had any previous ankle trauma. On average almost everyone sustains an inversion injury of the ankle once during their lifetime.Thirty nine percent of the volunteers had signs of minor injury of the collateral ankle ligaments, visible as a slight thickening of one or more of the collateral ankle ligaments. Although isolated injury of the syndesmosis, known as a high sprain, can occur, it often has a more protracted recovery period and therefore would be easier remembered. On the other hand minor syndesmotic injury could also go undetected and heal with a slight thickening or maybe wavy aspect of the ATIFL.
Clinically, information about the integrity of the syndesmotic ligaments is of importance, because it determines the kind of therapy the patient gets. Especially the ATIFL plays an important role in stability of the syndesmosis. In case of an isolated injury of the ATIFL (a high sprain) a complete rupture of the ATIFL should be treated with a no weight bearing cast or surgery, while a partly ruptured ATIFL can be treated functionally with a weight bearing cast.
Until now the ATIFL and PTIFL have been scanned in the usual orthogonal MRI scan planes. The advantage of scanning in an oblique image plane of about 45 degrees lies in a better depiction of both ligaments when compared to the axial plane and with it a better interpretation of continuity, thickening and wavy contour. This may lead to a reduction in false positive results, especially regarding partly or completely ruptured ligaments, and can be of considerable aid in therapeutic management.

Conclusion

The MRI scans for the syndesmosis ligaments ATIFL and PTIFL have been carried out in the three usual orthogonal scan planes. The advantage of scanning in an oblique image plane of about 45 degrees lies in a better depiction of both ligaments when compared to the axial plane, and with it a better interpretation of continuity, thickening and wavy contour. This may lead to a reduction in false positive results, especially regarding partly or completely ruptured ligaments, and can be of considerable aid in therapeutic management as demonstrated by the three clinical cases.

References

1. Cedell CA. Ankle lesions. Acta orthopaedica Scandinavica. 1975; 46(3):425-445.
2. Hopkinson WJ, St Pierre P, Ryan JB, Wheeler JH. Syndesmosis sprains of the ankle. Foot & ankle. 1990; 10(6):325-330.
3. Brostroem L. Sprained Ankles. I. Anatomic Lesions in Recent Sprains. Acta Chir Scand. 1964; 128:483-495.
4. Gerber JP, Williams GN, Scoville CR, Arciero RA, Taylor DC. Persistent disability associated with ankle sprains: a prospective examination of an athletic population. Foot & ankle international / American Orthopaedic Foot and Ankle Society [and] Swiss Foot and Ankle Society. 1998; 19(10):653-660.
5. Beumer A, Heijboer RP, Fontijne WP, Swierstra BA. Late reconstruction of the anterior distal tibiofibular syndesmosis: good outcome in 9 patients. Acta orthopaedica Scandinavica. 2000; 71(5):519-521.
6. Beumer A, Valstar ER, Garling EH, Niesing R, Ginai AZ, Ranstam J, et al. Effects of ligament sectioning on the kinematics of the distal tibiofibular syndesmosis: a radiostereometric study of 10 cadaveric specimens based on presumed trauma mechanisms with suggestions for treatment. Acta Orthop. 2006; 77(3):531-540.
7. Kelikian H KA. Disorders of the ankle. Philadelphia-London-Toronto: Saunders Company, 1985.
8. Cedell CA. Supination-outward rotation injuries of the ankle. A clinical and roentgenological study with special reference to the operative treatment. Acta orthopaedica Scandinavica. 1967:Suppl 110:113+.
9. Riede UN, Schenk RK, Willenegger H. [Joint mechanical studies on post-traumatic arthrosas in the ankle joint. I. The intra-articular model fracture]. Langenbecks Arch Chir. 1971; 328(3):258-271.
10. Ramsey PL, Hamilton W. Changes in tibiotalar area of contact caused by lateral talar shift. J Bone Joint Surg Am. 1976; 58(3):356-357.
11. Pneumaticos SG, Noble PC, Chatziioannou SN, Trevino SG. The effects of rotation on radiographic evaluation of the tibiofibular syndesmosis. Foot & ankle international / American Orthopaedic Foot and Ankle Society [and] Swiss Foot and Ankle Society. 2002; 23(2):107-111.
12. Beumer A, van Hemert WL, Niesing R, Entius CA, Ginai AZ, Mulder PG, et al. Radiographic measurement of the distal tibiofibular syndesmosis has limited use. Clinical orthopaedics and related research. 2004(423):227-234.
13. Brage ME, Bennett CR, Whitehurst JB, Getty PJ, Toledano A. Observer reliability in ankle radiographic measurements. Foot & ankle international / American Orthopaedic Foot and Ankle Society [and] Swiss Foot and Ankle Society. 1997; 18(6):324-329.
14. Wrazidlo W, Karl EL, Koch K. [Arthrographic diagnosis of rupture of the anterior syndesmosis of the upper ankle joint]. Rofo. 1988; 148(5):492-497.
15. Karl EL, Wrazidlo W. [Fresh rupture of the syndesmosis of the proximal ankle joint. Clinical significance and arthrographic diagnosis]. Der Unfallchirurg. 1987; 90(2):92-96.
16. Sanders HW. Ankle arthrography and ankle distortion. Radiol Clin (Basel). 1977; 46(1):1-10.
17. Milz P, Milz S, Steinborn M, Mittlmeier T, Putz R, Reiser M. Lateral ankle ligaments and tibiofibular syndesmosis. 13-MHz high-frequency sonography and MRI compared in 20 patients. Acta orthopaedica Scandinavica. 1998; 69(1):51-55.
18. Ebraheim NA, Lu J, Yang H, Mekhail AO, Yeasting RA. Radiographic and CT evaluation of tibiofibular syndesmotic diastasis: a cadaver study. Foot & ankle international / American Orthopaedic Foot and Ankle Society [and] Swiss Foot and Ankle Society. 1997; 18(11):693-698.
19. Brown KW, Morrison WB, Schweitzer ME, Parellada JA, Nothnagel H. MRI findings associated with distal tibiofibular syndesmosis injury. Ajr. 2004; 182(1):131-136.
20. Takao M, Ochi M, Oae K, Naito K, Uchio Y. Diagnosis of a tear of the tibiofibular syndesmosis. The role of arthroscopy of the ankle. The Journal of bone and joint surgery. 2003; 85(3):324-329.
21. Muhle C, Frank LR, Rand T, Ahn JM, Yeh LR, Trudell D, et al. Tibiofibular syndesmosis: high-resolution MRI using a local gradient coil. J Comput Assist Tomogr. 1998; 22(6):938-944.
22. Vogl TJ, Hochmuth K, Diebold T, Lubrich J, Hofmann R, Stockle U, et al. Magnetic resonance imaging in the diagnosis of acute injured distal tibiofibular syndesmosis. Investigative radiology. 1997; 32(7):401-409.
23. Schneck CD, Mesgarzadeh M, Bonakdarpour A, Ross GJ. MR imaging of the most commonly injured ankle ligaments. Part I. Normal anatomy. Radiology. 1992; 184(2):499-506.
24. Bartonicek J. Anatomy of the tibiofibular syndesmosis and its clinical relevance. Surg Radiol Anat. 2003; 25(5-6):379-386.
25. Oae K, Takao M, Naito K, Uchio Y, Kono T, Ishida J, et al. Injury of the tibiofibular syndesmosis: value of MR imaging for diagnosis. Radiology. 2003; 227(1):155-161.
26. Kim S, Huh YM, Song HT, Lee SA, Lee JW, Lee JE, et al. Chronic tibiofibular syndesmosis injury of ankle: evaluation with contrast-enhanced fat-suppressed 3D fast spoiled gradient-recalled acquisition in the steady state MR imaging. Radiology. 2007; 242(1):225-235.
27. Beumer A. Chronic instability of the anterior syndesmosis of the ankle. Acta orthopaedica. 2007; 78(327):4-36.
28. 28. Grass R, Herzmann K, Biewener A, Zwipp H. [Injuries of the inferior tibiofibular syndesmosis]. Der Unfallchirurg. 2000; 103(7):520-532.
29. Kapanji I. Funktionelle Anatomie der Gelenke. Gerlingen: Ferdinand Enke Verlag, 1985.
30. Ebraheim NA, Taser F, Shafiq Q, Yeasting RA. Anatomical evaluation and clinical importance of the tibiofibular syndesmosis ligaments. Surg Radiol Anat. 2006; 28(2):142-149.
31. Bassett FH, 3rd, Gates HS, 3rd, Billys JB, Morris HB, Nikolaou PK. Talar impingement by the anteroinferior tibiofibular ligament. A cause of chronic pain in the ankle after inversion sprain. J Bone Joint Surg Am. 1990; 72(1):55-59.

32. Subhas N, Vinson EN, Cothran RL, Santangelo JR, Nunley JA, 2nd, Helms CA. MRI appearance of surgically proven abnormal accessory anterior-inferior tibiofibular ligament (Bassett's ligament). Skeletal Radiol. 2008; 37(1):27-33.
33. Feinstein AR, Cicchetti DV. High agreement but low kappa: I. The problems of two paradoxes. J Clin Epidemiol. 1990; 43(6):543-549.

Chapter 5

Tibiofibular syndesmosis in acute ankle fractures: additional value of an oblique MR image plane

John J. Hermans
Annechien Beumer
Wim C.J. Hop
Adrianus F.C.M. Moonen
Abida Z. Ginai

Skeletal Radiology accepted 2011 Apr

Abstract

Objective: To evaluate the additional value of a 45° oblique MRI scan plane for assessing the anterior and posterior distal tibiofibular syndesmotic ligaments in patients with an acute ankle fracture.

Materials and Methods: Prospectively, data of 44 consecutive patients with an acute ankle fracture who underwent a radiograph (AP, lateral and mortise view) as well as a MRI, in both the standard three orthogonal planes and in an additional 45° oblique plane was collected. The fractures on the radiographs were classified according to Lauge-Hansen (LH). The aspect of the anterior (ATIFL) and posterior (PTIFL) distal tibiofibular ligaments, as well as the presence of a bony avulsion in both the axial and oblique planes were evaluated on MRI. MRI findings regarding syndesmotic injury in the axial and oblique planes were compared to syndesmotic injury predicted by LH. Kappa, and the agreement score was calculated to determine the interobserver agreement. The Wilcoxon signed rank test and McNemar's test were used to compare the two scan planes.

Results: The interobserver agreement (κ) and agreement score (AS (%)) regarding injury of the ATIFL and PTIFL, and the presence of a fibular or tibial avulsion fracture, was good to excellent in both the axial and oblique image planes ($0.61<\kappa<0.92$; $84\%<AS<95\%$). For both ligaments the oblique image plane demonstrated significantly less injury than the axial plane ($p<0.001$). There was no significant difference in detection of an avulsion fracture in the axial or oblique plane, neither anteriorly ($p=0.50$) nor posteriorly ($p=1.00$). With syndesmotic injury as predicted by LH as comparison, the specificity in the oblique MR plane increased for both anterior (from 7% to 86%) and posterior (from 48% to 86%) syndesmotic injury when compared to the axial plane.

Conclusion: Our results show the additional value of an 45° oblique MR image plane for detection of injury of the anterior and posterior distal tibiofibular syndesmosis in acute ankle fractures. Findings of syndesmotic injury in the oblique MRI plane were closer to the diagnosis as assumed by the Lauge-Hansen classification than in the axial plane. With more accurate information, the surgeon can better decide when to stabilize syndesmotic injury in acute ankle fractures.

Introduction

Disruption of the distal tibiofibular syndesmosis in ankle fractures is common and usually results from an external rotation injury. In up to 13% of all ankle fractures, and in 20% of patients requiring internal fixation, there will be an associated injury to the syndesmosis [1-4]. It is commonly agreed that adequate reduction of ankle fractures reduces late osteoarthritis. However, evaluating syndesmotic stability in ankle fractures is still a subject of debate as it is unclear when to stabilize an injured syndesmosis [5-12].

The value of MRI in acute and chronic syndesmotic injuries has been described in several articles, and the axial image is known to be the most useful image plane [13-17]. However, imaging in the axial plane can result in false positive findings [14, 18] since the anterior and posterior distal tibiofibular ligament run in an oblique plane [19, 20]. Several studies reported that the most commonly injured and reliably visualized anterior tibiofibular ligament on MRI might not be seen in its entire length on one single transverse image, and a partially imaged ligament may be mistaken as a tear despite careful observation of contiguous slices [16, 21, 22]. A recent study demonstrated that the anterior and posterior syndesmotic ligaments are better depicted in an oblique image plane of about 45° when compared to the axial plane, and that the integrity of the ligaments can be better evaluated [23]. Therefore, this prospective study evaluated the additional value of an oblique MRI scan plane for assessing the anterior and posterior distal tibiofibular syndesmotic ligaments in patients with an acute ankle fracture.

Materials and Methods

The data of 44 consecutive patients with an acute ankle fracture who underwent a radiograph as well as a MRI in both the standard three orthogonal planes and in an additional oblique plane was collected and analyzed. In the 44 patients, the fracture distribution according to Lauge-Hansen was 59% supination external rotation (SE), 5% pronation external rotation (PE), 25% supination adduction (SA), 9% pronation adduction (PA), 2% pronation dorsiflexion (PD). The mean age of the patients was 36 years and ranged between 16-61 years; 25 were men and 19 were women. In 24 patients the injury involved the left and in 20 the right ankle. In 16 patients the fracture was treated with an open reduction and internal fixation (ORIF), with a setscrew placed in 4 patients.

Written informed consent was obtained and the study was approved by the institutional review board. Inclusion criteria were an acute ankle fracture not older than 48 hours after trauma, and closure of the growth plates. Exclusion criteria were associated neurological or vascular injuries, fractures associated with a hindfoot or midfoot fracture, a former trauma of the ankle, contra-indications for MRI, and an insufficient knowledge of the Dutch language.

Radiographs obtained at presentation included AP, lateral and mortise views. The fractures on the radiographs were classified according to Lauge-Hansen (Table 1, *see next page*) by a radiologist with 11 years experience in musculoskeletal radiology (JH).

MRI was performed on a 1.5 T Gyroscan (Philips, Best, the Netherlands) with a wrap-around ankle coil (E1 coil). The foot was kept in a fixed (neutral) position and stabilized with sandbags or a plaster. Dual TSE images (TR=3500-4500ms; TE=11ms; TE=120ms; Echo train length=14) were performed in three orthogonal planes, i.e. axial, coronal and sagittal, and in an additional 45˚ oblique plane. The oblique image plane was defined in the coronal and sagittal views (Fig. 1).

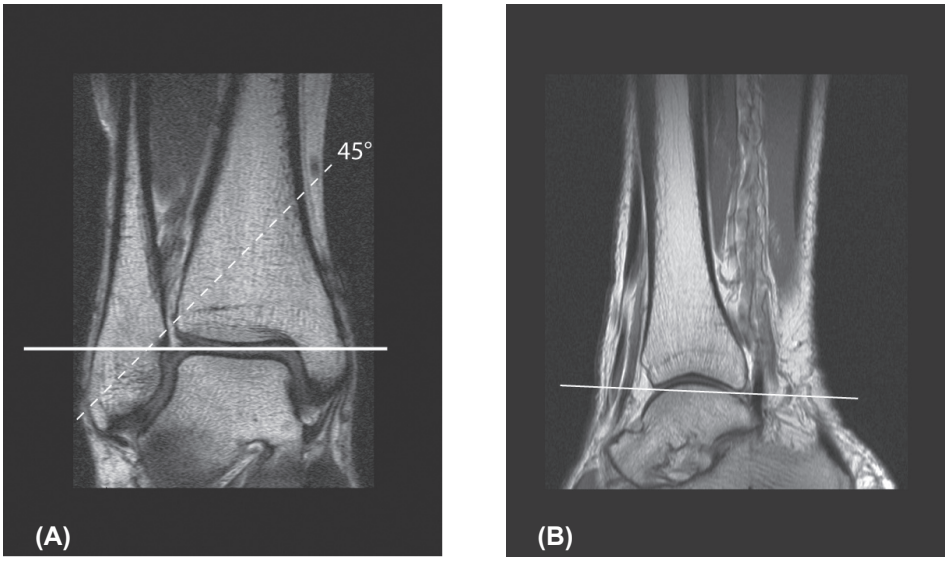

Fig. 1: Coronal (*A*) and sagittal (*B*) MR image, which indicate the angle of the 45º oblique image plane for the anterior and posterior distal tibiofibular ligament. In the coronal plane the angle of 45º is related to the tibial plafond. In the sagittal view the direction of the oblique plane runs parallel to a line along the inferior border of the anterior and posterior tibia.

In the coronal view the 45˚ angle of the oblique plane was related to the tibial plafond and ran in a caudal-cranial and lateral-medial direction through the distal fibula. In the sagittal view the direction of the oblique plane ran parallel to a line along the inferior border of the anterior and posterior tibia. All series were performed with a 512×512 matrix. The field of view was 18-20cm for coronal and sagittal imaging, and 12-15cm for axial and oblique imaging. The slice thickness of the images was 3.0mm (gap 0.3mm) with a NSA of 2. A STIR, i.e. a short tau inversion recovery image (TR=1460ms; TE=15ms; Echo train length=14), was performed in the coronal plane, with a field of view of 18-20cm, a slice thickness of 4mm (gap 0,4mm) and a 256x256 matrix.

Table 1. The Lauge-Hansen fracture classification describes the mechanisms of ankle fractures, based on the position of the foot at the time of injury and the direction in which the talus moves within the ankle mortise. It defines both the bony and ligamentous injury. The following five groups of ankle fractures can be discerned: supination-adduction, supination-eversion, pronation-abduction, pronation-eversion and pronation-dorsiflexion. Depending on the degree of severity the main groups can be further divided into stages.

Type of injury Foot position/ direction of force	**Pathology**
Supination adduction	1) Transverse fracture fibula at or distal to the level of the tibiofibular joint/ tear of collateral ligaments 2) Vertical, oblique fracture of the medial malleolus/ tear of the deltoid ligament
Supination eversion (external rotation)	1) Disruption of the anterior tibiofibular ligament or an avulsion of its tibial attachment (*Tillaux fracture*) or fibular attachment (*Wagstaffe-Le Fort fracture*) 2) Spiral, oblique fracture of the distal fibula. The fracture line runs from proximal posterior to distal anterior at a variable distance from the tibiotalar joint 3) Disruption of the posterior tibiofibular ligament or fracture of the posterior malleolus 4) Fracture of the medial malleolus or rupture of the deltoid ligament
Pronation abduction	1) Transverse fracture of the medial malleolus or rupture of the deltoid ligament 2) Rupture of the anterior and posterior syndesmotic ligaments or avulsion fracture of their insertion(s) 3) Short, oblique fracture of the fibula 0,5-1cm above the distal articular surface of the tibia
Pronation eversion (external rotation)	1) Transverse fracture of the medial malleolus or disruption of the deltoid ligament 2) Disruption of the anterior tibiofibular ligament. The ligament may avulse its tibial attachment (*Tillaux fracture*) 3) High oblique, spiral fibular fracture. No fracture is less than 2,5 cm above the tibiotalar joint. The fracture pattern runs from proximal anterior to distal posterior. The fibula may fracture proximally at the neck (*Maisonneuve fracture*) 4) Rupture of posterior tibiofibular ligament or avulsion fracture of the posterolateral tibia
Pronation dorsiflexion/ pilon fracture	1) Fracture of the medial malleolus 2) Fracture of the anterior margin of the tibia 3) Supramalleolar fracture of the fibula 4) Transverse fracture of the posterior tibial surface

The MR images were independently analyzed by two radiologists with respectively 11 and 31 years of musculoskeletal experience (JH, AG). They were blinded to the results of the radiographs. The majority of the patients were examined with MRI on the day of injury. All were examined within 10 days of injury and 5 patients were examined postoperatively.

The anterior and posterior syndesmosis consist of their ligament and their tibial and fibular attachment sites. We first evaluated these two aspects of the syndesmosis separately, and then combined these findings, as this coincides with clinical practice regarding syndesmotic injury. On MRI the syndesmotic ligaments, i.e. the anterior and posterior distal tibiofibular ligament, were evaluated in both the axial and oblique planes and assigned a score: 0 = normal; 1 = thickened; 2 = partially ruptured or 3 = completely ruptured. A normal distal tibiofibular ligament consisted of multiple continuous thin fibres interspersed with normal high signal intensity fat on dual TSE weighted images. In a thickened ligament the continuous fibres were thickened, not sharp and the signal intensity of fat was intermediate on dual TSE weighted images. A complete rupture was defined when the ligament was either discontinuous or invisible, or showed increased signal intensity with fluid in the ligament on T2-weighted TSE images. In a partially ruptured ligament the discontinuity was not complete [16, 18, 20, 23, 24].

The presence of a bony avulsion, both anteriorly and posteriorly, was also assigned a score: 0 = no avulsion; 1 = tibial avulsion; 2 = fibular avulsion; 3 = avulsion of both tibial and fibular tubercle. Anteriorly this classification was according to Wagstaffe. Posteriorly a fracture of the malleolus tertius, irrespective of its size, was defined as an avulsion.

The findings of the aspect of the distal tibiofibular ligament in combination with the presence of a bony avulsion were combined into the overall presence of anterior or posterior syndesmotic injury: 0 = normal syndesmosis, i.e. normal ligament without bony avulsion; 1 = thickened syndesmosis, i.e. thickened ligament without bony avulsion; 2 = partially ruptured syndesmosis, i.e. partially ruptured ligament without bony avulsion; 3 = completely ruptured syndesmosis, i.e. ruptured ligament without a bony avulsion or an intact ligament with a bony avulsion.

The interobserver agreement was determined by the kappa agreement score (κ) (0.00 – 0.20: poor; 0.21 – 0.40: fair; 0.41 – 0.60 moderate; 0.61 – 0.80 good; 0.81 – 0.90: very good; 0.91 – 1.00: excellent agreement). In case of ordinal scores, i.e. the aspect of the ATIFL and PTIFL, a weighted kappa agreement score was determined. The Wilcoxon signed rank test was used to compare the axial and oblique scan planes regarding the aspect of the ATIFL and PTIFL, and the overall injury scores of anterior and posterior syndesmotic injury. The McNemar test was used to compare the axial and oblique scan planes regarding the presence of an avulsion fracture. The sensitivity and specificity for detection of syndesmotic injury were determined when MRI findings were compared with Lauge-Hansen. A two-sided p-value less than 0.05 was considered as significant. Statistical analysis was performed with Stat (version 11.0; Statacorp., College station, Texas, USA).

Results

The kappa regarding the aspect of the ATIFL was respectively 0.61 and 0.92 for the axial respectively oblique image plane, with agreement scores (AS) of 84% and 91%, respectively (Table 2).The kappa regarding the presence of a tibial or fibular avulsion fracture of the ATIFL was respectively 0.71 and 0.84 for the axial and oblique image planes, with agreement scores (AS) of 91% and 95%, respectively.

Compared to the axial plane, the oblique plane demonstrated in 45% (20/44) lower injury scores and in 55% (24/44) equal injury scores of the ATIFL ($p<0.001$) (Fig. 2). Nine patients showed an avulsion fracture anteriorly. The presence of a tibial or fibular avulsion of the ATIFL was not significantly different in the axial and oblique planes ($p = 0.50$). Anteriorly, 2/3 patients with a tibial, and 5/6 patients with a fibular avulsion fracture showed injury of the ATIFL in the axial plane, whereas in the oblique plane none of the avulsion fractures was associated with injury of the ATIFL (Fig. 3, Fig. 4).

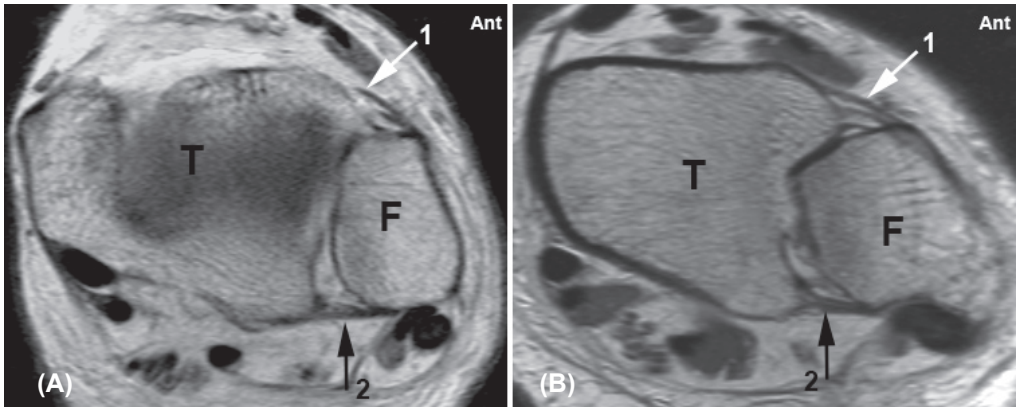

Fig. 2 Axial (*A*) and oblique (*B*) proton density TSE (turbo spin echo) image. In the axial plane (*A*) the multifascicular AITFL (1) is discontinuous, while in the oblique plane (*B*) the fascicles of the AITFL are intact. In both planes the PITFL (2) is intact. T, tibia; F, fibula; Ant, anterior.

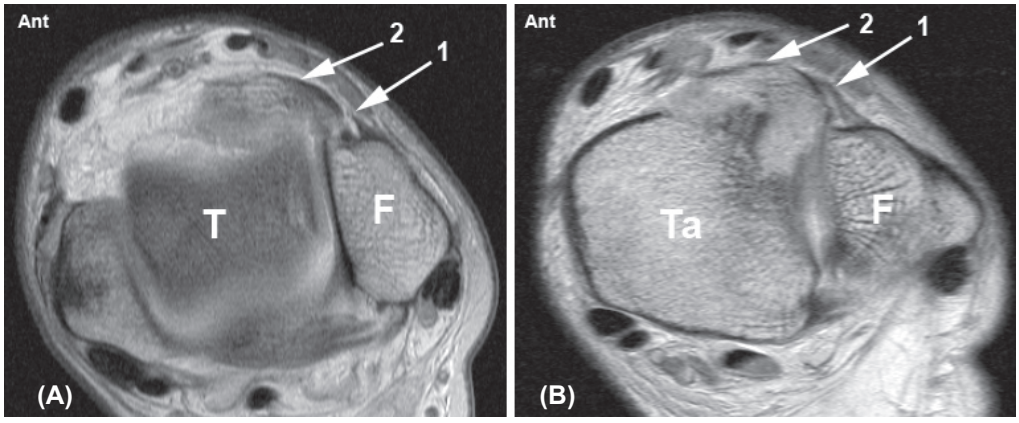

Fig. 3 Axial (*A*) and oblique (*B*) proton density TSE (turbo spin echo) image. In the axial plane (*A*) the AITFL (1) is discontinuous. There is a large avulsion fragment from the anterior tibial tubercle (2). (*B*) In the oblique plane the intact AITFL is attached to the tibial avulsion fracture. This is an example of a Wagstaffe type I fracture (or Chaput-Tillaux fracture) with an intact AITFL. T, tibia; F, fibula; Ta, talus; Ant, anterior.

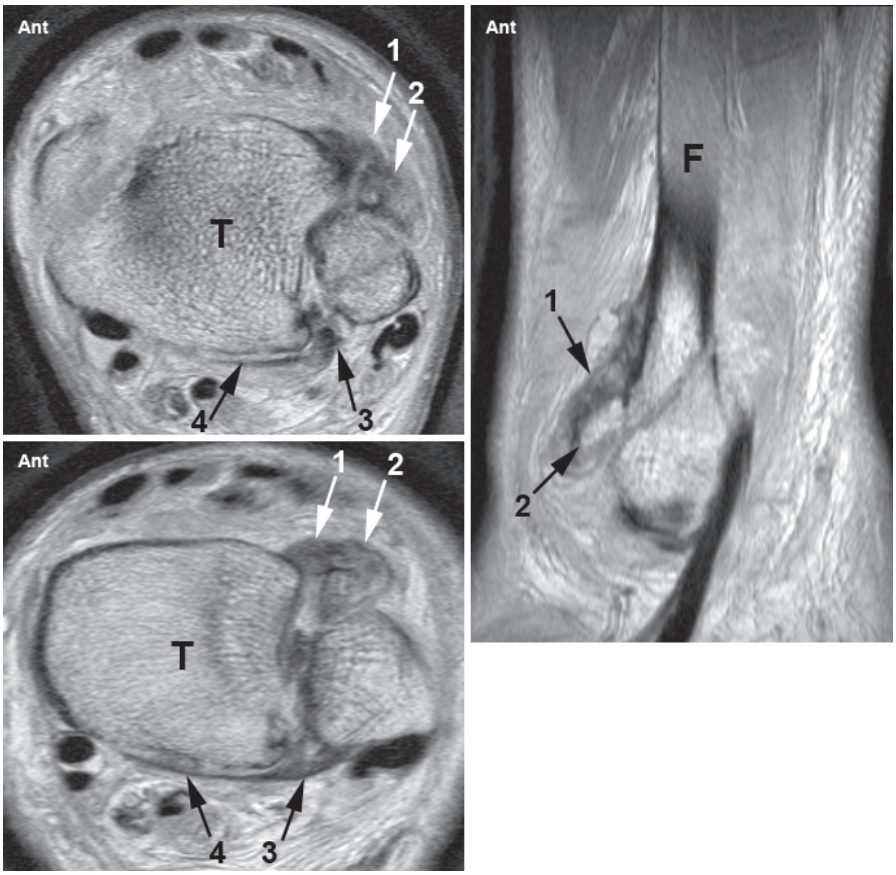

Fig. 4 Axial, oblique and sagittal proton density TSE (turbo spin echo) images. In the axial plane (*upper left*) the AITFL (1) is discontinuous. In front of the fibula lies an avulsed fibular fragment (2). In the oblique plane (lower left), the continuous AITFL (1) is attached to the fibular avulsion (2). On the sagittal image (*right*) the avulsion fracture from the anterior tubercle of the fibula is just visible above the obliquely running fibula fracture. This is a type II Wagstaffe fracture: a fibular avulsion fragment attached to an intact AITFL. Posteriorly the PITFL (3) is ruptured in the axial plane (upper left). In the oblique plane (*lower left*) the intact PITFL (3) is attached to a slip of periost from the posterior malleolus (4). T, tibia; F, fibula; Ant, anterior.

Table 2: Interobserver agreement (kappa) and agreement score (AS (%)) between the axial and oblique MRI planes regarding the aspect of the anterior (ATIFL) and posterior (PTIFL) distal tibiofibular ligament, the presence of a tibial or fibular avulsion fracture and overall presence of anterior or posterior syndesmotic injury. P-values refer to comparison between the axial and oblique plane.

	ATIFL					PTIFL				
	Axial		Oblique			Axial		Oblique		
	κ	AS (%)	κ	AS (%)	p	κ	AS (%)	κ	AS (%)	p
Ligament	0.61	84	0.92	91	<0.001	0.83	84	0.86	91	<0.001
Avulsion	0.71	91	0.84	95	0.50	0.83	93	0.83	91	1,00
Syndesmosis	0.48	84	0.81	86	<0.001	0.79	80	0.83	89	<0.001

The kappa for the aspect of the PTIFL was respectively 0.83 and 0.86 for the axial and oblique image planes, with agreement scores (AS) of 84% and 91%, respectively (Table 2). The kappa regarding the presence of a tibial or fibular avulsion fracture of the PTIFL was 0.83 for both the axial and oblique image plane, with an agreement score (AS) of 93% for both planes.
Compared to the axial plane, the oblique plane demonstrated in 62% (27/44) lower injury scores and in 36% (16/44) equal injury scores of the PTIFL ($p<0.001$). In 2% (1/44) the injury score in the oblique plane was higher than in the axial plane. Eleven patients showed an avulsion fracture posteriorly. The presence of a tibial or fibular avulsion of the PTIFL was not significantly different in the axial and oblique planes ($p = 1.00$). Posteriorly there were only avulsion fractures of the tibia and none of the fibula. In 6/11 patients with a posterior tibial avulsion, the PTIFL was injured in the axial plane but not in the oblique plane (Fig. 5)

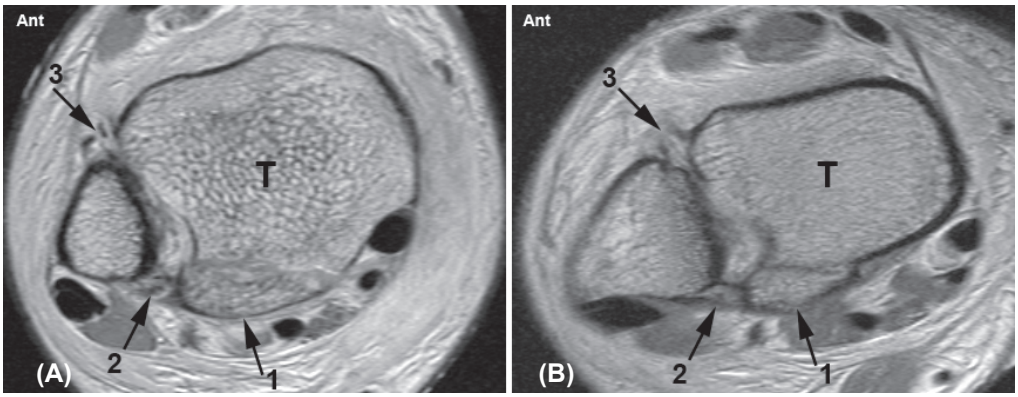

Fig. 5 Axial (*A*) and oblique (*B*) proton density TSE (turbo spin echo) image. (*A*) Posterolateral oblique fracture of the posterior malleolus (1) with a discontinuous PITFL (2) in the axial plane, but with an intact PITFL in the oblique plane (*B*). In both planes the AITFL (3) is ruptured. T, tibia; Ant, anterior.

Findings of ligament integrity and the presence of an avulsion fracture were combined to determine overall anterior or posterior syndesmotic injury. The kappa regarding anterior syndesmotic injury was respectively 0.48 and 0.81 in the axial and oblique image planes, with agreement scores (AS) of 84% and 86%, respectively. The oblique image plane demonstrated significantly less anterior syndesmotic injury than the axial plane ($p < 0.001$). Regarding posterior syndesmotic injury, the kappa was 0.76 resp. 0.79 for the axial resp. oblique image plane, with a respective agreement score (AS) of 75% and 79%. The oblique image plane showed significantly less posterior syndesmotic injury than the axial plane ($p < 0.001$).
We compared the overall anterior and posterior syndesmotic injury as found on MRI, with syndesmotic injury as defined by the Lauge-Hansen fracture classification on the radiograph (Table 3). In 14 patients Lauge-Hansen predicted absence of injury of the anterior syndesmosis, whereas MRI demonstrated absence of injury in 1 patient in the axial plane and in 12/14 patients in the oblique plane. In 30 patients Lauge-Hansen predicted presence of injury of the anterior syndesmosis, which was shown in 30 and 28 patients in the axial and oblique plane, respectively (Table 3). Compared to LH, this resulted in a sensitivity and specificity of respectively 100% and 7% for the axial plane, and a sensitivity and specificity of respectively 93% and 86% for the oblique plane for detection of anterior syndesmotic injury.

In 29 patients Lauge-Hansen predicted absence of injury of the posterior syndesmosis, whereas MRI demonstrated absence of injury in 14 patients in the axial plane and in 25 patients in the oblique plane (Fig. 6). In 15 patients Lauge-Hansen predicted presence of injury of the posterior syndesmosis, which was shown in 13 and 11 patients in the axial and oblique plane respectively (Table 3). Compared to LH, this resulted in a sensitivity and specificity of respectively 87% and 48% for the axial planes, and a sensitivity and specificity of respectively 73% and 86% for the oblique plane for detection of posterior syndesmotic injury.

Table 3: Anterior and posterior overall syndesmotic injury on MRI, i.e. injury to distal tibiofibular ligament or avulsion fracture, in the axial (ax) and oblique (obl) image planes, related to the Lauge-Hansen (LH) fracture classification on the radiograph. Normal and thickened ligament (0/1) and partial and ruptured ligament (2/3) are grouped together. Anterior or posterior syndesmotic injury in LH: absent = 0 and present = 1.

	LH anterior injury				LH posterior injury			
MRI	**0**		**1**		**0**		**1**	
	ax	*obl*	*ax*	*obl*	*ax*	*obl*	*ax*	*obl*
0/1	1	12	0	2	14	25	2	4
2/3	13	2	30	28	15	4	13	11

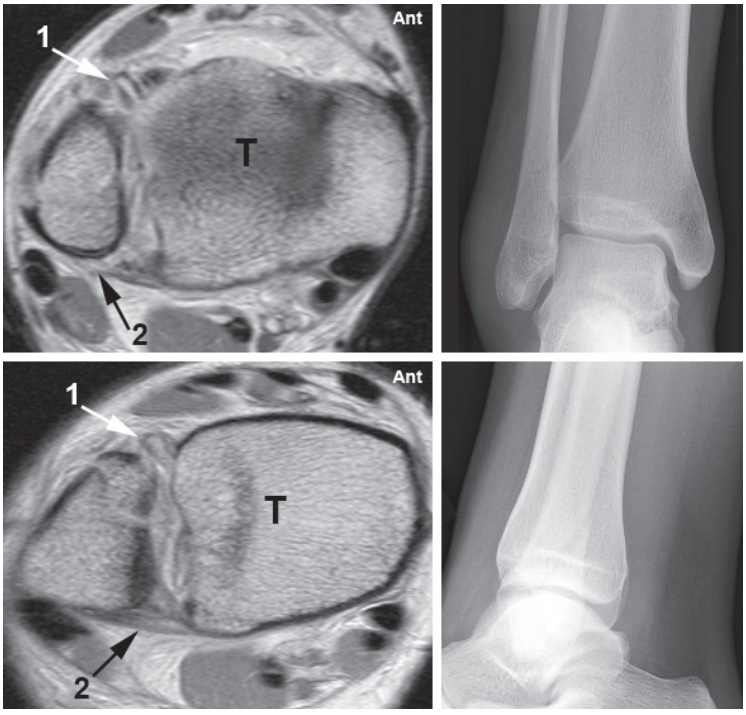

Fig. 6 Axial (*upper left*) and oblique (*lower left*) proton density TSE (turbo spin echo) image. AP (*upper right*) and lateral (*lower right*) radiograph. A local swelling at the level of the distal fibula is visible on the AP radiograph. The lateral radiograph shows an oblique fracture in the distal fibula. According to Lauge-Hansen this is a supination-external rotation type 2 fracture (SE2). In the axial plane (*upper left*) the AITFL (1) and PITFL (2) are both discontinuous. In the oblique plane (*lower left*) the AITFL is also discontinuous, but the multifascicular PITFL is intact. The fracture line through the fibula is visible in both planes. T, tibia; Ant, anterior.

Discussion

Our study population consisted of 44 consecutive patients with an acute ankle fracture. The fracture distribution was conform other studies with reported fracture types of LH type SE (42-72%), PE (7-22%), SA (6-20%) and PA (5-21%) [25].

Many clinical and radiographic tests have been suggested to diagnose a disruption of the syndesmosis. Clinical tests include the squeeze test, Cotton test, exorotation stress test and fibula translation test, but these are not reliable when syndesmotic injury is associated with an ankle fracture because of the pain, swelling and dislocation [26]. Radiologically the syndesmosis can be evaluated with a radiograph, ultrasound, CT or MRI. Several authors have described that a radiograph has limited value in the assessment of syndesmotic integrity [27-29]. Stress radiographs with the foot in external rotation may demonstrate the diastasis, but are rarely used in clinical practice [30]. Ultrasound can clearly depict a torn tibiofibular ligament in the acute stage but is less accurate after elapse of time, and the results are dependent on the skills of the radiologist [31]. With the use of CT, widening of the mortise exceeding 3 mm can reliably be assessed, as well as gross deformity or malreduction [32-34].

The value of MRI in acute and chronic syndesmotic injuries has been described in several articles. Vogl et.al. performed a contrast-enhanced MRI in patients with an acute ankle trauma and clinical suspicion of a syndesmotic tear, in which a tear of the ATIFL markedly enhanced in T1-weighted images [16]. Muratli et. al. used MR arthrography in the first few days after injury to demonstrate leakage of contrast into the tibiofibular space as a sign of syndesmotic diastasis [35]. Schneck et. al. paid attention to the position of the ligaments paraxial to the imaging plane, and concluded that axial imaging with the foot in full dorsiflexion provided optimal views of the anterior and posterior tibiofibular ligaments [17].

However, imaging in the axial plane can result in false positive findings [14, 18] as the anterior and posterior distal tibiofibular ligaments run in an oblique plane [19, 20]. Several studies reported that the most commonly injured and reliably visualized anterior tibiofibular ligament on MRI might not be seen in its entire length on one single transverse image, and a partially imaged ligament may be mistaken as a tear despite careful observation of contiguous slices [16, 21, 22, 24]. Boonthathip et. al. showed in cadavers that oblique image planes parallel to the long axis of the ligament better display the normal anatomy of the tibiofibular syndesmotic ligaments when compared with standard imaging planes [36]. Hermans et. al. demonstrated in a recent study in healthy volunteers that the ATIFL and PTIFL are better depicted in an oblique image plane of about 45° when compared to the axial plane, and that the integrity of the ligaments can be better evaluated [23]. We therefore imaged the ATIFL and PTIFL with an additional 45° oblique plane and compared this with the commonly used axial plane.

The interobserver agreement (κ) and agreement score (AS (%)) regarding injury of the ATIFL and PTIFL was good to excellent in both the axial and oblique image plane ($0.61<\kappa<0.92$; $84\%<AS<91\%$). For both ligaments the oblique image plane demonstrated significantly lower injury scores than the axial plane ($p < 0.001$). In a recent study of Hermans et. al. in 20 healthy volunteers, as well as in this study with 44 patients with an acute ankle fracture, the oblique image plane resulted in less false positive findings.

The interobserver correlation (κ) and agreement score (AS(%)) regarding the presence of a fibular or tibial avulsion fracture, was good to excellent in both the axial and oblique image planes ($0.71<\kappa.< 0.84$; $91\%<AS< 95\%$). There was no significant difference in detection of an avulsion fracture in the axial or oblique planes, neither anteriorly ($p = 0.50$) nor posteriorly

(p = 1.00). In the axial plane in 2/3 patients with a tibial avulsion and 5/6 patients with a fibular avulsion, injury of the ATIFL was detected, whereas in the oblique plane the bony avulsion was present without a rupture of the ATIFL.

In 1875 Wagstaffe was the first to describe two cases of an avulsion fracture from the anterior tibiofibular ligament [37]. In case of a Wagstaffe fracture combined with a lateral malleolar fracture, the ATIFL avulsion fragment was classified as type I, II or III. Type I is a displaced avulsion fracture of the distal end of the tibia, and is very rare. The most commonly occurring type is type II, which is a fracture of the anterior spike of the proximal fibular fragment. Type III is a fracture of the anterior tubercles from both the tibia and fibula, and is also very rare [38, 39]. In our study we found 7/44 patients with a type II Wagstaffe fracture on MRI but not on the radiograph. If the surgeon can reduce the avulsed fragment properly and obtain stable fixation, direct bone-to-bone union can be achieved, inducing more physiologic healing of the syndesmosis. Park et al described one case in which the Wagstaffe fracture was displaced into the joint and caused chronic ankle pain and restricted joint motion [38]. Nelson described in a series of 50 transmalleolar fractures, 18% fibular avulsions (Wagstaffe type II fractures) and 8% tibial avulsions (Wagstaffe type I or Chaput-Tillaux fractures). In some cases the avulsed fragment did wedge the joint open [9]. A Wagstaffe fracture can be easily overlooked because of a fracture hematoma, torn capsule or covering by an intact extensor retinaculum. Therefore careful examination of the anterior syndesmosis area is necessary after fixation of the lateral malleolar fracture.

Posteriorly we only found avulsion fractures of the tibia and no avulsion fractures of the fibula. In 6/11 patients with a tibial avulsion, the PTIFL appeared to be ruptured in the axial plane, and was shown to be intact in the oblique plane. Generally spoken, when an avulsion fracture occurs, the ligament attached to the avulsion remains intact. Therefore our findings in the oblique image plane were concordant with this generally accepted statement. This finding has important implications for treatment of unstable ankle fractures. In case of a fracture of the distal posterior tibia with an intact PTIFL, syndesmotic stability can be achieved by fixation of the posterior malleolus fragment, without the use of a syndesmotic screw [40]. An additional value of MRI is information about the exact size, location and orientation of the posterior malleolus fracture. This may help the surgeon in choosing the surgical approach to the fragment [41].

Injury of the anterior or posterior distal tibiofibular syndesmosis can be either a rupture of the distal tibiofibular ligament or a bony avulsion from either the fibula or tibia. The interobserver correlation (κ), regarding injury of the anterior syndesmosis was moderate (κ=0.48) for the axial plane and very good (κ=0.81) for the oblique plane, although the agreement score for both planes was good (84% and 86%, respectively). Discrepancy between the percentage agreement and kappa value can be explained by the skewed distribution of categories in our study. In case of the latter, kappa is known to have poor properties as an index for measuring agreement [42]. The interobserver correlation (κ) and agreement score for posterior syndesmosis injury were very good.

To further substantiate our data, we compared our findings at MRI with the Lauge-Hansen fracture classification, as with this classification it is possible to predict injury to the anterior and posterior syndesmosis. For the oblique MRI plane, the specificity increased for both anterior (from 7% to 86%) and posterior (from 48% to 86%) syndesmotic injury when compared to the axial plane. This means a substantial decrease in false positive injury of the ATIFL and PTIFL. Although we do not know if the Lauge-Hansen fracture classification allows an anatomically correct diagnosis, it is likely that the oblique images are closer to the diagnosis than the axial images.

Several studies focused on the position of the foot during imaging in order to evaluate the ankle ligaments. The best full-length visualization of the ATIFL and PTIFL would be obtained in the axial plane, with the foot taped into full dorsiflexion [15, 17]. As it is difficult to obtain a position of full dorsiflexion in a patient with an acute ankle fracture, we maintained the foot in a neutral position. It is hard to imagine what influence the foot in dorsiflexion would have on imaging in the axial plane of the obliquely running ATIFL and PTIFL. With dorsiflexion the only effect on the ligaments would be an increased tension, as the talus pushes the fibula outwards. It therefore seems more likely that, not the position of the foot but the angle of the image plane, plays a more important role in depicting the syndesmotic ligaments. This concept is confirmed in the current study, in which the oblique plane showed a decrease in false positive findings, especially regarding injury of the ATIFL. This finding is the more relevant as, until now, the ATIFL was the most reliably visualized syndesmotic ligament in an axial MRI. Thus, MRI could help in selecting patients for an open reduction with internal fixation (ORIF) in case of suspicion of syndesmotic injury in an acute ankle fracture.

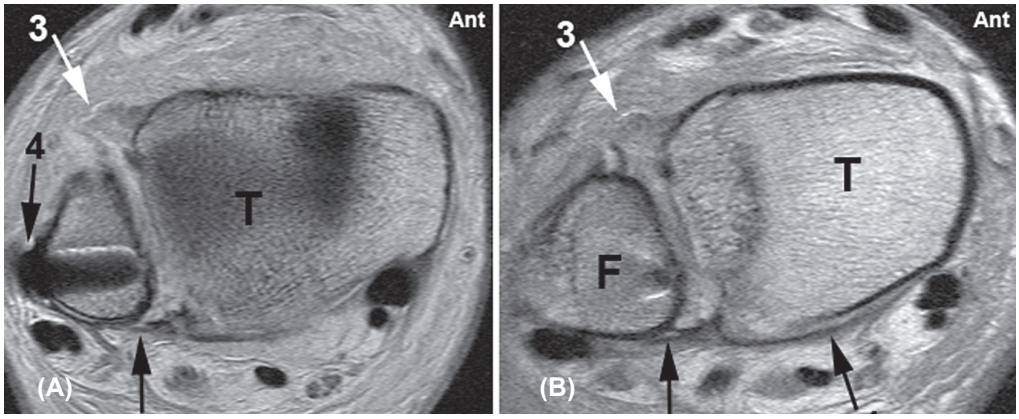

Fig. 7 Axial (*A*) and oblique (*B*) proton density TSE (turbo spin echo) image. Posterior tibial periost slip (1) with a discontinuous PITFL (2) in the axial plane (*A*) and an intact PTIFL in the oblique plane (*B*). In both planes the AITFL (3) is ruptured. Although there is a screw present in the fibula (4), the quality of the MR image is still good and the tibiofibular ligaments can be well evaluated. T, tibia; F, fibula; Ant, anterior.

A shortcoming of our study was firstly, due to logistic problems, in 5/44 of patients it was not possible to obtain a preoperative MRI. However, in the patients with a plate and screws, the quality of the MR image was still good, and the ATIFL and PTIFL as well as the presence of a tibial or fibular avulsion could be well evaluated (Fig. 7). Secondly, we did not have an invasive technique, like arthroscopy, available to confirm our MRI findings. However, in our opinion it would not be ethical to perform an ankle arthroscopy in patients who would be treated with only a plaster. Moreover, our study population now comprises both patients with and without syndesmotic injury, which therefore reduces a selection bias that would occur when only operated patients had been included. In the latter case, the a priori chance of syndesmotic injury would have been very high.

In conclusion, our results show the additional value of an oblique MR image plane for detection of injury of the anterior and posterior distal tibiofibular syndesmosis in acute ankle fractures. More accurate information about the tibiofibular syndesmosis could lead to a better treatment plan, resulting in fewer complaints of chronic syndesmotic injury or even early osteoarthritis.

Conclusion

Our results show the additional value of an oblique MR image plane for detection of injury of the anterior and posterior distal tibiofibular syndesmosis in acute ankle fractures. The 45° oblique MRI plane demonstrated significantly less ligamentous injury than the axial planes, for both the ATIFL and PTIFL. Findings of syndesmotic injury in the oblique MRI plane were closer to the diagnosis as assumed by the Lauge-Hansen classification than in the axial plane. With more accurate information, the surgeon can better decide when to stabilize syndesmotic injury in acute ankle fractures.

References

1. Kennedy JG, Johnson SM, Collins AL, DalloVedova P, McManus WF, Hynes DM, et al. An evaluation of the Weber classification of ankle fractures. Injury. 1998; 29(8):577-580.
2. Court-Brown CM, McBirnie J, Wilson G. Adult ankle fractures–an increasing problem? Acta Orthop Scand. 1998; 69(1):43-47.
3. Lindsjo U. Operative treatment of ankle fractures. Acta Orthop Scand Suppl. 1981; 189:1-131.
4. Pettrone FA, Gail M, Pee D, Fitzpatrick T, Van Herpe LB. Quantitative criteria for prediction of the results after displaced fracture of the ankle. J Bone Joint Surg Am. 1983; 65(5):667-677.
5. Yamaguchi K, Martin CH, Boden SD, Labropoulos PA. Operative treatment of syndesmotic disruptions without use of a syndesmotic screw: a prospective clinical study. Foot Ankle Int. 1994; 15(8):407-414.
6. Weening B, Bhandari M. Predictors of functional outcome following transsyndesmotic screw fixation of ankle fractures. J Orthop Trauma. 2005; 19(2):102-108.
7. Ramsey PL, Hamilton W. Changes in tibiotalar area of contact caused by lateral talar shift. J Bone Joint Surg Am. 1976; 58(3):356-357.
8. Cedell CA. [Total rupture of the syndesmosis in the ankle joint]. Lakartidningen. 1969; 66(23):2427-2433.
9. Nelson OA. Examination and repair of the AITFL in transmalleolar fractures. J Orthop Trauma. 2006; 20(9):637-643.
10. Hovis WD, Kaiser BW, Watson JT, Bucholz RW. Treatment of syndesmotic disruptions of the ankle with bioabsorbable screw fixation. J Bone Joint Surg Am. 2002; 84-A(1):26-31.
11. Kennedy JG, Soffe KE, Dalla Vedova P, Stephens MM, O'Brien T, Walsh MG, et al. Evaluation of the syndesmotic screw in low Weber C ankle fractures. J Orthop Trauma. 2000; 14(5):359-366.
12. Chissell HR, Jones J. The influence of a diastasis screw on the outcome of Weber type-C ankle fractures. J Bone Joint Surg Br. 1995; 77(3):435-438.
13. Brown KW, Morrison WB, Schweitzer ME, Parellada JA, Nothnagel H. MRI findings associated with distal tibiofibular syndesmosis injury. Ajr. 2004; 182(1):131-136.
14. Takao M, Ochi M, Oae K, Naito K, Uchio Y. Diagnosis of a tear of the tibiofibular syndesmosis. The role of arthroscopy of the ankle. The Journal of bone and joint surgery. 2003; 85(3):324-329.
15. Muhle C, Frank LR, Rand T, Ahn JM, Yeh LR, Trudell D, et al. Tibiofibular syndesmosis: high-resolution MRI using a local gradient coil. Journal of computer assisted tomography. 1998; 22(6):938-944.
16. Vogl TJ, Hochmuth K, Diebold T, Lubrich J, Hofmann R, Stockle U, et al. Magnetic resonance imaging in the diagnosis of acute injured distal tibiofibular syndesmosis. Invest Radiol. 1997; 32(7):401-409.
17. Schneck CD, Mesgarzadeh M, Bonakdarpour A, Ross GJ. MR imaging of the most commonly injured ankle ligaments. Part I. Normal anatomy. Radiology. 1992; 184(2):499-506.
18. Oae K, Takao M, Naito K, Uchio Y, Kono T, Ishida J, et al. Injury of the tibiofibular syndesmosis: value of MR imaging for diagnosis. Radiology. 2003; 227(1):155-161.
19. Bartonicek J. Anatomy of the tibiofibular syndesmosis and its clinical relevance. Surg Radiol Anat. 2003; 25(5-6):379-386.
20. Hermans JJ, Beumer A, De Jong AW, Kleinrensink GJ. Anatomy of the distal tibiofibular syndesmosis in adults: a pictorial essay with a multimodality approach. J Anat. 2010.
21. Han SH, Lee JW, Kim S, Suh JS, Choi YR. Chronic tibiofibular syndesmosis injury: the diagnostic efficiency of magnetic resonance imaging and comparative analysis of operative treatment. Foot Ankle Int. 2007; 28(3):336-342.
22. Lee SH, Jacobson J, Trudell D, Resnick D. Ligaments of the ankle: normal anatomy with MR arthrography. J Comput Assist Tomogr. 1998; 22(5):807-813.
23. Hermans JJ, Ginai AZ, Wentink N, Hop WC, Beumer A. The additional value of an oblique image plane for MRI of the anterior and posterior distal tibiofibular syndesmosis. Skeletal Radiol. 2010.
24. Kim S, Huh YM, Song HT, Lee SA, Lee JW, Lee JE, et al. Chronic tibiofibular syndesmosis injury of ankle: evaluation with contrast-enhanced fat-suppressed 3D fast spoiled gradient-recalled acquisition in the steady state MR imaging. Radiology. 2007; 242(1):225-235.
25. Lindsjo U. Classification of ankle fractures: the Lauge-Hansen or AO system? Clin Orthop Relat Res. 1985(199):12-16.
26. van den Bekerom MP, Lamme B, Hogervorst M, Bolhuis HW. Which ankle fractures require syndesmotic stabilization? J Foot Ankle Surg. 2007; 46(6):456-463.
27. Pneumaticos SG, Noble PC, Chatziioannou SN, Trevino SG. The effects of rotation on radiographic evaluation of the tibiofibular syndesmosis. Foot & ankle international / American Orthopaedic Foot and Ankle Society [and] Swiss Foot and Ankle Society. 2002; 23(2):107-111.
28. Beumer A, van Hemert WL, Niesing R, Entius CA, Ginai AZ, Mulder PG, et al. Radiographic measurement of the distal tibiofibular syndesmosis has limited use. Clinical orthopaedics and related research. 2004(423):227-234.
29. Brage ME, Bennett CR, Whitehurst JB, Getty PJ, Toledano A. Observer reliability in ankle radiographic measurements. Foot & ankle international / American Orthopaedic Foot and Ankle Society [and] Swiss Foot and Ankle Society. 1997; 18(6):324-329.
30. Dattani R, Patnaik S, Kantak A, Srikanth B, Selvan TP. Injuries to the tibiofibular syndesmosis. J Bone Joint Surg Br. 2008; 90(4):405-410.
31. Milz P, Milz S, Steinborn M, Mittlmeier T, Putz R, Reiser M. Lateral ankle ligaments and tibiofibular syndesmosis. 13-MHz high-frequency sonography and MRI compared in 20 patients. Acta orthopaedica Scandinavica. 1998; 69(1):51-55.

32. Ebraheim NA, Lu J, Yang H, Mekhail AO, Yeasting RA. Radiographic and CT evaluation of tibiofibular syndesmotic diastasis: a cadaver study. Foot & ankle international / American Orthopaedic Foot and Ankle Society [and] Swiss Foot and Ankle Society. 1997; 18(11):693-698.
33. Elgafy H, Semaan HB, Blessinger B, Wassef A, Ebraheim NA. Computed tomography of normal distal tibiofibular syndesmosis. Skeletal Radiol. 2010; 39(6):559-564.
34. Gardner MJ, Demetrakopoulos D, Briggs SM, Helfet DL, Lorich DG. Malreduction of the tibiofibular syndesmosis in ankle fractures. Foot Ankle Int. 2006; 27(10):788-792.
35. Muratli HH, Bicimoglu A, Celebi L, Boyacigil S, Damgaci L, Tabak AY. Magnetic resonance arthrographic evaluation of syndesmotic diastasis in ankle fractures. Arch Orthop Trauma Surg. 2005; 125(4):222-227.
36. Boonthathip M, Chen L, Trudell DJ, Resnick DL. Tibiofibular syndesmotic ligaments: MR arthrography in cadavers with anatomic correlation. Radiology. 2010; 254(3):827-836.
37. Wagstaffe W. An unusual form of fracture of the fibula. Cited by: St Thomas Hosp Rep; 6:43. 1875.
38. Park JW, Kim SK, Hong JS, Park JH. Anterior tibiofibular ligament avulsion fracture in weber type B lateral malleolar fracture. J Trauma. 2002; 52(4):655-659.
39. Pankovich AM. Fractures of the fibula at the distal tibiofibular syndesmosis. Clin Orthop Relat Res. 1979(143):138-147.
40. Gardner MJ, Brodsky A, Briggs SM, Nielson JH, Lorich DG. Fixation of posterior malleolar fractures provides greater syndesmotic stability. Clin Orthop Relat Res. 2006; 447:165-171.
41. Haraguchi N, Haruyama H, Toga H, Kato F. Pathoanatomy of posterior malleolar fractures of the ankle. J Bone Joint Surg Am. 2006; 88(5):1085-1092.
42. Feinstein AR, Cicchetti DV. High agreement but low kappa: I. The problems of two paradoxes. J Clin Epidemiol. 1990; 43(6):543-549.

Chapter 6

Correlation between radiological assessment of acute ankle fractures and syndesmotic injury on MRI

John J. Hermans
Noortje Wentink
Annechien Beumer
Wim C.J. Hop
Marinus P. Heijboer
Adrianus F.C.M. Moonen
Abida Ginai

Submitted

Abstract

Objective: Through the shortcomings of clinical examination and radiographs, injury to the syndesmotic ligaments is often misdiagnosed. When there is no indication to operate the fractured ankle, the syndesmosis is not tested intra-operatively and rupture of this ligament may be missed. Subsequently the patient is not treated properly leading to chronic complaints such as instability, pain and swelling. We evaluated three fracture classification methods and radiographic measurements with respect to syndesmotic injury.

Materials and Methods: Prospectively the radiographs of 51 consecutive ankle fractures were classified according to Weber, AO-Müller and Lauge-Hansen. Both the fracture type and additional measurements of the tibiofibular clear space (TFCS), tibiofibular overlap (TFO), medial clear space (MCS) and superior clear space (SCS) were used to assess syndesmotic injury. MRI, as standard of reference, was performed to evaluate the integrity of the distal tibiofibular syndesmosis. The sensitivity and specificity for detection of syndesmotic injury with radiography was compared to MRI.

Results: The Weber and AO-Müller fracture classification system, in combination with additional measurements, detected syndesmotic injury with a sensitivity of 47% and a specificity of 100%, and Lauge-Hansen with a sensitivity and specificity of both 92%. TFCS and TFO were not correlated with syndesmotic injury and a widened MCS was not associated with deltoid ligament injury.

Conclusion: Syndesmotic injury as predicted by the Lauge-Hansen fracture classification correlated well with MRI findings. With MRI the extent of syndesmotic injury and therefore fracture stage can be assessed more accurately compared to radiographs.

Introduction

Treatment of ankle fractures is determined by several factors such as patient age, soft tissue status, dislocation of the fracture and integrity of the distal tibiofibular syndesmosis. As the major stabilizer of the distal tibiofibular joint, the ligamentous complex of the syndesmosis is critical in maintaining normal ankle function. The lateral malleolus of the fibula is firmly held in the fibular notch of the tibia, providing a tight elastic ankle mortise. There are four syndesmotic ligaments: the anterior distal tibiofibular ligament (ATIFL) and posterior distal tibiofibular ligament (PTIFL) which attach the anterior and posterior tibial and fibular tubercles respectively; the interosseous ligament (IOL) which is the thickened continuation of the interosseous membrane (IOM) and the transverse ligament extending between the malleolar fossa of the fibula and the dorsal rim of the distal tibia [1-4].
The classification of malleolar fractures constitutes the basis for treatment of acute ankle fractures. Three frequently used methods to describe ankle fractures are the Danis-Weber, AO-Müller and Lauge-Hansen fracture classification [5-7]. According to Weber and AO-Müller, a fracture is classified based on the level of the fibular fracture in relation to the syndesmotic ligaments. Lauge-Hansen describes the trauma mechanism of ankle fractures, based on the position of the foot at the time of injury and the direction in which the talus moves within the ankle mortise.
Additionally a number of radiographic parameters are used to evaluate the integrity of the syndesmotic and deltoid ligaments. Absence of tibiofibular overlap (TFO) at one side, and a tibiofibular clear space (TFCS) larger than 6mm may be an indication of syndesmotic injury [8-10]. A medial clear space (MCS) surpassing the tibial clear space (TCS) is indicative of deltoid injury, which regularly accompanies injury of the syndesmosis [10].
As it is difficult to assess injury to the syndesmosis on radiographs, the true incidence is a matter of speculation. Through the shortcomings of clinical examination and radiographs [2, 11], injury to the syndesmotic ligaments is often misdiagnosed. Subsequently the patient is not treated properly, leading to chronic complaints such as instability, pain, swelling and early osteoarthritis [12, 13]. MR imaging enables identification of syndesmotic injuries that were not diagnosed at the initial radiographs and clinical examination [14-17].
The primary goal of this study is to correlate three clinically often used facture classification systems with MR findings, regarding injury of the syndesmosis in acute ankle fractures. Secondary goals are to determine the correlation between the radiographic measurements and fracture treatment in relation to syndesmotic injury.

Materials and methods

In a prospective study, between April 2004 and February 2007, 51 consecutive skeletally mature patients with an acute ankle fracture not older than 48 hours after trauma, who underwent radiographs as well as a MRI at the Erasmus University Medical Center in Rotterdam, were included. Exclusion criteria were, associated neurological or vascular injuries, fractures that were associated with a hindfoot or midfoot fracture, a former trauma of the ankle, contraindications for MRI, and an insufficient knowledge of the Dutch language. Informed consent was obtained and the study was approved by the institutional review board.
Radiographs obtained at presentation included antero-posterior, lateral and mortise views. The fractures on the radiographs were classified according to the Weber, AO-Müller and Lauge-Hansen fracture classification systems [5-7]. Both the fracture type and additional mea-

surements of the TFCS, TFO, and MCS/SCS ratio were used to assess possible syndesmotic injury on a radiograph (Fig. 1). The TFCS is the horizontal distance between the posterolateral border, the anterolateral border or the incisura fibularis of the tibia and the medial border of the fibula. The TFO is the horizontal distance between the medial border of the fibula and the lateral border of the anterior tubercle, and was measured at 1cm above, and parallel to the tibial plafond. The MCS is the widest distance between the medial border of the talus and the lateral border of the medial malleolus and was measured 0.5cm beneath the talar dome, on a line parallel to the superior talar joint surface. The SCS was the vertical distance between the talar dome and the tibial plafond (Fig. 1) [8, 9, 18-22]. A TFCS larger than 6mm, the absence of tibiofibular overlap (TFO < 0mm), a MCS/SCS ratio larger than 1 or a MCS larger than 4mm, were considered deviated and indicative for possible syndesmotic injury. The radiographs were blinded for identity and evaluated by a radiologist with 11 years experience in musculoskeletal radiology (JH). For the Weber and AO-Müller fracture classification expected syndesmotic injury was determined by the fracture type in combination with the measurements. For the Lauge-Hansen fracture classification expected syndesmotic injury was based on the trauma mechanism deducted from the radiographs.

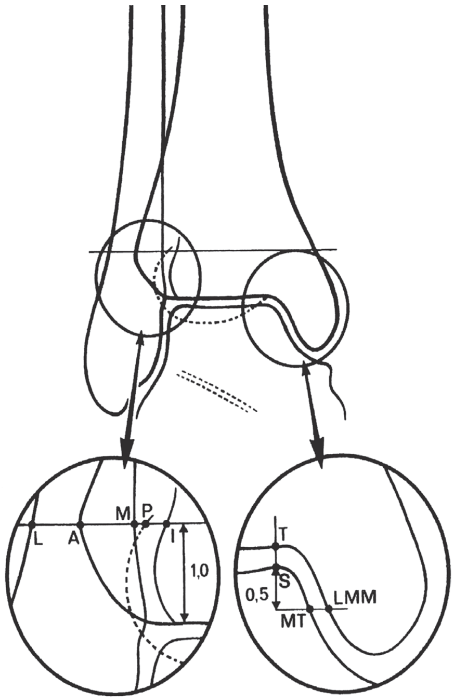

Fig 1. A schematic drawing of the ankle shows landmarks used for measurements of the different radiologic parameters. L=lateral border of the fibula; M=medial border of the fibula; A=anterior tibial tubercle; P=posterior tibial tubercle; I=floor of incisura fibularis; T=tibial plafond; S=superior point of medial talus; MT=medial side of talus; LMM=lateral side medial malleolus. AM is tibiofibular overlap (TFO). MI is tibiofibular clear space (TFCS). TS is superior clear space (SCS) and MTLMM is medial clear space (MCS). (Copy with permission from A. Beumer Clin. Orthop. Rel. Res 2004;423:227-234).

MRI was performed on a 1.5 T Gyroscan (Philips, Best, Netherlands) with a wrap-around ankle coil (E1 coil). The foot was kept in a fixed (neutral) position and stabilized with sandbags or a plaster. Dual TSE images (TR=3500-4500ms; TE=11ms; TE=120ms; Echo train length=14) were performed in three orthogonal planes, i.e. axial, coronal and sagittal, and in an additional 45° oblique plane. The oblique image plane was defined in the coronal and sagittal views. In the coronal view the 45° angle of the oblique plane was related to the tibial plafond and

ran in a caudal-cranial and lateral-medial direction through the distal fibula. In the sagittal view the direction of the oblique plane ran parallel to a line along the inferior border of the anterior and posterior tibia [23]. All series were performed with a 512×512 matrix. The field of view was 18-20cm for coronal and sagittal imaging and 12-15cm for axial and oblique imaging. The slice thickness of the images was 3,0mm with a NSA of 2. For cartilage analysis a sagittal T1 FFE (TE 20ms, TR7.8ms, flip angle 25˚), with a FOV of 15cm, matrix 512x243, slice thickness of 3.0mm with 1.5mm overlap, and NSA=2 was performed. A STIR, i.e. a short tau inversion recovery image (TR=1460ms; TE=15ms; Echo train length=14), was performed in the coronal plane, with a field of view of 18-20cm, a slice thickness of 4mm (gap 0,4mm) and a 256x256 matrix.

The MR images were independently analyzed by two radiologists with 11 respectively 31 years of musculoskeletal experience, and finally read in consensus (JH, AG). They were blinded to the results of the radiographs. The majority of the patients were examined with MRI on the day of injury. Nineteen patients were treated with an open reduction with internal fixation (ORIF), of whom six underwent a MRI postoperatively. In all patients a MRI was obtained within 7 days after starting treatment, either plaster or surgery.

The presence of anterior or posterior syndesmotic injury was defined as: 0 = normal syndesmosis, i.e. normal ligament without bony avulsion; 1 = thickened syndesmosis, i.e. thickened ligament without bony avulsion; 2 = partially ruptured syndesmosis, i.e. partially ruptured ligament without bony avulsion; 3 = completely ruptured syndesmosis, i.e. ruptured ligament without a bony avulsion or an intact ligament with a bony avulsion. The anterior and posterior distal tibiofibular ligament, were evaluated in both the axial and oblique plane. A normal distal tibiofibular ligament consisted of multiple continuous thin fibres interspersed with normal high signal intensity fat on dual TSE weighted images. In a thickened ligament the continuous fibres were thickened, not sharp and the signal intensity of fat was intermediate on dual TSE weighted images. A complete rupture was defined when the ligament was either discontinuous or invisible, or showed increased signal intensity with fluid in the ligament on T2-weighted TSE images. In a partially ruptured ligament the discontinuity was not complete [14, 17, 23-25]. A tibial or fibular avulsion, both anteriorly and posteriorly, was evaluated as either present or absent. Posteriorly a fracture of the malleolus tertius, irrespective of its size, was defined as an avulsion. The interosseous and transverse ligament were evaluated as: 0 = normal, 1 = thickened, 2 = partially ruptured or 3 = completely ruptured.

The treatment plan was based on the radiographs, without knowledge of MRI findings, and was denoted as: 0 = plaster, 1 = open reduction and internal fixation (ORIF) without setscrew, or 2 = ORIF with setscrew.

With MRI as gold standard, the sensitivity and specificity in assessing syndesmotic injury with the Weber, AO-Müller and Lauge-Hansen fracture classification, were calculated. Correlation between the MCS-SCS ratio and deltoid ligament injury, as well as the correlation between the TFCS and TFO and syndesmotic injury were analyzed with the Mann-Whitney U test. All analyses were conducted using SPSS (version 15.0, SPSS Inc., Chicago, USA). A two-sided p-value <0.05 was considered statistically significant.

Results

In total 51 patients were included with a mean age of 37 years and a range between 16 - 62 years; 28 were men and 23 were women. In 27 patients the injury involved the left and in 24 the right ankle. In six patients the MRI was performed postoperatively, within 2 days of the injury in five, and after 7 days in one patient. The other 45 patients underwent a MRI before treatment was started. Treatment consisted of a plaster in 32 patients, and ORIF with or without a setscrew in 6 and 13 patients respectively.

Weber and AO-Müller fracture classification

According to Weber 11 (21.6%) fractures were classified as type A, 23 (45.1%) as type B and 11 (21.6%) as type C (Table 1, *see end of chapter 6*). Six fractures (11.8%) could not be classified and involved either a solitary fracture of the medial malleolus with unknown status of the lateral collateral ligaments or a tibial avulsion fracture.

According to AO-Müller 11 (21.6%) fractures were classified as type A, 20 (39.3%) as type B and 9 (17.7%) as type C, with referral to table 1 for detailed sub classifications. In 11 (21.6%) patients the fracture could not be described. Those involved, in addition to the six fractures that also could not be classified according to Weber, five fibula fractures combined with either a fracture of the medial malleolus or the posterior malleolus.

In 33 patients with normal measurements on the radiographs, MRI showed absence of syndesmotic injury in 13 cases, consisting of nine patients with a Weber type A and 4 patients with a no classifiable fracture (Table 2, *see next page*). In the remaining 20 patients with normal measurements, anterior syndesmotic injury was present in 9 (Fig. 2, *see next page*), and both anterior as well as posterior syndesmotic injury in 11 patients. Syndesmotic injury was defined as either a rupture of the tibiofibular ligament or an intact tibiofibular ligament attached to an avulsion fracture. The measurements were normal in two patients with a Weber type A, or AO-Müller A1.2 and A1.3 fracture, with only anterior syndesmotic injury, and in 10 patients with a Weber type B (3 with only anterior and 7 with anterior and posterior injury), or 7 with a AO-Müller B1.1 fracture (3 with only anterior and 4 with anterior and posterior injury) and one AO-Müller B3.3 fracture (anterior and posterior injury). The measurements were also normal in 6 patients with a Weber type C fracture, with only anterior syndesmotic injury present in 3 and both anterior and posterior injury in another 3 cases, and in 4 patients with an AO-Müller type C fracture, 3 with anterior and 1 with both anterior and posterior injury. Two fractures that could not be classified by Weber and six not by AO-Müller also showed syndesmotic injury.

In 18 patients with deviating measurements syndesmotic injury was present in all of them, with only anterior syndesmotic injury in eight and both anterior and posterior injury in 10 patients. These involved 13 patients with a Weber type B fracture, and 12 patients with AO-Müller type B fracture (at least B1.2) and one no classifiable fracture, with only anterior syndesmotic in 8 and both anterior and posterior syndesmotic injury in 5 patients. The measurements deviated in 5 patients with a Weber or AO-Müller type C fracture with both anterior and posterior syndesmotic injury.

With MRI as gold standard, both the Weber and AO-Müller classification in association with the additional measurements, detected injury of the anterior and posterior syndesmosis with a sensitivity of 47% (95%CI: 31-64%), and a specificity of 100% (95%CI: 75-100%). No correlation was found between the TFCS and TFO and the presence of syndesmotic injury (p=0.152 and p=0.682 respectively). With a MCS/SCS ratio>1 or MCS>4mm, no correlation could be demonstrated with a rupture of the superficial or deep deltoid ligament (p=1.00).

Table 2. Predicted syndesmotic injury in acute ankle fractures, classified on radiographs according to Weber and AO-Müller and additional measurements, compared with syndesmotic injury on MRI. Associated measurements on radiographs: 0 = normal; 1 = deviated. Syndesmotic injury on MRI: 0 = no injury; 1 = anterior syndesmotic injury; 3 = anterior and posterior syndesmotic inj

Weber		Syndesmotic injury (MRI)			AO-Müller		Syndesmotic injury (MRI)		
		0	1	3			0	1	3
A	0	9	2	0	44A	0	9	2	0
	1	0	0	0		1	0	0	0
B	0	0	3	7	44B	0	0	3	5
	1	0	8	5		1	0	7	5
C	0	0	3	3	44C	0	0	3	1
	1	0	0	5		1	0	0	5
nc	0	4	1	1	nc	0	4	1	5
	1	0	0	0		1	0	1	0

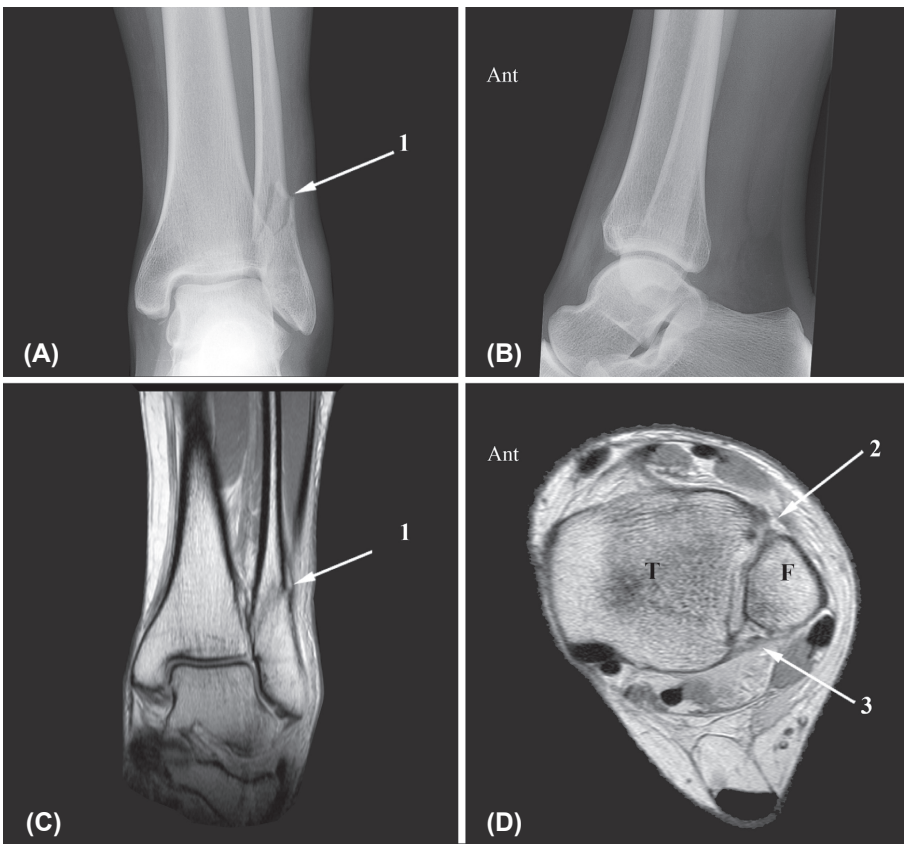

Fig. 2. AP (*A*) and lateral (*B*) radiograph, show a distal fibula fracture (1). Measurements are normal. The coronal proton-density-weighted MR image (*C*) also shows the fibula fracture (1). The axial proton-density-weighted MR image (*D*) is just below the level of the fibula fracture, and demonstrates the rupture of the ATIFL (2). The fascicles of the PTIFL (3) are a little thickened but intact. This is a Weber type B, AO-Müller type B1.1, Lauge-Hansen SE2 fracture, with normal measurements but with anterior syndesmotic injury. Ant, anterior; T, tibia; F, fibula.

Lauge-Hansen fracture classification

According to Lauge-Hansen, 28 (54.8%) fractures were classified as supination external rotation (SE), 4 (7.8%) as pronation external rotation (PE), 11 (21.6%) as supination adduction (SA), 3 (5.9%) as pronation adduction (PA), and 1 (2.0%) as pronation dorsiflexion (PD), with referral to table 1 for detailed sub classifications. In 4 (7.8%) patients the fracture could not be classified. These involved either a solitary fracture of the medial malleolus with unknown status of the collateral ligaments, a tibial avulsion fracture and a fibula fracture not visible on the radiographs.

In 15 patients without expected syndesmotic injury on the radiographs, MRI showed anterior syndesmotic injury in 3 patients (two SA1 and one no classifiable fracture) (Table 3). In 36 patients with expected syndesmotic injury on the radiographs, MR showed one patient without injury (PD2 fracture). Compared to MRI, Lauge-Hansen under- resp. overestimated syndesmotic injury in 9 and 5 patients respectively (Table 3).

With MRI as gold standard, the Lauge-Hansen classification detected injury of the anterior and posterior syndesmosis with a sensitivity of 92% (95%CI: 79-98%), and a specificity of 92% (95%CI: 64-99.8%).

Table 3: Predicted syndesmotic injury as expected by Lauge-Hansen based on trauma mechanism deducted from the radiographs (Synd-X) compared with syndesmotic injury on MRI (Synd-MR). Syndesmotic injury: 0 = no injury; 1 = anterior syndesmotic injury; 3 = anterior and posterior syndesmotic injury.

Synd-X	Synd-MR		
	0	*1*	*3*
0	12	3	0
1	1	10	6
3	0	4	15

Syndesmotic injury on MRI

Syndesmotic injury consisted of either a rupture of the distal tibiofibular ligament or an intact tibiofibular ligament with a bony avulsion from either the tibia or fibula. Anteriorly, the distal tibiofibular ligament was ruptured in 27 patients and intact but associated with a fibular avulsion in 8 patients, and a tibial avulsion in one. On the radiographs, however, only the tibial avulsion and 3/8 fibular avulsion fractures were visible. Posteriorly, the distal tibiofibular ligament was ruptured in 3 patients. An intact ligament associated with an avulsion fracture occurred in 18 patients, but only at the tibia, and was defined as any size of posterior malleolus fracture. The posterior malleolus fracture was not visible on the radiographs in 6/18 patients, although it involved a large posteromedial fragment in three. Injury of the posterior syndesmosis occurred only in combination with anterior injury (n = 21).

The interosseous ligament was injured in 7 patients, and in 6/7 patients showed intact fascicles with an avulsed periost from its tibial attachment. The interosseous ligament was ruptured in 3 patients in association with a ruptured anterior syndesmosis (Fig. 3, *see next page*) and in 3 patients with a ruptured anterior as well as posterior syndesmosis. In one patient it involved a ruptured interosseous ligament in combination with only a fracture of the medial malleolus. The transverse ligament was completely ruptured in 1 patient with only anterior syndesmotic injury, and partially ruptured in another with both anterior and posterior syndesmotic injury. The interosseous membrane (IOM) was intact in 39 patients, and its integrity could not be determined in one. The IOM was injured in 11 patients, with a rupture in 4 and intact but attached to an avulsion of tibial periost in 7 patients. Both findings were interpreted as a rupture of the membrane. In 8/11 cases the rupture of the interosseous membrane was above the level of the fibula fracture and involved, in the majority, a supination-external rotation trauma (n=7). In 3/11 cases with a ruptured membrane at or below the level of the fibula fracture, it involved a pronation-external-rotation trauma in two.

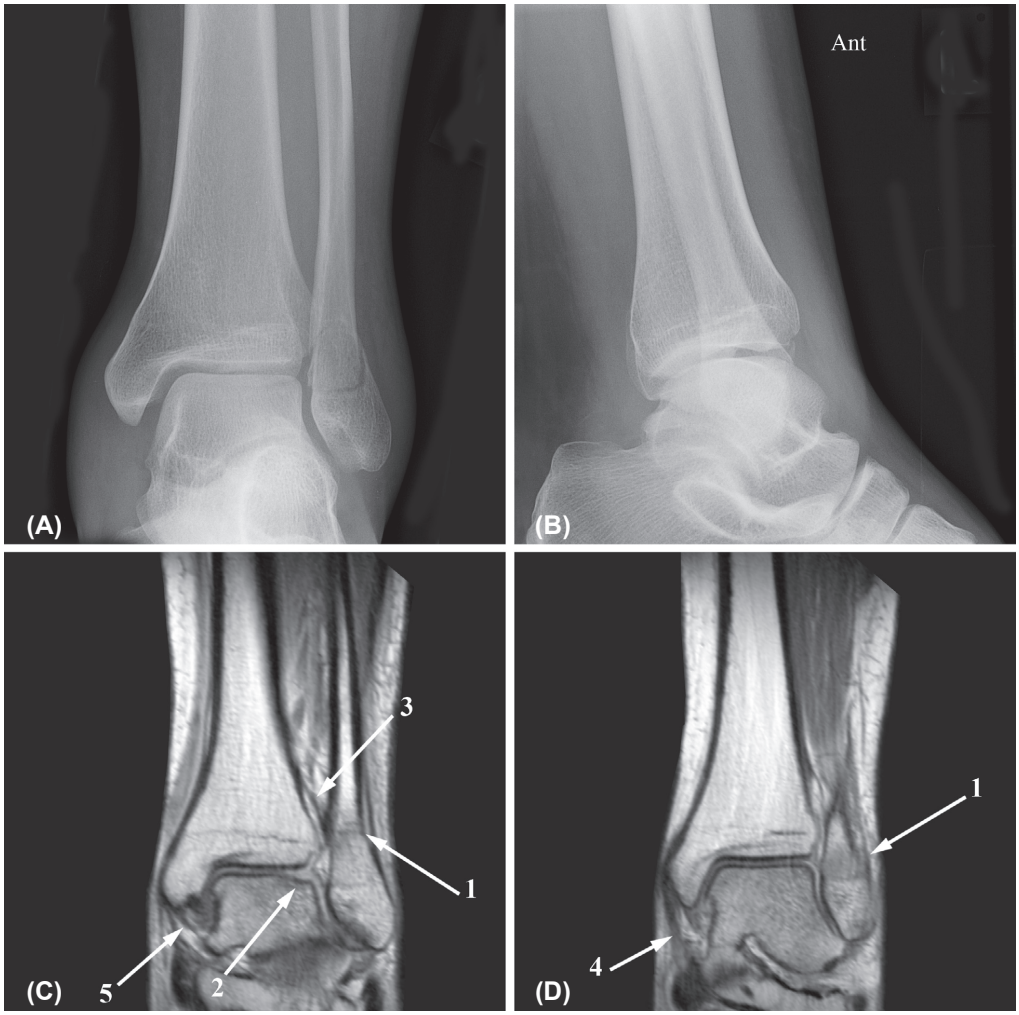

Fig. 3. A, B, C and D

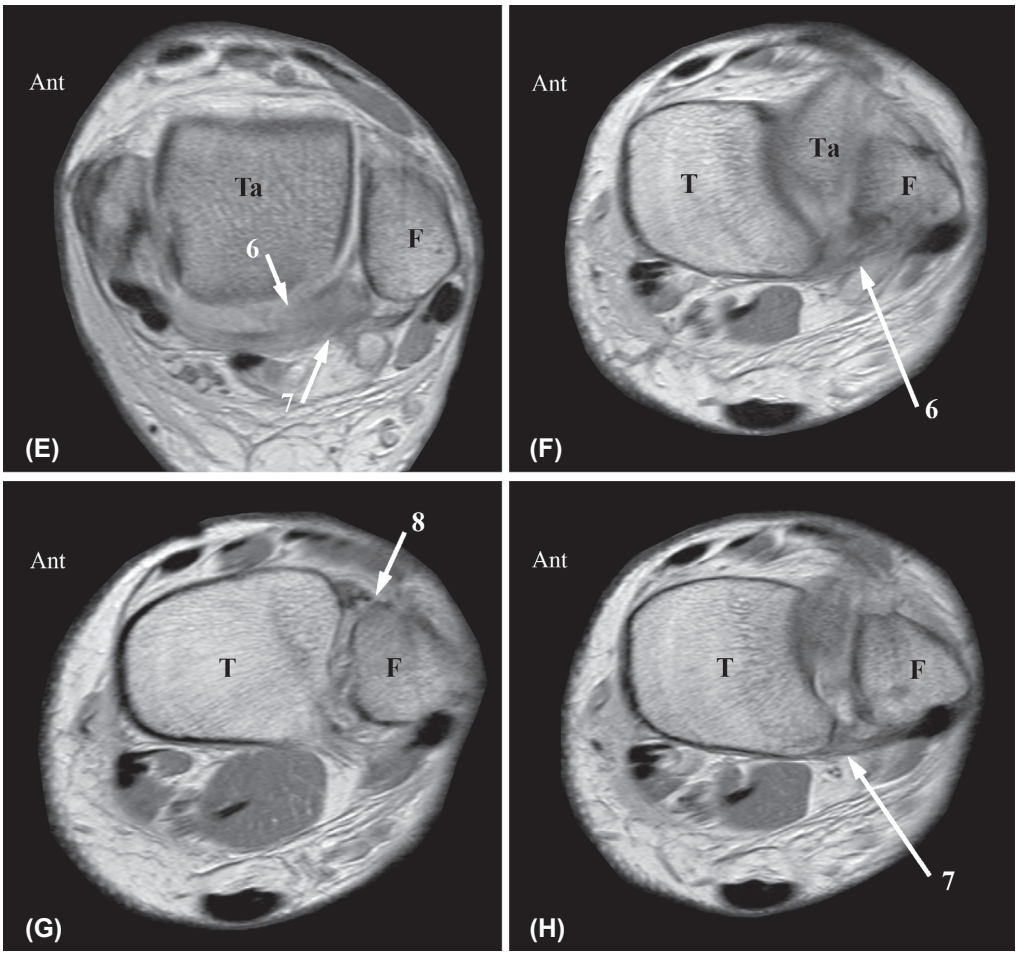

Fig. 3. AP (*A*) and lateral (*B*) radiograph. Short distal fibula fracture (1) extending from just below till just above the level of the tibiotalar joint line. Measurements are normal. This fracture is classified as: Weber type B, AO-Müller type B1.1 and Lauge-Hansen SE2. Coronal (*C, D*), axial (*E*) and 45° oblique (*F, G, H*) proton-density-weighted MR images. The coronal MRI (*C, D*) shows the fibula fracture (1), a postero-lateral osteochondral lesion of the talar dome (2), a normal interosseous ligament (3), a thickened superficial (4) and a normal deep (5) deltoid ligament. On the axial (*E*) and oblique MR image (*F*) the transverse ligament (6) is ruptured. The PTIFL (7) appears to be ruptured in the axial plane (*E*) but is still continuous, although thickened, in the 45° oblique plane (*B*). The ATIFL (8) is ruptured (*G*). With the MRI findings this would change the fracture into a AO-Müller type B1.2 but it would still be Lauge-Hansen SE2. Ant, anterior; Ta, talus; T, tibia; F, fibula.

Treatment

Treatment was based on radiographs and peroperative findings, but without knowledge of MRI findings. In 19 patients the fracture was treated with an open reduction and internal fixation (ORIF), and in six of them the syndesmosis was fixated with a setscrew (Table 4, *see next page*). ORIF with a setscrew involved 1 patient with a rupture of the anterior syndesmosis associated with a rupture of the interosseous ligament, 3 patients with a rupture of both the anterior as well as posterior syndesmosis, and 2 patients with a rupture of both the anterior as well as posterior syndesmosis in association with a rupture of the interosseous ligament. All were Weber type C fractures or PE4 (n=4), PA3 (n=1) or SE3 (n=1). The syndesmosis was fixated with a setscrew in 4 patients with an intact and in 2 patients with a ruptured inte-

rosseous membrane. In 0% (0/10) of Weber type B fractures and 86% (6/7) of Weber type C fractures treated with ORIF a setscrew was required.

Table 4. Treatment in relation to syndesmotic injury on MRI. Treatment consists of plaster or open reduction and internal fixation (ORIF) with or without setscrew. Syndesmotic injury on MRI: 0 = no injury; 1 = anterior syndesmotic injury; 3 = anterior and posterior syndesmotic injury.

Treatment	Syndesmotic injury (MRI)		
	0	*1*	*3*
Plaster	12	13	7
ORIF - setscrew	1	3	9
ORIF + setscrew	0	1	5

Discussion

Our study population consisted of 51 consecutive patients with an acute ankle fracture. The fracture distribution was conform to other studies with reported fracture types of LH type SE (42-72%), PE (7-22%), SA (6-20%) and PA (5-21%) [26].

Anterior or posterior syndesmotic injury was defined as a rupture of the tibiofibular ligament or as an intact tibiofibular ligament attached to an avulsion fracture. With MRI as gold standard, both the Weber and AO-Müller classification, in association with the additional measurements, detected injury of the anterior and posterior syndesmosis with a sensitivity of 47% and a specificity of 100%. LH detected syndesmotic injury with a sensitivity and specificity of both 92%. To compare the sensitivity and specificity of the 3 fracture classification systems, no distinction was made in the extent of syndesmotic injury, as with Weber and AO-Müller it is not possible to differentiate between anterior and posterior syndesmotic injury. With LH however, syndesmotic injury can be evaluated in more detail. In 14 cases we found a discrepancy between syndesmotic injury as predicted by LH and findings at MRI. LH underrespectively overestimated syndesmotic injury in 9 respectively 5 patients. Underestimation involved three cases in which LH missed a rupture of the anterior syndesmosis, and six cases in which not only the anterior but also the posterior syndesmosis was injured.

In 3 cases syndesmotic injury was underestimated by LH as MRI showed a rupture of the anterior syndesmosis. On radiographs, a transverse fibular fracture below the level of the tibiotalar joint space was present, suggesting a supination adduction type 1 (SA1) fracture. MRI showed, in addition to the transverse fibular fracture, injury of the anterior syndesmosis (Fig. 4). This is therefore not compatible with the general statement that the syndesmosis is not involved in supination-adduction injury, which is by definition an infrasyndesmotic injury. Gardner et. al also found one case, in a series of 59 patients, with a supination-adduction trauma in which the anterior tibiofibular ligament was ruptured [27]. As the ATIFL runs approximately in a 45° oblique plane from the anterior tibial tubercle to the anterior fibular tubercle, and just crosses the anterolateral talar corner, its fibular insertion point lies a little below the level of the tibiotalar joint space [24, 28]. A fibula fracture at this level could therefore result in injury of the ATIFL. This finding could affect treatment outcome, as in the presence of syndesmotic injury a non-weightbearing cast would be the preferred treatment. In case of anterior syndesmotic injury, early weightbearing could result in an elongated healed ATIFL leading to complaints of chronic instability or even early osteoarthritis.

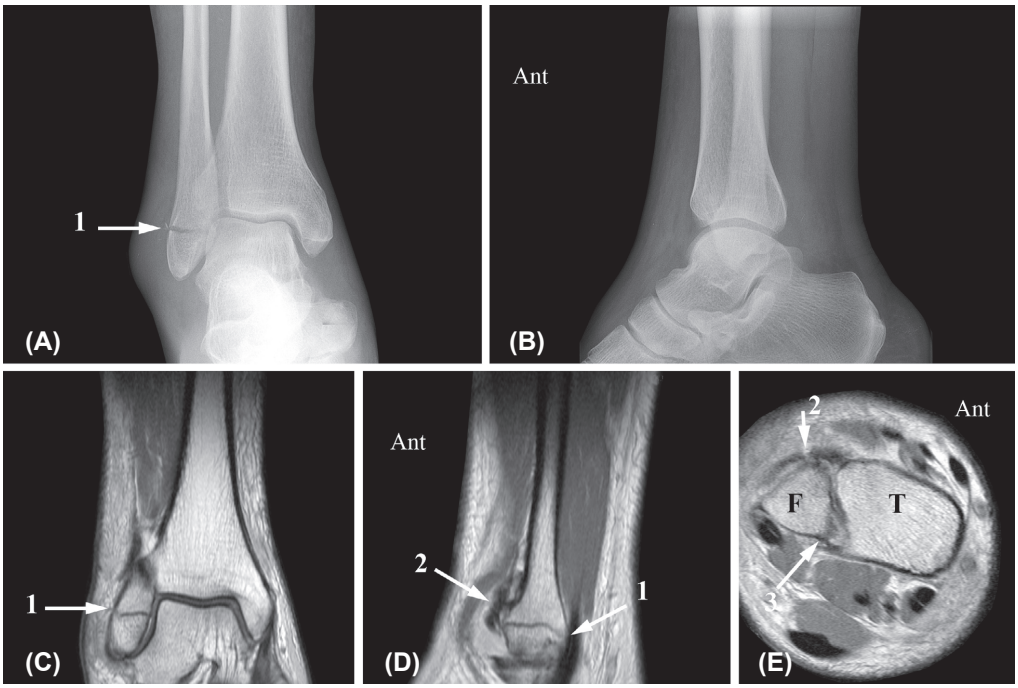

Fig. 4. AP (*A*) and lateral (*B*) radiograph. A transverse fibular malleolar fracture (1) below the level of the tibiotalar joint line is visible. No fracture is visible at the medial or posterior malleolus. Measurements are normal. The fracture was classified as: Weber A, AO-Müller A1.3, Lauge-Hansen SA1. Coronal (*C*), sagittal (*D*) and axial (*E*) proton-density-weighted MR image. The transverse fibula fracture (1) is visible on the coronal and sagittal MR image. The lower border of the ruptured ATIFL (2) just lies across the fibula fracture as can be seen on the sagittal MR image (*D*). In the 45° oblique image (*E*) the ATIFL (2) is thickened and avulsed from the fibula. The PTIFL (3) is intact. Ant, anterior; T, tibia; F, fibula.

In 6 other cases of underestimated syndesmotic injury, LH predicted only anterior syndesmotic injury, whereas MRI showed also posterior injury. Anterior syndesmotic injury consisted of a ruptured ATFIL in 4 and an anterior fibular avulsion fracture in 2 patients. Posterior syndesmotic injury involved 5 patients with an intact PTIFL attached to an avulsed fragment of the posterior malleolus, which was not visible on the radiographs, and one patient with a ruptured posterior tibiofibular ligament (Fig. 5, *see next page*). In 2 patients the superficial deltoid ligament was partially or completely ruptured. With these findings on MRI the fracture would change from SE2 into SE3 in 3 cases, from SE2 into SE4 in two cases and from a no classifiable SE1/PE1 into PA2 in one case. For therapeutic management it is important to know whether a fracture is stable or unstable. An unstable fracture should be treated with an open reduction and internal fixation (ORIF) and, if necessary, syndesmotic stability should be regained with a setscrew. In two patients with an underestimated SE4 fracture ORIF was performed without fixation of the syndesmosis with a setscrew, although on MRI the superficial deltoid ligament was partially or completely ruptured, and the deep deltoid ligament was intact in both. The measurements deviated only in one case. It is likely that the deep deltoid ligament prevents a lateral shift of the talus, when the fibula is pulled laterally with the hook test [29], whereas the superficial deltoid ligament gives restraint to a valgus position of the talus.

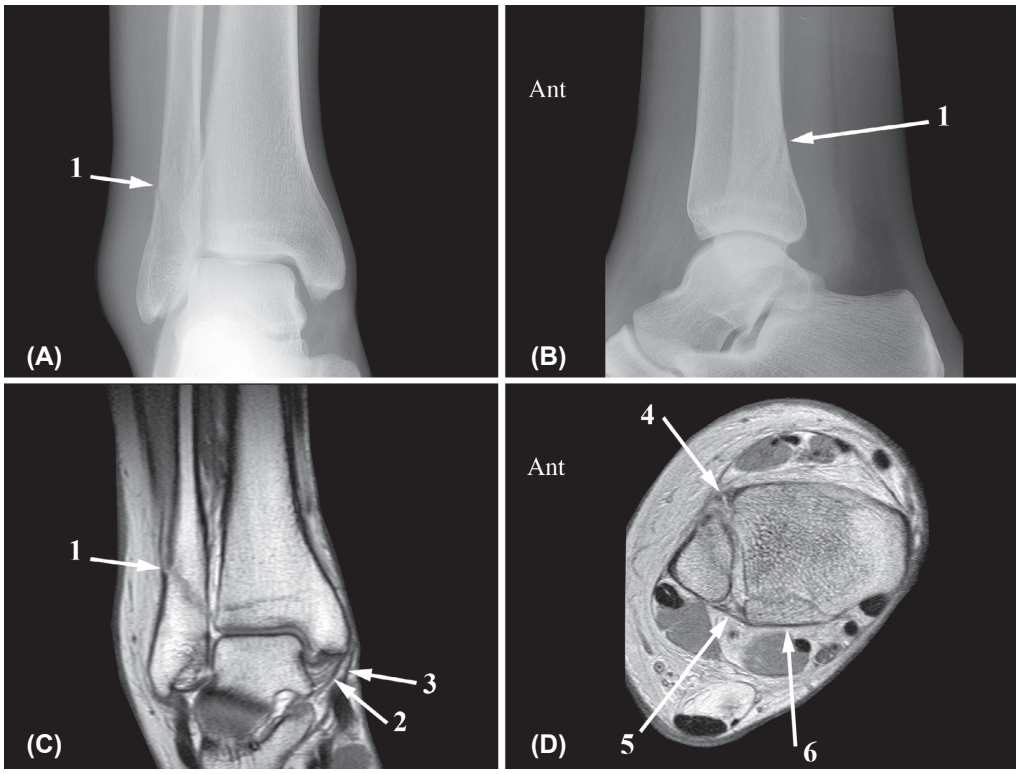

Fig. 5. AP (*A*) and lateral (*B*) radiograph show a distal fibula fracture (1) at the level of the syndesmosis, running obliquely from antero-inferior to postero-superior, characteristic of a supination-external rotation trauma. Measurements are normal. This fracture is classified as: Weber type B, AO-Müller type B1.1 and Lauge-Hansen SE2. Coronal (*C*) and 45º oblique (*D*) proton-density-weighted MR image demonstrate the fibula fracture (1), and a normal deep (2) and superficial (3) deltoid ligament. The ATIFL is ruptured (4), whereas the intact PTIFL (5) is attached to an avulsion fracture of the posterolateral malleolus (6). This is therefore a Weber type B fracture with normal measurements but with anterior as well as posterior syndesmotic injury. According to Lauge-Hansen this is a SE3 fracture.

Overestimation of syndesmotic injury occurred in five cases. In one case with a pronation-dorsiflexion type2 injury (PD2), the radiographs showed a transverse fracture of the medial malleolus and a fracture of the anterior rim of the distal tibia, which was interpreted as a possible Chaput-Tillaux fracture, implying anterior syndesmotic injury. On MRI the fracture of the medial malleolus was well visualized. The intact multifascicular ATIFL was attached to a normal tubercle of Chaput, that was adjacent to a comminute impression fracture of the anterior tibial rim.

In 4 other cases of overestimation, injury of both the anterior and posterior syndesmosis was expected on the radiographs but MRI showed only anterior injury. In one case with a suspected SE4 trauma, based on a fibula fracture, a suspected medial malleolus avulsion fracture and posterior syndesmotic injury inferred from the type of trauma mechanism, MRI showed neither posterior nor medial injury, resulting in down staging of the fracture into SE2. In two cases, a supination external rotation type 3 and 4 trauma were based on an obliquely running fibula fracture, from antero-inferior to postero-superior, associated with either an avulsion fracture of the medial malleolus or suspected posterior malleolus avulsion fracture. MRI, however, showed in both cases no posterior malleolus fracture or ruptured posterior tibiofibu-

lar ligament, but did show either a medial malleolus avulsion fracture or a possibly ruptured deltoid ligament. Both experimentally and clinically a SE4 injury can exist without damage to the posterior tibiofibular ligament [30, 31]. The absence of posterior injury suggests these fractures could also be a pronation external rotation injury type 3 (PE3). In that case, however, the direction of the fibula fracture line should be from antero-superior to postero-inferior, and usually the level of the fracture is above the syndesmosis, which was not the case in these 2 patients. In a study with cadavers, Haraguchi et.al. showed that a pronation external rotation trauma could result in a fibula fracture at the level of the syndesmosis with a fracture line running from antero-inferior to postero-superior [32]. They also noted that medial injury occurred after the fracture of the fibula and posterior injury was absent in 4/8 cadavers. This means that a PE3 and SE4 type of fracture cannot always be distinguished on radiographs or MRI only. The clinical relevance of this distinction is based on the stability of the tibiotalar and tibiofibular joint. Because with PE fractures the level of the fibula fracture is above the syndesmosis and could be accompanied by a rupture of the interosseous membrane, this fracture type would benefit from a setscrew, whereas fibula fractures within 3.0 – 4.5cm of the tibiotalar joint do not need a setscrew [33].

The fourth case of overestimated syndesmotic injury involved a pronation-external rotation type 4 trauma (PE4, i.e. Maisonneuve fracture), based on a proximal fibula fracture, an avulsed medial malleolus and possible fracture of the posterior malleolus. Although MRI showed an intact posterior malleolus, the posterior tibiofibular ligament was thickened and attached to a slip of avulsed tibial periosteum from the posterior malleolus, suggesting at least some kind of posterior traumatic stress. Therefore, based on these findings the fracture should be classified as PE3.

On radiographs, injury of the distal tibiofibular syndesmosis can be predicted based on the type of fracture. According to Weber the more proximal the fibula fracture, the greater the risk of a disrupted syndesmosis and ankle instability. A rupture of the syndesmotic ligaments is assumed in all type C and in 50% type B fractures [5]. In the AO-Müller classification, syndesmotic injury is expected in all fractures with at least a type B1.2 fracture. However it is not possible to predict which of the Weber type B or AO-Müller type B1.1 fractures will have injury of the syndesmotic ligaments, and for that reason radiographic measurements can be used to deduce syndesmotic injury. In our study the Weber and AO-Müller fracture classification showed a low sensitivity of 47% for prediction of syndesmotic injury. In contrast to the literature in which 50% of Weber type B fractures are expected to have syndesmotic injury, our study showed syndesmotic injury in all patients, either anterior (48%) or both anterior as well as posterior (52%). Measurements, however, were normal in 64% with only anterior and in 67% with both anterior and posterior syndesmotic injury. In all Weber type C fractures syndesmotic injury was present, as expected, although the measurements were normal in 55%. Nielson et. al. showed that the tibiofibular clear space (TFCS) and tibiofibular overlap (TFO) did not correlate with anterior and posterior tibiofibular ligament injuries [34]. According to Beumer et. al. there is no optimal radiographic parameter to assess the integrity of the syndesmosis. Absence of tibiofibular overlap at one side may be an indication of syndesmotic injury and a medial clear space surpassing the tibial clear space is indicative of deltoid injury [22]. As a secondary question in this study, we looked at the additional value of the measurements and also concluded that the TFCS and TFO did not correlate with syndesmotic injury and neither did a widened medial clear space correlate with deltoid ligament injury [35]. A possible explanation for normal measurements in the presence of syndesmotic injury, could be the spontaneous reduction of the tibiofibular diastasis after the acute injury. But whenever measurements deviated syndesmotic injury was always present, whereas normal measurements did not exclude syndesmotic injury.

Syndesmotic injury is also underestimated due to the low detection rate of avulsion fractures on radiographs. When compared to MRI, radiographs detected only 50% (2/9) of anterior avulsion fractures from either the fibula (n=8) or tibia (n=1) and 67% of the posterior malleolus avulsion fractures. Park et. al. found a fibula avulsion fracture (Wagstaffe type II fracture) in 13/52 (25%) of Weber type B fractures, with an associated diastasis in 11/13 (85%) [36]. In our study 4/23 (17%) patients with a Weber type B fracture showed a Wagstaffe fracture, and in only one the measurements deviated. Harper showed in 18 patients with a SE2 fracture that CT detected occult avulsion fractures of the distal tibia in 39% of the cases [37]. In our series a distal anterior tibial avulsion was present in only one no classifiable fracture with normal measurements. To detect a posterior malleolus fracture Ebraheim et. al. advocated a 50º external rotation radiograph [38], although Ferries et. al showed that radiographs poorly assessed the posterior fragment size when compared to CT [39]. Nielson et. al. described a series of ligamentous Weber B or SE4 fractures, in which the fibula was fractured without associated fracture of the medial and posterior malleolus, based on only radiographs and intraoperative exorotational stress tests. Although CT has been used to evaluate the distal tibiofibular syndesmosis postoperatively, no studies have been performed to compare the detection rate of avulsion fractures of the distal tibiofibular joint between radiography, CT and MRI preoperatively. It seems likely however, that CT is superior in detecting especially small bony avulsions.

Syndesmotic stability occurs in the coronal, sagittal, rotational and axial planes but only the coronal and rotational plane instability are routinely addressed clinically [40]. Coronal plane stability is tested intraoperatively with the hook test by pulling laterally on the fibula with a bone hook. Lateral movement of the fibula or widening of the mortise on the AP radiograph suggests the need for a setscrew. Van den Bekerom reported a sensitivity of 39% and specificity of 96% of the hook test with a cut-off of the height of the fibula fracture of 4.5cm [41]. Rotational plane instability can be tested with an intraoperative fluoroscopic external rotation stress test and is based on radiographic tibiofibular clear space measurements. With intraoperative fluoroscopy Jenkinson et. al. detected syndesmotic instability in 37% of ankle fractures [42]. Xenos et. al. evaluated syndesmotic instability with the external rotation stress test by assessing posterior movement of the fibula on lateral radiographs [43], suggesting instability of the syndesmosis in a sagittal plane. These studies show that syndesmotic instability can occur in different planes and depends on which of the osseoligamentous structures are disrupted and therefore play a role in the discussion which ankle fractures need to be stabilized with a setscrew. Therefore when the surgeon would know preoperatively which syndesmotic ligaments are injured, application and interpretation of available intraoperative tests could be optimized and result in a better evaluation of syndesmotic instability and aid in the decision of using a setscrew.

In this study six fractures were treated with ORIF and a setscrew, including four pronation-external rotation fractures (PE4), one SE3 and one PA3 fracture, all of which were Weber type C fractures (Table 15). According to. Egol et. al., in a series of 347 patients with unstable ankle fractures, 18% type B fractures and 79% type C fractures required syndesmotic stabilization [44, 45]. In another study 50% of unstable AO type B fractures needed a setscrew [46]. In our study 0% (0/10) type B fractures and 86% (6/7) type C fractures treated with ORIF required a setscrew. This is remarkable as anterior and posterior syndesmotic injury occurred in 70% (7/10) Weber type B fractures and was associated with a ruptured, possibly ruptured or avulsed interosseous ligament in 30% (3/10). In this study in only 56% (5/9) of SE4 fractures, which are unstable ankle fractures, ORIF was performed, however, without syndesmotic stabilization. Stark et. al. observed syndesmotic instability in 39% of unstable Weber

B lateral malleolar fractures or ligamentous SE4 fractures, i.e. without associated fractures of the medial and posterior malleolus [42, 47]. These findings raise the question how accurate intraoperative stabilization tests are, not only regarding the way they are performed but also in interpretation of fluoroscopic findings. Regaining a normal ankle stability is important, as several studies have shown that surgical treatment yields improved results in unstable ankle fractures [48, 49].
The interosseous membrane also plays an important role in the stability of ankle fractures, and the relation between the level of the fibula fracture and extension of the ruptured membrane has frequently been discussed [50, 51]. In our study injury of the interosseous membrane occurred in 11 patients and was located at or below the level of the fibula fracture in 3 cases and above the fibula fracture in 8 cases. The majority of these 8 fractures involved a supination-external rotation trauma (SE2 (n=3); SE3 (n=1); SE4 (n=4)) and one pronation-external rotation trauma (PE4). This is the only case in which the interosseous membrane itself was ruptured. It is also the only case in which ORIF was performed with a setscrew. In two SE2 and three SE4 fractures ORIF without a setscrew was performed (Fig. 6, *see next page*).
Our study showed several shortcomings. Not in all patients a MRI could be performed preoperatively, but the presence of a plate and screws did not influence image quality and the syndesmotic ligaments could still be well evaluated. The presence of a setscrew could influence the observer regarding the extent of syndesmotic injury. This occurred only in two cases in which both anterior and posterior syndesmotic were obviously present, and a bias therefore not likely. We did not perform a standardized preoperative stress test, and neither was the intra-operatively used stress test performed in a standardized way, but this is conform daily routine in our clinic. This study was a radiographic analysis without clinical or long-term follow-up.

Overall we can conclude that, in this study, the sensitivity for detecting syndesmotic injury with the Weber and AO-Müller fracture classification in combination with additional measurements is low, and much higher with the Lauge-Hansen fracture classification. We showed that syndesmotic injury was present in all Weber type B fractures, although measurements were normal in 65%. Remarkably, none of the Weber type B fractures treated with ORIF required a setscrew, although both anterior and posterior syndesmotic injury was present. MRI showed that posterior syndesmotic injury only occurred in association with anterior syndesmotic injury and consisted in 80% of an intact posterior tibiofibular ligament attached to an avulsion fracture of the posterior malleolus, which was not visible on the radiographs in 33%. Anterior avulsion fractures were only visible on the radiographs in 50%. Although Lauge-Hansen is the best available fracture classification in predicting syndesmotic injury, MRI can be of additional value in determining its exact extent, as until now when referring to syndesmotic injury the exact extent of osseoligamentous involvement is not defined.

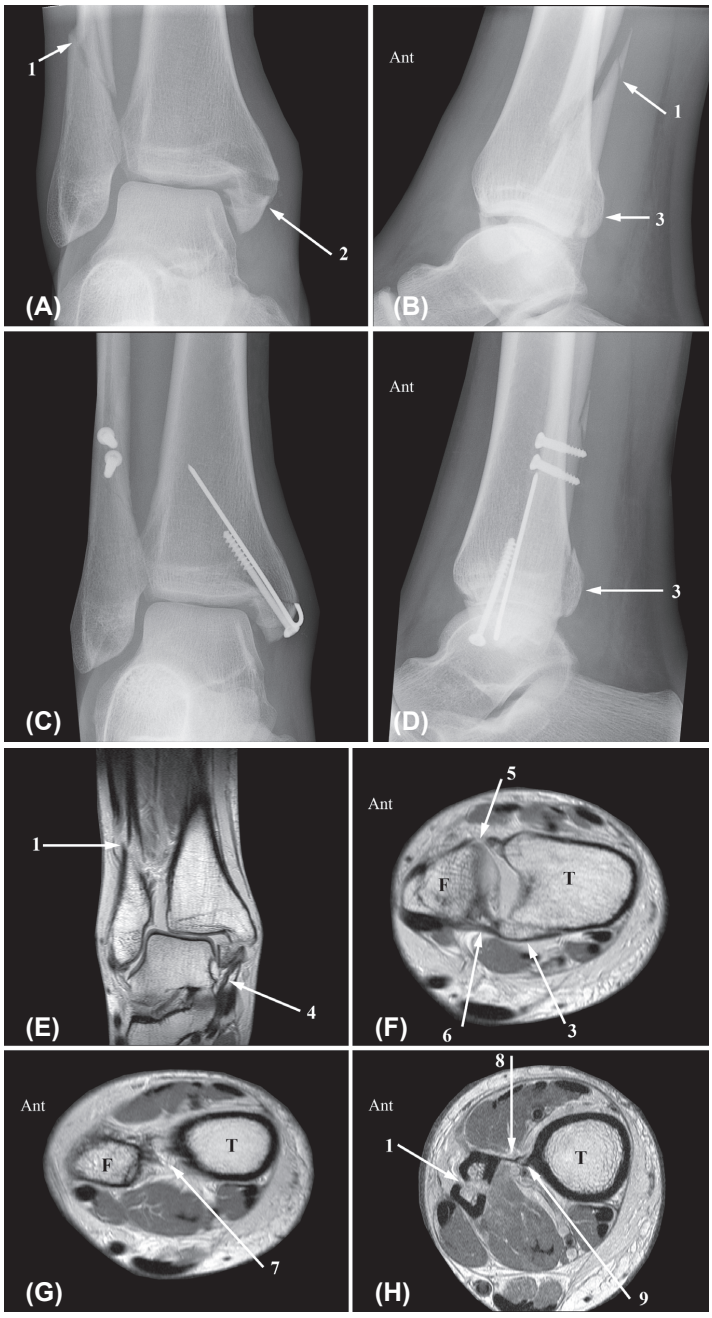

Fig. 6. AP (*A*) and lateral (*B*) radiograph show an oblique fibula fracture (1), running from antero-inferior to postero-superior, characteristic of a supination-external rotation injury. The medial malleolus (2) and posterior malleolus (3) are avulsed. AP (*C*) and lateral (*D*) radiograph after open reduction and internal fixation without a setscrew. The fracture of the posterior malleolus (3) is visible and not fixated. The fracture was classified as: Weber type C, AO-Müller C2.3, Lauge-Hansen SE4. Coronal (*E*), 45° oblique (*F, G*), and axial proton-density-weighted (*H*) MR image. The coronal MRI shows the laterally dislocated talus, with a distal fibula fracture (1) and an avulsion fracture of the medial malleolus (2) attached to a thickened but intact superficial deltoid ligament (4). In (*F*) the ATIFL (5) is ruptured, whereas the PTIFL (6) is intact and attached to an avulsion fracture of the posterolateral malleolus (3). In (*G*) the ruptured interosseous ligament (7) is visible. In (*H*) the fibula fracture (1) runs proximal to the interosseous membrane (8) which has a small tibial avulsion (9) up to this level. Ant, anterior; T, tibia; F, fibula.

Conclusion

Lauge-Hansen is the best fracture classification to predict syndesmotic injury with a sensitivity and specificity of both 92%. The Weber and AO-Müller fracture classification system detected syndesmotic injury with a sensitivity of 47% and a specificity of 100%. In this study 100% of Weber type B fractures showed a rupture of the syndesmosis, in contrast to 50% reported in the literature. On radiographs underestimation of anterior and posterior syndesmotic injury is partly due to missed fibular or tibial avulsion fractures in 50% and 67% respectively. Posterior syndesmotic injury occurred only in association with anterior syndesmotic injury and consisted in 86% of a posterior malleolus fracture. TFCS and TFO did not correlate with syndesmotic injury, and neither did a widened MCS correlate with deltoid ligament injury. In 12% of patients ORIF with a setscrew was performed, but not only in unstable fractures.

Table 1. Predicted syndesmotic injury based on three fracture classification systems and measurements on X-ray. Findings at MRI regarding the anterior (ATIFL) and posterior tibiofibular ligament (PTIFL), transverse ligament, interosseous membrane and ligament, deep and superficial deltoid ligament. Type of treatment.

Table 1					X-ray										MRI											
					Fracture classification			Measurements				Syndesmosis injury			Anterior			Posterior								
Nr	*age*	*sex*	*MRI*	*Side*	*WE*	*AO*	*LH*	*TFCS*	*TFO*	*MCS*	*SCS*	*WE*	*AO*	*LH*	*Injury*	*ATIFL*	*AvAnt*	*Injury*	*PTIFL*	*AvPos*	*IOL*	*TRL*	*IOM*	*De Δ*	*Su Δ*	*OR*
1	24	m	0	R	C	C.2.3	SE4	4,3	11,9	5,7	3,9	1	1	3	1	3	0	1	1	1	2	0	3	1	1	1
2	48	f	0	L	C	*	SE3	4,6	3,8	1,7	3,6	1	0	3	1	3	0	1	0	1	0	0	0	0	1	0
3	33	m	0	L	*	*	SE1-PE2	5,7	6,3	3,3	4,4	1	1	1	1	0	1	1	3	0	0	2	0	0	2	1
4	26	m	0	R	B	B.1.1	SE2	5,1	5,9	1,7	3,4	0	0	1	1	3	0	1	0	1	1	0	0	0	0	0
5	39	m	0	L	B	B.1.2	SE2	6,3	5,7	4,7	3,8	1	1	1	1	3	0	0	1	0	0	0	1	0	1	1
6	26	m	0	R	B	B.1.2	SE2	6,5	0,0	7,9	5,9	1	1	1	1	3	0	1	1	1	1	1	*	1	3	1
7	41	f	0	L	C	C.1.2	SE4	3,2	7,5	1,7	3,2	1	1	3	1	3	0	0	1	0	1	0	1	0	0	0
8	58	f	0	R	C	C.2.2	SE4	3,6	4,4	3,4	5,3	1	1	3	1	1	2	1	1	1	0	0	0	1	1	0
9	48	m	0	R	A	A.1.3	SA1	3,4	7,1	2,3	3,3	0	0	0	1	1	2	0	0	0	0	0	0	0	1	0
10	17	f	0	L	*	*	PD2	4,4	5,6	2,8	2,8	0	0	1	0	0	0	0	0	0	0	0	0	1	1	1
11	57	f	0	L	A	A.1.3	SA1	3,3	5,3	2,1	3,1	0	0	0	0	0	0	0	0	0	0	0	0	1	1	0
12	22	m	0	R	A	A.1.2	SA1	4,9	8,0	1,9	2,7	0	0	0	0	0	0	0	0	0	0	0	0	1	1	0
13	41	m	0	L	B	B.1.1	SE2	2,8	7,6	2,1	2,9	0	0	1	1	3	0	0	1	0	0	0	0	0	0	0
14	23	m	0	L	B	*	SE3	4,5	3,2	1,3	3,1	1	0	3	1	3	0	1	0	1	0	0	0	3	3	1
15	48	m	0	L	B	B.2.2	SE4	5,7	9,8	3,1	2,9	1	1	3	1	3	0	0	0	0	1	1	0	1	1	0
16	21	m	0	R	C	C.2.3	PE4	11,6	0,0	*	*	1	1	3	1	3	0	1	0	1	4	1	3	1	0	2
17	51	m	0	R	B	B.3.2	SE4	*	0,0	*	*	1	1	3	1	3	0	1	1	1	1	1	0	0	1	1
18	41	m	0	R	B	B.1.1	SE2	4,0	12,8	3,8	4,6	0	0	1	1	3	0	1	1	1	0	1	0	1	1	0
19	58	f	0	L	A	A.1.2	SA1	4,4	3,7	1,7	2,4	0	0	0	0	0	0	0	0	0	0	0	0	0	0	0
20	58	m	0	L	B	*	SE4	3,9	9,6	2,5	2,7	0	0	3	1	1	2	1	1	1	1	1	0	0	1	0
21	20	f	1	R	B	B.2.1	SE4	2,5	0,0	12,7	2,9	1	1	3	1	3	0	1	1	1	0	0	0	3	3	1
22	18	f	0	R	B	B.1.1	SE2	6,0	2,6	2,7	2,9	0	0	1	1	3	0	0	0	0	1	0	0	1	1	0
23	55	m	0	L	*	*	PA1-PE1	4,8	4,2	2,5	2,9	0	0	0	0	0	0	0	0	0	4	0	0	0	0	0
24	25	f	0	L	B	B.1.2	SE2	5,1	6,0	3,8	3,0	1	1	1	1	3	0	0	1	0	0	3	0	0	1	0
25	53	f	0	L	C	C.2.2	PA3	9,8	0,0	2,5	2,9	1	1	3	1	0	2	1	3	0	1	1	0	0	1	2
26	62	f	0	L	B	B.1.2	SE2	4,1	10,4	2,3	2,2	1	1	1	1	3	0	0	1	0	1	0	0	0	0	0
27	33	f	0	R	B	B.1.1	SE2	4,6	3,3	3,1	3,4	0	0	1	1	3	0	0	1	0	0	0	0	0	0	0
28	52	f	1	R	C	C.3.3	PE4	7,7	0,0	3,5	5,0	1	1	3	1	3	0	1	3	0	1	1	0	2	3	2
29	48	m	1	L	B	*	SE3	6,9	3,0	4,6	5,0	1	1	3	1	1	2	0	1	0	4	1	1	2	2	0

Table 1					X-ray										MRI										
					Fracture classification			Measurements				Syndesmosis injury			Anterior			Posterior							
Nr	*age*	*sex*	*MRI*	*Side*	*WE*	*AO*	*LH*	*TFCS*	*TFO*	*MCS*	*SCS*	*WE*	*AO*	*LH*	*Injury*	*ATIFL*	*AvAnt*	*Injury*	*PTIFL*	*AvPos*	*IOL*	*TRL*	*IOM*	*De Δ*	*Su Δ*	*OR*
30	29	m	0	R	*	*	PA1	2,9	2,8	2,2	4,1	0	0	0	0	1	0	0	0	0	0	0	0	2	3	0
31	58	m	1	L	B	B.3.2	SE4	*	*	*	*	1	1	3	1	3	0	1	1	1	2	1	1	1	1	1
32	28	f	0	R	A	A.1.2	SA1	5,3	3,6	2,5	3,9	0	0	0	0	0	0	0	1	0	0	0	0	0	0	0
33	27	f	0	R	B	B.1.1	SE2	4,0	3,2	3,3	3,1	1	1	1	1	3	0	0	0	0	1	0	0	0	0	1
34	27	m	0	L	B	B.3.3	SE4	5,4	4,5	3,7	3,0	1	1	3	1	3	0	1	1	1	0	0	1	0	0	1
35	56	f	0	L	A	A.1.2	SA1	3,8	6,9	2,4	2,6	0	0	0	0	0	0	0	0	0	0	0	0	0	0	0
36	56	m	0	R	C	C.1.1	SE2	2,5	9,4	2,7	4,3	1	1	1	1	0	2	0	0	0	0	0	0	1	0	0
37	16	f	0	L	A	A.2.2	SA2	3,9	5,4	3,1	3,2	0	0	0	0	0	0	0	0	0	0	0	0	0	1	0
38	18	m	0	R	C	*	SE3	4,6	4,9	2,6	5,0	1	0	3	1	3	0	1	0	1	0	0	0	3	3	2
39	53	f	0	L	B	B.1.1	SE2	3,9	3,7	2,6	3,1	0	0	1	1	3	0	1	0	1	4	0	0	1	1	0
40	51	f	0	R	B	B.1.1	SE2	3,5	3,7	2,3	2,9	0	0	1	1	0	2	1	1	1	0	0	0	1	1	0
41	56	m	1	L	B	B.1.2	SE2	0,8	3,1	7,8	2,6	1	1	1	1	3	0	0	1	0	4	0	1	1	2	1
42	27	f	0	L	A	A.1.1	SA1	5,1	0,6	2,3	3,0	0	0	0	0	0	0	0	0	0	0	0	0	1	1	0
43	18	m	1	R	C	C.1.3	PE4	6,2	1,4	2,7	3,5	1	1	3	1	1	0	1	0	1	4	0	0	0	0	2
44	30	f	0	L	*	*	PA1-PE1	5,0	4,4	2,1	3,8	0	0	0	0	0	0	0	0	0	0	0	0	0	0	0
45	27	m	0	R	C	C3.3	PE4	4,3	2,1	4,0	4,3	1	1	3	1	3	0	0	2	0	3	0	2	3	3	2
46	20	m	0	R	A	A1.2	SA1	5,1	6,2	2,9	4,8	0	0	0	1	0	2	0	0	0	0	0	0	1	0	0
47	61	f	0	L	B	B3.3	PA3	3,0	4,5	2,1	3,0	0	0	3	1	3	0	1	1	1	0	0	0	0	0	1
48	36	m	0	L	A	A1.2	SA1	3,9	8,1	2,1	3,6	0	0	0	0	0	0	0	0	0	0	0	0	0	0	0
49	17	m	0	R	*	*	*	4,1	1,4	2,5	2,8	0	0	0	1	3	0	0	0	0	1	0	0	0	0	0
50	22	f	0	R	B	B.1.2	SE2	7,1	0,0	2,3	2,4	1	1	1	1	3	0	0	2	0	0	0	1	0	0	0
51	17	m	0	L	A	A.1.3	SA1	2,4	6,9	3,2	4,0	0	0	0	0	0	0	0	0	0	0	0	1	1	0	0

Legends:
Age (years). Sex (m = male; f = female). MRI (0 = performed before treatment; 1 = performed postoperatively). Side of ankle fracture (R = right; L = left).
X-ray:
Fracture classification (WE = Weber; AO = AO-Müller, LH = Lauge Hansen).
X-ray measurements (TFCS = tibiofibular clear space (normal value TFCS ≤ 6 mm); TFO = tibiofibular overlap (normal value TFO > 0 mm); MCS = medial clear space; SCS = superior clear space (normal value MCS ≤ 4 mm or MCS/SCS ≤ 1)).
Syndesmosis injury based on X-ray and measurements for WE and AO (0 = no injury; 1 = injury); for LH based on trauma mechanism deducted from X-ray (0 = no injury, 1 = anterior injury, 2 = posterior injury, 3 = anterior and posterior injury).
MRI:
ATIFL and PTIFL: 0 = normal tibiofibular ligament; 1 = thickened tibiofibular ligament; 2 = possibly ruptured tibiofibular ligament; 3 = ruptured tibiofibular ligament.
Avulsion fracture anterior (AvAnt) or posterior (AvPos): 0 = no avulsion; 1 = tibial avulsion; 2 = fibular avulsion.
Syndesmosis injury anterior or posterior on MRI (i.e. ruptured tibiofibular ligament or intact tibiofibular ligament with an avulsion fracture): 0 = no injury; 1 = injury.
Interosseous ligament (IOL), Transverse Ligament (TRL), Deep deltoid ligament (De Δ) and Superficial deltoid ligament (Su Δ): 0 = normal; 1 = thickened; 2 = partially ruptured; 3 = completely ruptured.
Interosseous membrane (IOM): 0 = normal; 1 = rupture of membrane higher than fibula fracture; 2 = rupture of membrane at the same level as fibula fracture; 1 = rupture of membrane lower than fibula fracture;
Operation (OR): 0 = no ORIF; 1 = ORIF without setscrew; 2 = ORIF with setscrew.

References

1. Bartonicek J. Anatomy of the tibiofibular syndesmosis and its clinical relevance. Surg Radiol Anat. 2003; 25(5-6):379-386.
2. Kelikian H, Kelikian S. Disorders of the ankle. Philadelphia, London, Toronto: W.B. Saunders Company, 1985.
3. Kapandji IA. Funktionelle Anatomie der Gelenke. Schematisierte und kommentierte Zeichnungen zur menslichen Biomechanik: Ferdinand Enke Verlag; 1985:148-165.
4. Lutz W. Zur Struktur der unteren Tibiofibularverbindung und der Membrana interossea cruris. Anat Entwickl Gesch. 1942; 111:315-321.
5. Weber BG. Die Verletzungen des oberen Sprunggelenkes. Zweite, überarbeitete und ergänzte Auflage ed: Hans Huber Bern Stuttgart Wien, 1972.
6. Lauge-Hansen N. Fractures of the ankle. II. Combined experimental-surgical and experimental-roentgenologic investigations. Arch Surg. 1950; 60(5):957-985.
7. Müller ME, Nazarian S, Koch P, Schatzker J. The comprehensive classification of fractures of long bones. Berlin: Springer-Verlag, 1990.
8. Harper MC, Keller TS. A radiographic evaluation of the tibiofibular syndesmosis. Foot Ankle. 1989; 10(3):156-160.
9. Pneumaticos SG, Noble PC, Chatziioannou SN, Trevino SG. The effects of rotation on radiographic evaluation of the tibiofibular syndesmosis. Foot Ankle Int. 2002; 23(2):107-111.
10. Beumer A. Chronic instability of the anterior syndesmosis of the ankle: biomechanical, kinematical, radiological and clinical aspects. Rotterdam: Erasmus University Rotterdam, The Netherlands; 2007.
11. Xenos JS, Hopkinson WJ, Mulligan ME, Olson EJ, Popovic NA. The tibiofibular syndesmosis. Evaluation of the ligamentous structures, methods of fixation, and radiographic assessment. J Bone Joint Surg Am. 1995; 77(6):847-856.
12. Hopkinson WJ, St Pierre P, Ryan JB, Wheeler JH. Syndesmosis sprains of the ankle. Foot Ankle. 1990; 10(6):325-330.
13. Boytim MJ, Fischer DA, Neumann L. Syndesmotic ankle sprains. Am J Sports Med. 1991; 19(3):294-298.
14. Vogl TJ, Hochmuth K, Diebold T, Lubrich J, Hofmann R, Stockle U, et al. Magnetic resonance imaging in the diagnosis of acute injured distal tibiofibular syndesmosis. Invest Radiol. 1997; 32(7):401-409.
15. Brown KW, Morrison WB, Schweitzer ME, Parellada JA, Nothnagel H. MRI findings associated with distal tibiofibular syndesmosis injury. AJR Am J Roentgenol. 2004; 182(1):131-136.
16. Takao M, Ochi M, Oae K, Naito K, Uchio Y. Diagnosis of a tear of the tibiofibular syndesmosis. The role of arthroscopy of the ankle. J Bone Joint Surg Br. 2003; 85(3):324-329.
17. Oae K, Takao M, Naito K, Uchio Y, Kono T, Ishida J, et al. Injury of the tibiofibular syndesmosis: value of MR imaging for diagnosis. Radiology. 2003; 227(1):155-161.
18. Pettrone FA, Gail M, Pee D, Fitzpatrick T, Van Herpe LB. Quantitative criteria for prediction of the results after displaced fracture of the ankle. J Bone Joint Surg Am. 1983; 65(5):667-677.
19. Sclafani SJ. Ligamentous injury of the lower tibiofibular syndesmosis: radiographic evidence. Radiology. 1985; 156(1):21-27.
20. Ebraheim NA, Lu J, Yang H, Rollins J. The fibular incisure of the tibia on CT scan: a cadaver study. Foot Ankle Int. 1998; 19(5):318-321.
21. Joy G, Patzakis MJ, Harvey JP, Jr. Precise evaluation of the reduction of severe ankle fractures. J Bone Joint Surg Am. 1974; 56(5):979-993.
22. Beumer A, van Hemert WL, Niesing R, Entius CA, Ginai AZ, Mulder PG, et al. Radiographic measurement of the distal tibiofibular syndesmosis has limited use. Clin Orthop Relat Res. 2004(423):227-234.
23. Hermans JJ, Ginai AZ, Wentink N, Hop WC, Beumer A. The additional value of an oblique image plane for MRI of the anterior and posterior distal tibiofibular syndesmosis. Skeletal Radiol. 2010.
24. Hermans JJ, Beumer A, De Jong AW, Kleinrensink GJ. Anatomy of the distal tibiofibular syndesmosis in adults: a pictorial essay with a multimodality approach. J Anat. 2010.
25. Kim S, Huh YM, Song HT, Lee SA, Lee JW, Lee JE, et al. Chronic tibiofibular syndesmosis injury of ankle: evaluation with contrast-enhanced fat-suppressed 3D fast spoiled gradient-recalled acquisition in the steady state MR imaging. Radiology. 2007; 242(1):225-235.
26. Lindsjo U. Classification of ankle fractures: the Lauge-Hansen or AO system? Clin Orthop Relat Res. 1985(199):12-16.
27. 27. Gardner MJ, Demetrakopoulos D, Briggs SM, Helfet DL, Lorich DG. The ability of the Lauge-Hansen classification to predict ligament injury and mechanism in ankle fractures: an MRI study. J Orthop Trauma. 2006; 20(4):267-272.
28. Boonthathip M, Chen L, Trudell DJ, Resnick DL. Tibiofibular syndesmotic ligaments: MR arthrography in cadavers with anatomic correlation. Radiology. 2010; 254(3):827-836.
29. Snedden MH, Shea JP. Diastasis with low distal fibula fractures: an anatomic rationale. Clin Orthop Relat Res. 2001(382):197-205.
30. Michelson J, Solocoff D, Waldman B, Kendell K, Ahn U. Ankle fractures. The Lauge-Hansen classification revisited. Clin Orthop Relat Res. 1997(345):198-205.
31. Yde J, Kristensen KD. Ankle fractures. Supination-eversion fractures stage II. Primary and late results of operative and non-operative treatment. Acta Orthop Scand. 1980; 51(4):695-702.
32. Haraguchi N, Armiger RS. A new interpretation of the mechanism of ankle fracture. J Bone Joint Surg Am. 2009; 91(4):821-829.
33. Boden SD, Labropoulos PA, McCowin P, Lestini WF, Hurwitz SR. Mechanical considerations for the syndesmosis screw. A cadaver study. J Bone Joint Surg Am. 1989; 71(10):1548-1555.

34. Nielson JH, Gardner MJ, Peterson MG, Sallis JG, Potter HG, Helfet DL, et al. Radiographic measurements do not predict syndesmotic injury in ankle fractures: an MRI study. Clin Orthop Relat Res. 2005(436):216-221.
35. Koval KJ, Egol KA, Cheung Y, Goodwin DW, Spratt KF. Does a positive ankle stress test indicate the need for operative treatment after lateral malleolus fracture? A preliminary report. J Orthop Trauma. 2007; 21(7):449-455.
36. Park JW, Kim SK, Hong JS, Park JH. Anterior tibiofibular ligament avulsion fracture in weber type B lateral malleolar fracture. J Trauma. 2002; 52(4):655-659.
37. Harper MC. The short oblique fracture of the distal fibula without medial injury: an assessment of displacement. Foot Ankle Int. 1995; 16(4):181-186.
38. Ebraheim NA, Mekhail AO, Haman SP. External rotation-lateral view of the ankle in the assessment of the posterior malleolus. Foot Ankle Int. 1999; 20(6):379-383.
39. Ferries JS, DeCoster TA, Firoozbakhsh KK, Garcia JF, Miller RA. Plain radiographic interpretation in trimalleolar ankle fractures poorly assesses posterior fragment size. J Orthop Trauma. 1994; 8(4):328-331.
40. Candal-Couto JJ, Burrow D, Bromage S, Briggs PJ. Instability of the tibio-fibular syndesmosis: have we been pulling in the wrong direction? Injury. 2004; 35(8):814-818.
41. van den Bekerom MP, Haverkamp D, Kerkhoffs GM, van Dijk CN. Syndesmotic Stabilization in Pronation External Rotation Ankle Fractures. Clin Orthop Relat Res. 2009.
42. Jenkinson RJ, Sanders DW, Macleod MD, Domonkos A, Lydestadt J. Intraoperative diagnosis of syndesmosis injuries in external rotation ankle fractures. J Orthop Trauma. 2005; 19(9):604-609.
43. Grath GB. Widening of the ankle mortise. A clinical and experimental study. Acta Chir Scand Suppl. 1960; Suppl 263:1-88.
44. Egol KA, Pahk B, Walsh M, Tejwani NC, Davidovitch RI, Koval KJ. Outcome after unstable ankle fracture: effect of syndesmotic stabilization. J Orthop Trauma. 2010; 24(1):7-11.
45. Heim D, Schmidlin V, Ziviello O. Do type B malleolar fractures need a positioning screw? Injury. 2002; 33(8):729-734.
46. Hoiness P, Stromsoe K. Early complications of surgically managed ankle fractures related to the AO classification. A review of 118 ankle fractures treated with open reduction and internal fixation. Arch Orthop Trauma Surg. 1999; 119(5-6):276-279.
47. Stark E, Tornetta P, 3rd, Creevy WR. Syndesmotic instability in Weber B ankle fractures: a clinical evaluation. J Orthop Trauma. 2007; 21(9):643-646.
48. Xu YQ, Zhan BL, He FX, Wei HD. [Surgical treatment of pronation and supination external rotation trimalleolar fractures]. Zhongguo Gu Shang. 2008; 21(4):300-301.
49. Zalavras C, Thordarson D. Ankle syndesmotic injury. J Am Acad Orthop Surg. 2007; 15(6):330-339.
50. Nielson JH, Sallis JG, Potter HG, Helfet DL, Lorich DG. Correlation of interosseous membrane tears to the level of the fibular fracture. J Orthop Trauma. 2004; 18(2):68-74.
51. Ebraheim NA, Mekhail AO, Gargasz SS. Ankle fractures involving the fibula proximal to the distal tibiofibular syndesmosis. Foot Ankle Int. 1997; 18(8):513-521.

Chapter 7

Conclusion

Conclusion

Ankle fractures are usually diagnosed with two or three standardized radiographs, i.e. the anteroposterior, lateral and mortise views. These radiographs are subsequently used to classify the fracture according to one of three clinically frequently used fracture classification systems: the Weber, AO-Müller and Lauge-Hansen classification. A fracture classification system is useful because it describes the fracture localisation or fracture pattern, which forms the basis for a treatment plan. Furthermore it has a prognostic value.

In contrast to the Lauge-Hansen fracture classification, which is based on the trauma mechanism, the Weber and AO-Müller fracture classifications are based on the level of the fibula fracture in relation to the distal tibiofibular syndesmosis. This implies that the exact boundaries of the syndesmosis and its composing osseoligamentous structures should be well defined. However, neither in the literature nor in daily practice is specified what is meant by injury of the syndesmosis nor which and how many of the four tibiofibular ligaments are involved.

As radiologists are the clinical anatomists, or to be more precise: the (consulting) anatomist in the clinic, I posed a question at a radiological congress about skeletal radiology, in which both consultants and residents were asked to demarcate the anatomical lower and upper border of the syndesmosis on a presented AP radiograph of a normal ankle. A bell shaped frequency distribution showed that 80% of the radiologists defined the lower border at the level of the tibiotalar joint line, whereas a wide frequency distribution was observed when the definition of the upper border was asked. The explanation is that syndesmotic injury is most likely perceived as injury to the distal anterior tibiofibular ligament, and possibly also to the posterior tibiofibular ligament, as these ligaments are located in a narrow range around the tibiotalar joint line. The wide range of the perceived upper limit of the syndesmosis can only be explained by lack of knowledge regarding its anatomy. This means that a distinction between a Weber type B and C fracture is probably based on a subjective interpretation of the level of the fibula fracture in relation to the syndesmosis rather than an objective one based on the exact anatomical extent of the tibiofibular joint.

We therefore performed an extensive analysis of the distal tibiofibular syndesmotic anatomy in human cadaver specimens, and correlated findings regarding microscopy, macroscopy, plastination and cross sectional imaging techniques like CT and MRI. This resulted in the application of a 45° oblique imaging plane for MRI of the ankle, in addition to the commonly used three orthogonal imaging planes, to depict the anterior and posterior tibiofibular ligaments along their entire length. Both in healthy volunteers as in patients with an acute ankle fracture, this additional 45° oblique imaging plane resulted in less false positive findings when compared to the axial imaging plane.

Not only is the distal tibiofibular syndesmosis a point of reference for the fracture classification systems, but also the other way around can the fracture classification be used to predict syndesmotic injury. We showed however, that with Weber and AO-Müller syndesmotic injury can be poorly predicted, especially in the type B fractures which showed at least anterior syndesmotic injury in all cases when compared to findings at MRI. This is in contrast with the literature which describes that injury to the syndesmosis is expected in 50% of type B fractures. Injury to the syndesmosis is better predicted with the Lauge-Hansen classification, although both under- as well as overestimation did occur.

Detailed knowledge of the anatomy of the distal tibiofibular joint plays an essential role in interpretation of plain radiographs and cross sectional imaging techniques like MRI.
This knowledge can only be acquired in the dissection room because the basis of interpreting the 'sliced anatomy' produced by imaging techniques as CT and MRI is the three dimensional form. Behind each slice lies a three dimensional form. And to really understand the form, it should be studied by taking the road back in history, back to the time one was a student, and re-visiting the dissection room. This visit will result in a completely different experience. Now that one has encountered the many problems (and really experienced them as problems) of clinical care, one will study the specimen in a much more specific way, and the effect of one's visit will be much higher when compared to the time one was 'forced' to attend and take exams.
Only through dynamic interaction between the anatomist, the surgeon and the radiologist, can increasing anatomic knowledge result in better application and evaluation of fracture classifications and aid in developing a better treatment plan with an improved clinical outcome.

Chapter 8

Recommendations

Recommendations

To date many studies have been performed regarding fractures of the ankle. However, only few studies have been performed in which MRI was used to evaluate not only the osseoligamentous structures but also the surrounding soft tissue structures of the ankle joint. With the currently available MRI techniques (1.5T or 3.0T) it is possible to acquire a nearly isovolumetric 3D dataset of the ankle, with an imaging voxel of less than 1 mm^3. From this dataset each individual ligament, of both the collateral as well as the tibiofibular ligaments, can be reconstructed in a plane along its longitudinal axis. With this detailed anatomic information, and because the greater part of the tibiofibular ligaments are extra-articularly located, MRI and not arthroscopy should serve as the gold standard. Therefore, with an isovolumetric MRI scan the following three questions could be addressed.

1. Which of the tibiofibular ligaments are exactly involved in a fractured ankle?

Three of the four tibiofibular ligaments lie in an obliquely running plane when compared to the commonly used three orthogonal planes. With only a fixed additional 45° oblique plane for both the anterior and posterior tibiofibular ligaments, we showed an improved interpretation of the continuity of these ligaments. With a tailored plane for each ligament this would improve even more. The interosseous ligament is to date rather difficult to image because it consists of multiple thin fibres running in three different directions. A tailored plane for this ligament could also better detect injury. Although the interosseous ligament plays an important role in the stability of the syndesmosis, it is not mentioned in fracture classifications. Therefore tailored imaging planes will enable a more accurate evaluation of the involved syndesmotic ligaments in acute ankle fractures.

2. Which of the tibiofibular ligaments are exactly involved in unstable ankle fractures?

An important decision in treatment of ankle fractures is based on the stability of the fracture. Several guidelines have been developed as to which ankle fractures are unstable and should be treated with an open reduction and internal fixation (ORIF). When, after fixation of the fibula and/or medial malleolus fracture, instability at the tibiofibular joint persists, the syndesmosis should be fixated with a setscrew. Tibiofibular instability can be tested intra-operatively with one of several techniques available. Two frequently used methods are the hook test in which the fibula is pulled laterally, and the exorotation stress test. However these tests are not performed in a standardized way and interpretation of residual instability is therefore subjective. With preoperative information available about the status of each individual ankle ligament, obtained with a 3D isovolumetric MRI, and a standardized way of performing these tests, remaining instability would be better evaluated and therefore be more uniformly treated. Also, an intra-operatively performed dynamic MRI could address whether the fracture is adequately stabilized and whether the fibula is correctly positioned in the tibial incisure. Therefore preoperatively tailored imaging planes and intra-operative dynamic MRI probably enable better interpretation of instability and guide the necessity for fixation with a setscrew.

3. Which trauma mechanism leads to which injured tibiofibular ligaments?

With the use of cadaveric specimens more insight has been gained into the trauma mechanism. Lauge-Hansen was the first to relate the position of the foot and direction of the force to a specific fracture pattern. However, his fracture classification has never been validated and in recent studies its reproducibility is questioned, mostly because his experiments were not performed under standardized conditions. Therefore a new cadaver study should be conducted in which the trauma mechanism is standardized and the tibiofibular ligaments as well as the interosseous membrane are evaluated with a 3D isovolumetric MRI, both before and after the induced trauma. In addition, stability tests can be performed both before and after the induced trauma. Thereafter the specimen can be dissected and anatomic findings be correlated with findings at MRI and the stability tests. This will result in information about osseoligamentous injury in relation to the stability tests, which in turn are related to the type of fracture, i.e. type of trauma mechanism.

Chapter 9

Summary

Summary

In chapter one the subject of this thesis is introduced: imaging of the anatomy of the distal tibiofibular syndesmosis in human cadavers, healthy volunteers and patients with an acute ankle fracture.
Injury to the distal tibiofibular syndesmosis can occur after an ankle sprain or after an acute ankle fracture. Several fracture classification systems have been developed which are based on radiographic findings of the ankle.These classifications can aid in predicting the presence of syndesmotic injury in relation to the level of the fibula fracture or to the mechanism of trauma. Clinically frequently used fracture classification systems are the Danis-Weber and AO-Müller classifications that pertain to the level of the distal fibula fracture, and the Lauge-Hansen classification which is based on the trauma mechanism, i.e. the position of the foot at the moment of injury and the direction of the occurring force.
However, from a questionnaire completed at a congress on skeletal radiology, it appears that the perceived anatomic boundaries of the syndesmosis vary tremendously.Also, the direction of the syndesmotic ligaments has repercussions for imaging techniques like MRI. A general concept is that ligaments can be best depicted along their longitudinal length. This means that when ligaments do not parallel the commonly used three orthogonal planes, this can lead to incorrect interpretation of imaging findings, resulting in chronic ankle instability or even early osteoarthritis.

Chapter two is a pictorial essay in which we endeavour to fill the hiatus in anatomic knowledge of the distal tibiofibular joint and provide a detailed anatomic description of the syndesmotic bones with the incisura fibularis, the syndesmotic recess, synovial fold and tibiofibular contact zone and the four syndesmotic ligaments, followed by their clinical relevance and discussion of remaining questions.
A syndesmosis is defined as a fibrous joint in which two adjacent bones are linked by a strong membrane or ligaments. This definition also applies for the distal tibiofibular syndesmosis, which is a syndesmotic joint formed by two bones and four ligaments. The distal tibia and fibula form the osseous part of the syndesmosis and are linked by the distal anterior tibiofibular ligament (ATIFL), the distal posterior tibiofibular ligament (PTIFL), the transverse ligament and the interosseous ligament.Although the syndesmosis is a joint, in literature the term syndesmotic injury is used to describe injury of the syndesmotic ligaments.
In an estimated 1-11% of all ankle sprains, injury of the distal tibiofibular syndesmosis occurs. Forty percent of patients do still have complaints of ankle instability six months after an ankle sprain.This could be due to widening of the ankle mortise as a result of increased length of the syndesmotic ligaments after acute ankle sprain. Since widening of the ankle mortise by 1mm decreases the contact area of the tibiotalar joint by 42%, this could lead to instability and hence an early osteoarthritis of the tibiotalar joint.
In fractures of the ankle, syndesmotic injury occurs in about 50% of type Weber B and in all of type Weber C fractures. However, it seems in discussing syndesmotic injury, the exact proximal and distal boundaries of the distal tibiofibular syndesmosis are not well defined. There is no clear statement in the Ashhurst and Bromer etiological, the Lauge-Hansen genetic or the Danis-Weber topographical fracture classifications about the extent of the syndesmosis. This joint is also not clearly defined in anatomical textbooks, such as Lanz and Wachsmuth. Kelikian and Kelikian postulate that the distal tibiofibular joint begins at the level of origin of the tibiofibular ligaments from the tibia and ends where these ligaments insert into the fibular malleolus.

In **chapter three** a new technique is described to study both intra- and extra-articular anatomy of a synovial joint, called MR-plastination-arthrography. As the syndesmosis of the ankle plays an important role in the stability of the talocrural joint, understanding of the exact anatomy of both the osseous and ligamentous structures is essential in interpreting plain radiographs, CT and MR images, in ankle arthroscopy and in therapeutic management.
In six human cadaveric lower legs, MR arthrography was performed in either a one-step or two-step procedure. In the former a mixture of diluted Gadolinium and dyed polymer was injected. In the latter the dyed polymer was injected after arthrography with diluted Gadolinium. Three-millimeter slices of these legs, obtained in a plane identical to that of the MR images, were plastinated according to the E12 technique of Von Hagens. The plastination slices were subsequently compared with the MR images. The one-step procedure resulted in an inhomogeneous arthrogram. The two-step procedure resulted in a good correlation between the high-resolution MR images and plastination slices, as expressed by a good comparison of anatomic detail of the small syndesmotic recess. Images of the distal tibiofibular syndesmosis obtained with plastination arthrography correlated well with images acquired by MR arthrography when performed in a two-step procedure.

In **chapter four** the optimal scan plane for depicting the ATIFL and PTIFL is assessed. MRI is a well proven technique to depict the osseoligamentous components of the ankle joint. Optimal MRI scan planes for the collateral ligaments of the ankle have been described extensively, however, with exception for the syndesmotic ligaments. Until now the usual three orthogonal planes have been used to image the ankle and its syndesmotic ligaments. But, as is known from detailed anatomic studies, the anterior (ATIFL) and posterior (PTIFL) tibiofibular ligament run in an oblique plane relative to the tibial plafond. In two fresh frozen cadaveric ankles we determined the optimum angle of the oblique caudal-cranial and lateral-medial MRI scan plane. The angle of the scan plane that demonstrated the anterior and posterior distal tibiofibular ligament uninterrupted in their full length was about 45 degrees. Subsequently we tested this oblique plane in healthy volunteers and evaluated the ATIFL and PTIFL regarding the continuity of the individual fascicles, thickness and wavy contour of the ligaments in both the axial and oblique planes. When compared to the axial plane, the oblique plane demonstrated significantly less discontinuity for both the ATIFL and PTIFL.

In **chapter five** the additional value of this 45° oblique MRI scan plane for assessing the anterior and posterior distal tibiofibular syndesmotic ligaments in patients with an acute ankle fracture is evaluated. Fractures on the radiographs were classified according to Lauge-Hansen (LH), and the aspect of the ATIFL and PTIFL as well as the presence of a bony avulsion, in both the axial and oblique planes, were evaluated on MRI. MRI findings regarding syndesmotic injury in the axial and oblique planes were compared to syndesmotic injury predicted by LH. The 45° oblique MRI plane demonstrated significantly less ligamentous injury than the axial plane, for both the ATIFL and PTIFL. There was however, no significant difference in detection of an avulsion fracture in the axial or oblique planes, neither anteriorly nor posteriorly. When compared with the Lauge-Hansen fracture classification, the oblique MRI plane showed a decrease in false positive syndesmotic injuries, anteriorly even more than posteriorly, which could be of considerable aid in therapeutic management.

Three frequently used methods to describe ankle fractures are the Danis-Weber, AO-Müller and Lauge-Hansen fracture classifications. In chapter six we correlate these fracture classification systems with MR findings regarding injury of the syndesmosis in acute ankle fractures. Treatment of ankle fractures is determined by several factors such as patient age, soft tissue status, dislocation of the fracture and integrity of the distal tibiofibular syndesmosis. Through the shortcomings of clinical examination and radiographs, injury to the syndesmotic ligaments is often misdiagnosed leading to chronic complaints such as instability, pain and swelling. As the major stabilizer of the distal tibiofibular joint, the ligamentous complex of the syndesmosis is critical in maintaining normal ankle function.

The classification of malleolar fractures constitutes the basis for treatment of acute ankle fractures. Additionally a number of radiographic parameters were used to evaluate the integrity of the syndesmotic and deltoid ligaments. Absence of tibiofibular overlap (TFO) at one side, and a tibiofibular clear space (TFCS) larger than 6mm may be an indication of syndesmotic injury. A medial clear space (MCS) surpassing the superior clear space (SCS) is indicative of deltoid injury, which regularly accompanies injury of the syndesmosis. We showed that the sensitivity for detecting syndesmotic injury with the Weber and AO-Müller fracture classifications in combination with additional measurements is low and much higher with the Lauge-Hansen fracture classification. Remarkably, syndesmotic injury was present in all Weber type B fractures, although measurements were normal in 65%.

None of the Weber type B fractures treated with ORIF required a setscrew although both anterior and posterior syndesmotic injury was present. MRI showed that posterior syndesmotic injury only occurred in association with anterior syndesmotic injury and mostly consisted of an intact posterior tibiofibular ligament attached to an avulsion fracture of the posterior malleolus. Both anterior and posterior avulsion fractures are frequently missed on radiographs when compared to MRI.

Chapter 10

Samenvatting

Samenvatting

Hoofdstuk 1 is de introductie van dit proefschrift dat gaat over het afbeelden van de anatomie van het distale tibiofibulaire gewricht in menselijke kadaverbenen, gezonde vrijwilligers en patiënten met een acute enkel fractuur.
Letsel van de distale tibiofibulaire syndesmose komt zowel voor bij een distorsie als ook bij een acute fractuur van de enkel. Op basis van bevindingen bij röntgenfoto's zijn meerdere fractuur classificaties voor de enkel ontwikkeld. Deze fractuurclassificaties kunnen helpen bij het voorspellen van syndesmose letsel in relatie tot het niveau van de fibula fractuur of in relatie tot het trauma mechanisme. In de kliniek veel gebruikte fractuur classificaties zijn de Weber en AO-Müller classificatie, die gerelateerd zijn aan het niveau van de fibula fractuur en de Lauge-Hansen classificatie, die gebaseerd is op het trauma mechanisme, i.e. de positie van de voet/talus op het moment van trauma en de richting van de optredende kracht.
Echter, zoals bleek uit een enquête tijdens een congres over skelet radiologie, was er een grote variatie in de interpretatie van de anatomische grenzen van de syndesmose. Echter, niet alleen de positie van, maar ook de richting waarin de syndesmose ligamenten lopen zijn van invloed op afbeeldingtechnieken zoals MRI. Een algemeen uitgangspunt is dat ligamenten het beste langs hun lengteas kunnen worden afgebeeld. Dit betekent dat, wanneer het verloop van de ligamenten niet parallel is aan de drie meestal gebruikte orthogonale scanvlakken, dit kan leiden tot een onjuiste interpretatie van de bevindingen. De gevolgen hiervan kunnen zijn dat er chronische enkel klachten ontstaan of zelfs vervroegde arthrose.

In **hoofdstuk twee** wordt geprobeerd om aan de hand van gedetailleerde afbeeldingen het hiaat in de kennis over de anatomie van het distale tibiofibulaire gewricht op te vullen en wordt er een gedetailleerde beschrijving gegeven van de incisura tibiae, de tibiofibulaire recessus, de synoviale plooi, de tibiofibulaire contact zone en de vier syndesmose ligamenten, gevolgd door hun klinische relevantie en bespreking van nog openstaande vragen.
Een syndesmose is gedefinieerd als een fibreus gewricht waarin twee botten met elkaar zijn verbonden door middel van een sterk membraan of ligamenten. Deze definitie is ook van toepassing op de distale tibiofibulaire syndesmose. De distale tibia en fibula vormen het ossale deel van de syndesmose en zijn met elkaar verbonden door het distale lig. tibiofibulare anterius, het distale lig. tibiofibulare posterius, het lig. tansversum en het lig interosseum. Alhoewel de syndesmose een gewricht is, wordt in de literatuur met letsel van de syndesmose niet zozeer het gewricht als wel de ligamenten van de syndesmose bedoeld.
Bij circa 1-11% van alle enkel distorsies komt letsel van de distale tibiofibulaire syndesmose voor. Zes maanden na een enkel distorsie heeft veertig procent van de patiënten nog klachten van een instabiele enkel. Dit kan zijn omdat de enkelvork verwijd is ten gevolge van uitgerekte syndesmose ligamenten na een enkel distorsie. Verwijding van de enkelvork met 1 mm leidt tot een afname van het tibiotalaire contact oppervlak met 42%. Dit kan leiden tot instabiliteit van de enkel en dientengevolge tot vroegtijdige artrose van het bovenste sprong-gewricht.
Indien er sprake is van enkel fracturen komt letsel van de syndesmose voor bij circa 50% van de Weber type B en bij alle Weber type C fracturen. Echter in discussies over syndesmose letsel blijkt dat de exacte proximale en distale begrenzing van de syndesmose niet goed zijn gedefinieerd. Er is geen duidelijke uitspraak over deze begrenzing te vinden noch in de etiologische fractuur classificatie volgens Ashhurst en Bromer, noch in de genetische volgens Lauge-Hansen of de topografische volgens Danis-Weber. Ook in tekstboeken over de anato-

mie, zoals dat van Lanz en Wachsmuth, is er geen duidelijke definitie te vinden. Kelikian en Kelikian postuleren dat het distale tibiofibulaire gewricht begint op het niveau van de origo van de tibiofibulaire ligamenten aan de tibia en eindigt daar waar de ligamenten insereren aan de malleolus van de fibula.

In **hoofdstuk drie** wordt een beschrijving gegeven van een nieuwe techniek, MR-plastinatie-arthrografie genoemd, om zowel de intra- als extra-articulaire anatomie van een synoviaal gewricht te kunnen bestuderen. Aangezien de syndesmose van de enkel een belangrijke rol speelt in de stabiliteit van het talocrurale gewricht, is gedetailleerde kennis van zowel de ossale als ligamentaire structuren essentieel voor het kunnen interpreteren van röntgenfoto's, CT en MR onderzoeken, voor het verrichten van arthroscopie van de enkel en voor opstellen van een behandeling.
In zes benen, door mensen ter beschikking gesteld voor de wetenschap, werd MR-arthrografie verricht in een één-stap dan wel twee-stappen procedure. In het eerste geval werd een mengsel van verdund Gadolinium en een gekleurd polymeer geïnjecteerd. In het tweede geval werd het gekleurde polymeer pas geïnjecteerd nadat de arthrografie met verdund Gadolinium was verricht. Drie millimeter plakken van deze benen, verkregen in hetzelfde vlak als waarin de MRI was verricht, werden geplastineerd volgens de E12 techniek van Von Hagens. De geplastineerde plakken werden vervolgens vergeleken met de MR afbeeldingen. De één-stap procedure leidde echter tot een inhomogeen arthrogram. De twee-stappen procedure daarentegen resulteerde in een goede correlatie tussen de hoge resolutie MR afbeeldingen en de geplastineerde plakken, zoals zichtbaar werd in de gedetailleerde anatomie van de kleine syndesmotische recessus.

In **hoofdstuk vier** wordt bepaald wat het optimale scanvlak is om de ATIFL en PTIFL af te beelden. In de loop der tijd heeft MRI zichzelf bewezen als een techniek waarmee het goed mogelijk is om zowel de ossale als de ligamentaire structuren van de enkel af te beelden. Er zijn uitgebreide beschrijvingen voor de optimale MRI scanvlakken voor de collaterale ligamenten van de enkel, maar niet voor de syndesmose ligamenten. Tot op heden worden meestal de drie gebruikelijke orthogonale scanvlakken gebruikt om de enkel en zijn syndesmose ligamenten af te beelden. Maar uit anatomische studies is bekend dat het ligamentum tibiofibulare anterius (ATIFL) en posterius (PTIFL) in een schuin vlak verlopen ten opzichte van het tibia plafond. In twee vers gevroren benen, door mensen ter beschikking gesteld voor de wetenschap, werd de optimale hoek van een scanvlak bepaald met een caudo-craniaal en latero-mediaal verloop. Het vlak waarin het ligamentum tibiofibulare anterius en posterius over hun gehele lengte ononderbroken zichtbaar waren bedroeg 45 graden. Vervolgens is dit schuine vlak getest bij gezonde vrijwilligers en zijn de ATIFL en PTIFL geëvalueerd, in zowel het axiale als schuine vlak, met betrekking tot de continuïteit van hun afzonderlijke vezels, de dikte en een golvend aspect van het ligament. Wanneer vergeleken werd met het axiale vlak bleek dat in het schuine vlak beduidend minder vaak discontinuïteit van zowel de ATIFL als de PTIFL voorkwam.

Nadat het nut van het schuine vlak in gezonde vrijwilligers is aangetoond, wordt in **hoofdstuk vijf** de toegevoegde waarde van dit schuine vlak voor analyse van letsel van de ATIFL en PTIFL bij patiënten met een acute enkel fractuur onderzocht. Fracturen op de röntgenfoto werden geclassificeerd volgens Lauge-Hansen (LH) en het aspect van de ATIFL en PTIFL, alsook de aanwezigheid van een avulsie fractuur, werden in zowel het axiale als het schuine vlak met een MRI geëvalueerd. Bevindingen op MRI, met betrekking tot letsel van de syndesmose

in het axiale en schuine vlak, werden vergeleken met syndesmose letsel zoals dat voorspeld werd door Lauge-Hansen. Het 45 graden schuine vlak toonde significant minder ligamentair letsel aan dan het axiale vlak, voor zowel de ATIFL als de PTIFL. Er was echter geen significant verschil in detectie van een avulsie fractuur in het axiale en schuine vlak, noch aan de voorzijde noch aan de achterzijde. In vergelijking met de Lauge-Hansen fractuur classificatie toonde het schuine MRI vlak een afname van fout positief syndesmose letsel aan, voor zelfs meer dan achter. Deze bevindingen kunnen een aanzienlijke ondersteuning zijn bij het opstellen van een behandelplan.

Drie veel gebruikte methoden om enkel fracturen te beschrijven zijn de Danis-Weber, AO-Müller en Lauge-Hansen fractuur classificaties. In **hoofdstuk zes** worden deze fractuur classificaties gecorreleerd met de bevindingen op MRI met betrekking tot letsel van de syndesmose in acute enkel fracturen. Behandeling van enkel fracturen wordt bepaald door een aantal factoren zoals de leeftijd van patiënt, de weke delen status, dislocatie van de fractuur en integriteit van de syndesmose. Door beperkingen van zowel lichamelijk onderzoek als röntgenfoto's, wordt letsel van de syndesmose vaak onderschat wat kan leiden tot chronische klachten als instabiliteit, pijn en zwelling. Als belangrijkste stabilisator van het distale tibiofibulaire gewricht, vormt het ligamentaire complex van de syndesmose derhalve een kritische rol bij het handhaven van een normale enkel functie.
De classificatie van malleolaire fracturen vormt de basis voor behandeling van acute enkel fracturen. Daarnaast kunnen een aantal röntgenologische parameters gebruikt worden om de integriteit van de syndesmose en het ligamentum deltoideum te evalueren. Het aan één zijde afwezig zijn van de tibiofibulaire overlap en een tibiofibulaire "clear space" die groter is dan 6 mm, zijn een indicatie voor letsel van de syndesmose. Een mediale "çlear space" die groter is dan de superior "clear space" wijst op letsel van het ligamentum deltoideum, wat vaak gepaard gaat met syndesmose letsel. Wij hebben aangetoond dat de sensitiviteit voor het detecteren van syndesmose letsel met de Weber en AO-Müller fractuur classificatie in combinatie met de aanvullende metingen laag is en een stuk hoger met de Lauge-Hansen fractuur classificatie. Opvallend was dat syndesmose letsel in alle Weber type B fracturen voorkwam, terwijl de metingen in 65% van de gevallen normaal waren.
Geen van de Weber type B fracturen die behandeld werden met een open reductie en interne fixatie (ORIF) kregen een stelschroef, alhoewel er zowel aan de voor- als achterzijde syndesmose letsel aanwezig was. MRI liet zien dat letsel van de achterste syndesmose alleen voorkwam in combinatie met letsel van de voorste syndesmose en meestal bestond uit een intact ligamentum tibiofibulare posterius dat vastzat aan een avulsie fractuur van de posterior malleolus. In vergelijking met MRI werden avulsie fracturen op röntgenfoto's vaak gemist, zowel aan de voor- als achterzijde.

Curriculum Vitae

Curriculum Vitae

After receiving his secondary education diploma from the Marnix Gymnasium, Rotterdam, he studied Chemical Technology at the Technical University in Delft (TUD). One year later he entered medical school at the Erasmus University Medical Center, Rotterdam. From that moment on he was fascinated by the combination of both technical and medical knowledge, and successfully became an engineer in 1988 and a medical doctor in 1990. He may in all probability therefore be the only medical doctor who ever designed a factory.

During that period (1986-1987) he also worked at the department of Clinical Chemistry at the Erasmus University Rotterdam (prof. dr. B. Leijnse) and developed an expert system in the area of haematology. Thereafter he collaborated for half a year in a project developing a model for estimating the distribution of toxic compounds in the ecosystem after a major calamity. This was at the Gesellschaft für Strahlen- und Umwelt Forschung in Munich, Germany (dr. M. Mathies).

In expectation of joining the military service, he worked as a resident at the department of general surgery at the Ruprecht-Karls University in Heidelberg, Germany. During his military service he was a resident in orthopaedic surgery at the Military Hospital dr. A. Mathijsen in Utrecht (1991). Following the latter, he spent one and a half years as resident (AGNIO) in general surgery at the Ruwaard van Putten Hospital, Spijkenisse, where he performed his first appendectomy with his father, a general surgeon (1993). From 1990-1994, he was also an instructor and examiner in surgery and traumatology at the School for Health Care in Rotterdam.

His first interest in the field of radiology commenced in 1993 with his traineeship as a resident at the St. Franciscus Hospital, Rotterdam, followed by his specialization in radiology at the University Medical Center in Groningen (prof. dr. C.J.P. Thijn). In 1999 he joined the medical staff at the radiology department of the Erasmus University Medical Center in Rotterdam (prof. dr. G.P. Krestin), and specialized in imaging of pancreas pathology. Early into his appointment at the Erasmus University Medical Center, he forged close collaboration with the department of neurosciences-anatomy (prof. dr. C.I. de Zeeuw) where he performed anatomic studies on the ankle culminating in this thesis. In 2010 he continued his career at the radiology department of the Radboud University Nijmegen Medical Center, in Nijmegen (prof. dr. W.M. Prokop), where he is currently forming a multidisciplinary working group on pancreas pathology.

PhD Portfolio

Summary of PhD training and teaching

Name PhD student: J.J. Hermans
Erasmus MC Department: Neuroscience – Anatomy

PhD period: 2006 – 2011
Promotor: prof.dr. G.J. Kleinrensink

1. PhD training

	Year	Workload (ECTS)
General courses		
Professional ICH GCP	2007	0.1
Specific courses		
MR fysica cursus	2007	0.4
Workshop endovascular techniques	2009	0.4
Presentations		
ISMRM MRI of chronic syndesmotic injury	2002	1.0
SICOT MRI of chronic syndesmotic injury	2002	0.4
Nederlandse Radiologendagen Chronisch syndesmoseletsel	2002	0.4
Alvleesklliervereniging	2002	0.2
Nederlandse Radiologendagen s-MRCP after Whipple	2003	0.5
RSNA Lipomatous tumors of the pancreas	2005	0.5
ECR Correlation X-ray and MRI in ankle fractures	2005	0.6
ESGAR Algorithm workup pancreas trauma	2007	0.6
RSNA Central venous catheter for power injection	2007	0.1
Desi Erasmus Local operability pancreas carcinoma	2007	1.0
EMCR Klinische anatomie thorax en abdomen	2008	1.0
NVvR MRI bij enkel letsel	2010	1.0

(Inter)national conferences		
European Congress of Radiology	2000	1.2
International Society for Magnetic Resonance in Medicine	2000	1.4
Erasmus Course MRI MSK	2002	1.2
International Diagnostic Course Davos	2002	1.4
International Society for Magnetic Resonance in Medicine	2002	1.4
NNvR Sandwich cursus Acute Radiologie	2004	0.4
European Society of Gastrointestinal and Abdominal Radiology	2004	1.2
International Society for Magnetic Resonance in Medicine	2005	1.4
European Society of Gastrointestinal and Abdominal Radiology	2005	1.2
Radiological Society of North America	2005	1.4
European Congress of Radiology	2006	1.2
European Congress of Radiology	2007	1.2
European Congress of Radiology	2008	1.2
European Society of Gastrointestinal and Abdominal Radiology	2008	1.2
Computer Assisted Radiology and Surgery	2008	0.6
European Congress of Radiology	2009	1.2
NNvR Sandwich cursus Acute Radiologie	2009	0.4
NVvR Sandwich cursus MSK	2010	0.4
European Congress of Radiology	2010	1.2

2. Teaching

	Year	Workload (ECTS)
Oncomotief Neuroendocriene Tumoren	2009	0.1
Junior Medical School	2010	0.3

Supervising Student's theses		
MRI morphometry of the distal tibiofibular syndesmosis	2003	0.6
Correlation between X-ray and MRI of ankle fractures	2004	0.6
Mathematisch-modelmatige analyse van het enkelgewricht	2005	0.6
Algoritme work-up en behandeling pancreas trauma	2006	0.6
Measurement of sternum width from Computed Tomography	2006	0.6
Local resectability of GIST on CT	2006	0.6
Yearly performed ultrasonography after liver transplantation	2006	0.6
Kwaliteit aanvraagproces radiologisch onderzoek	2007	0.6
Procesverantwoordelijkheid vanuit de afdeling radiologie	2008	0.6
Workflow driven user interface for radiological system	2008	0.6
Automated quantification of visceral and subcutaneous fat	2010	0.6

List of publications

List of publications

Van Dijken J.P., van den Bosch E., Hermans J.J., Rodrigues de Miranda L. & Scheffers W.A.. Alcoholic Fermentation by 'non-fermentative yeasts'.
Yeast 1986 Jun;2(2):123-127.

Hermans J.J., Hermans A.L., Risseeuw G.A., Verhaar J.C., Meradji M.. Appendicitis Caused by Carcinoid Tumor.
Radiology 1993 Jul; 188(1):71-72.

Hermans J.J., Mooyaart E.L., Hendriks J.G., Diercks R.L.. Familial congenital bilateral agenesis of the acromion: a radiologically illustrated case report.
Surg Radiol Anat. 1999;21(5):337-339.

Hansel D.E., Rahman A., Hermans J., de Krijger R.R., Ashfaq R., Yeo C.J., Cameron J.L., Maitra A.. Liver metastases arising from well-differentiated pancreatic endocrine neoplasms demonstrate increased VEGF-C expression.
Mod Pathol. 2003 Jul;16(7):652-9.

Beumer A., Hermans J.J., Niesten D., Heijboer M.P. Late reconstruction of the anterior tibiofibular syndesmosis for ankle diastasis with talar shift in a 12 year old boy.
Foot Ankle Surg 2005; 11: 49-53.

Hermans J.J., Beumer A., Mulder P.G..Ankle stress test for predicting the need for surgical fixation of isolated fibular fractures: statistical analysis.
J Bone Joint Surg Am. 2005 Aug; 87(8):1885-6.

Wolters L.M., Hermans J.J., van Dekken H., Kazemier G., Schouten W.R., Kuipers E.J..
Incidental cystic structures in the upper abdomen: to remove or not to remove.
NTVG 2006 Jan 28; 150(4): 169-174.

Van Vliet E.P., Eijkemans M.J., Kuipers E.J., Hermans J.J., Steyerberg E.W., Tilanus H.W., van der Gaast A., Siersema P.D.. A comparison between low-volume referring regional centers and a high-volume referral center in quality of preoperative metastasis detection in esophageal carcinoma.
Am J of Gastroenterol. 2006 Feb; 101(2): 234-242.

Smits M., Hermans J.J.. Arteriovenous malformation: a dynamic anomaly. Case report and literature review.
Radiological Archives of Serbia, Vol (13), 2007, p5-10.

Van Vliet E.P., van der Lugt A., Kuipers E.J., Tilanus H.W., van der Gaast A., Hermans J.J., Siersema P.D.. Ultrasound, computed tomography, or the combination for the detection of supraclavicular lymph nodes in patients with esophageal or gastric cancer: a comparative study.
J Surg Oncol. 2007 Sep 1; 96(3):200-6.

Van Santvoort H.C., Bollen T.L., Besselink M.G., Banks P.A., Boermeester M.A., van Eijck, C.H., Evans J., Freeny P.C., Grenacher L., Hermans J.J., Horvath K.D., Hough D.M., Lameris J.S., van Leeuwen M.S., Mortele K.J., Neoptolemos J.P., Sarr M.G., Vege S.S., Werner J., Gooszen H.G.. Describing peripancreatic collections in severe acute pancreatitis using morphologic terms: an international interobserver agreement study.
Pancreatology 2008; 8(6): 593-9.

Kompanje E.J., Hermans J.J.. Cephalopagus conjoined twins in a Leopard cat (Prionailurus bengalensis).
J Wildl Dis. 2008 Jan; 44(1): 177-180.

Van Buuren H.R., Hermans J.J., van Eijck C.H..Accidental placement of a biliary endoprosthesis in the portal vein.
Endoscopy 2008 Sep; 40 Suppl 2:E29.

Van Vliet E.P., Hermans J.J., de Wever W., Eijkemans M.J., Steyerberg E.W., Faasse C., van Helmond E.P., de Leeuw A.M., Sikkenk A.C., de Vries A.R., de Vries E.H., Kuipers E.J., Siersema P.D.. Radiologist experience and CT examination quality determine metastasis detection in patients with esophageal or gastric cardia cancer.
Eur Radiol. 2008 Nov;18(11):2475-84.

Morak M.J., van der Gaast A., Incrocci L., van Dekken H., Hermans J.J., Jeekel J., Hop W.C., Kazemier G., van Eijck C.H.. Adjuvant intra-arterial chemotherapy and radiotherapy versus surgery alone in resectable pancreatic and periampullary cancer: a prospective randomized controlled trial.
Ann Surg. 2008 Dec; 248(6):1031-41.

Lans T.E., van Ramshorst G.H., Hermans J.J., den Bakker M.A., Tran T.C., Kazemier G..
Perivascular epithelioid cell tumor of the retroperitoneum in a young woman resulting in an abdominal chyloma.
J Gastrointest Surg. 2009 Feb;13(2):389-92.

Hermans J.J., Wentink N., Kleinrensink G.J., Beumer A.. MR - Plastination arthrography: a new technique used to study the distal tibiofibular syndesmosis.
Skeletal Radiol. 2009 Jul;38(7):697-701.

Hermans, J.J., Kompanje, E.J.O., Krestin, G.P., Moeliker, C.W.. First Magnetic Resonance Imaging (MRI) of a complete specimen of Bruijn's brush-turkey Aepypodius bruijnii (Aves, Megapodiidae).
Deinsea 2009(13): 1–8.

Den Hartog D., Dur A.H.M., Kamphuis A.G.A., Tuinebreijer W.E., Hermans J.J., Kreiss R.W.. Pre-, intra-, and postoperative sonography of the abdominal wall in patients with incisional hernias repaired via a three-layered operative suture method.
J Clin Ultrasound 2009 Sep; 37(7):394-8.

Morak M.J., Hermans J.J., Smeenk H.G., Renders W.M., Nuyttens J.J., Kazemier G., van Eijck C.H.. Staging for locally advanced pancreatic cancer.
Eur J Surg Oncol. 2009 Sep;35(9):963-8.

Van Ramshorst G.H., Kleinrensink G.J., Hermans J.J., Terkivatan T., Lange J.F.. Abdominal wall paresis as a complication of laparoscopic surgery.
Hernia 2009 Oct;13(5):539-43.

Carbognin G., Girardi V., Biasiutti C., Camera L., Manfredi R., Frulloni L., Hermans J.J., Pozzi Mucelli R.P.. Autoimmune pancreatitis: imaging findings on contrast-enhanced MR, MRCP and dynamic secretin-enhanced MRCP.
Radiol. Med. 2009, Dec 114(8):1214-31.

Faccioli N, Molinari E, Hermans JJ, Comai A, D'Onofrio M, Bassi C, Pozzi Mucelli R.
Role of fistulography in characterizing pancreatic fistula after pancreaticoduodenectomy (accepted Br J Radiology May 2010).

De Jong K., Nio Y.C., Hermans J.J., Dijkgraaf M.G., Gouma D.J., van Eijck C.H., van Heel E., Klass G., Fockens P., Bruno M.J.. High prevalence of pancreatic cysts detected by screening magnetic resonance imaging examinations.
Clin. Gastroenterol. Hepatol. 2010 Sep; 8(9):806-811.

Hermans J.J., Beumer A., de Jong T.A., Kleinrensink G.J.. Anatomy of the distal tibiofibular syndesmosis in adults: a pictorial essay with a multimodality approach
J Anat 2010 Dec;217(6):633-45.

Hermans J.J., Ginai A.Z., Wentink N., Hop W.C., Beumer A.. The additional value of an oblique image plane for MRI of the anterior and posterior distal tibiofibular syndesmosis Skeletal Radiol. 2011 Jan;40(1):75-83.

Hermans J.J., Beumer A., Hop W.C.J., A.F.C.M. Moonen, Ginai A.Z.. Tibiofibular syndesmosis in acute ankle fractures: additional value of an oblique MR image plane.
Skeletal Radiology (accepted Apr 2011).

Hermans J.J., Wentink N., Beumer A., Hop W.C.J., Heijboer M.P., Moonen A.F.C.M., Ginai A.Z.. Correlation between radiological assessment of acute ankle fractures and syndesmotic injury on MRI.
Skeletal Radiology (submitted Apr 2011).

Croles F.N., Hebeda K.M., Kats-Ugurlu G., Hermans J.J., Bonenkamp J.J., van der Velden W.J.F.M.. Splenic gas due to a non-Hodgkin lymphoma in a patient with CVID.
(accepted JCO Apr 2011).